

Enamel-dentine junction morphology  
in hominin mandibular third  
premolars

Thomas Davies

MSc dissertation

University of Kent

Supervisor: Dr Matthew Skinner



---

*Abstract*

---

In non-human apes, as in most catarrhines, the P<sub>3</sub> is adapted for a role in honing the large upper canine, a feature which was lost early in hominin evolution. No longer adaptively constrained to the morphology required for canine honing, the hominin P<sub>3</sub> evolved in a variety of ways, mostly to improve its masticatory ability. This change in function makes the P<sub>3</sub> a particularly important tooth position in hominin evolution and it has featured prominently in systematic analyses of the hominin clade. However, due to dental wear much of the original morphology of the P<sub>3</sub> crown is lost in many hominin teeth. Analyses of other tooth positions have demonstrated that examining the enamel-dentine junction (EDJ) can improve the taxonomic signal in tooth crown morphology as well as reveal detailed insights into the presence and manifestation of discrete dental traits.

This study uses geometric morphometric techniques to analyse the shape of the P<sub>3</sub> EDJ in a broad sample of fossil hominins, modern humans, and extant non-human apes (n = 118), aiming to characterise the major differences in P<sub>3</sub> morphology between apes and hominins, and then within the hominin clade. The study also tests the utility of P<sub>3</sub> EDJ shape for distinguishing among major hominin species, and addresses the affinities of a number of hominin specimens of uncertain taxonomic affiliation. Moreover, the EDJ expression of a number of P<sub>3</sub> discrete traits are identified and investigated for the first time.

The results suggest that the morphology of the P<sub>3</sub> EDJ is effective in distinguishing among taxa, with a very high level of classification accuracy. Further, P<sub>3</sub> morphology is linked to previously discussed trends in hominin evolution such as the unique dental adaptations seen in *Paranthropus* species. The EDJ expression of discrete traits such as the transverse crest, buccal grooves and the marginal ridge are found to be variable among taxonomic groups. Potential developmental links to other features identified in molars are discussed.

# Acknowledgements

I would like to thank my supervisor, Dr Matthew Skinner, for all of his help and guidance throughout the project. I would like to thank everyone in the Virtual Paleoanthropology Lab; Bill Plumber, for our many discussions about teeth, and Leoni Georgiou, Christopher Dunmore and Klara Komza for their help (and patience) across the year. I would also like to thank Dr Tracy Kivell, and everyone in the APE lab for their help and advice in lab meetings, and everyone in the Anthropology department for making the year so enjoyable. For his assistance with Mathematica, I would like to thank Philipp Gunz. For access to specimens, I would like to thank Witwatersrand University, Naturmuseum Senckenberg, Ditsong Museum, National Museums of Kenya, National Museum of Ethiopia, Tel Aviv University, INSAP Rabat, ASBL Archéologie Andennaise, Musée national de Préhistoire, Institut für Geowissenschaften (Universität Heidelberg) and the Croatian Natural History Museum. For CT scanning I would like to thank Jean-Jacques Hublin and the technical staff of the Department of Human Evolution, Max Planck Institute for Evolutionary Anthropology.

# Table of Contents

List of Tables and Figures.....	6
Introduction .....	7
Literature review.....	8
1. Teeth in the fossil record .....	8
2. Premolars.....	15
3. Geometric morphometrics .....	19
4. Enamel-Dentine Junction.....	22
Manuscript.....	28
1. Introduction .....	28
2. Materials and methods.....	30
2.1. Study sample.....	30
2.2. Microtomography .....	32
2.3. Image filtering.....	33
2.4. Tissue segmentation .....	34
2.5. Landmark collection.....	35
2.6. Derivation of homologous landmark sets.....	36
2.7. Analysis of EDJ and CEJ shape and size.....	37
2.8. Visualisation of EDJ shape variation .....	38
2.9. Classification of additional specimens.....	38
2.10. Discrete traits.....	38
3. Results.....	44
3.1. Changes in P <sub>3</sub> morphology through time.....	44
3.2. Classification accuracies.....	56
3.3. Specimens of uncertain taxonomic affinity .....	57
3.4. Discrete traits.....	57
4. Discussion.....	63
4.1. Premolar morphology for taxonomy .....	63
4.2. Specimens of uncertain taxonomic affinity .....	64
4.3. Major EDJ shape trends .....	66
4.4. Discrete Traits .....	74
5. Conclusion.....	80
Reference List.....	82
Supplementary information.....	95

## List of Tables and Figures

<b>Table 1</b> – Study sample summary.....	31
<b>Table 2</b> – Geometric morphometric analyses summary.....	35
<b>Table 3</b> – Pairwise comparisons of P3 centroid size.....	45
<b>Table 4</b> – Classification accuracies.....	52
<b>Figure 1</b> – Landmarking protocol and P3 terminology guide.....	33
<b>Figure 2</b> – Transverse crest variation.....	38
<b>Figure 3</b> – Marginal ridge form.....	39
<b>Figure 4</b> – Buccal groove variation.....	40
<b>Figure 5</b> – Wireframe models for each taxa.....	42
<b>Figure 6</b> – PCA plots of EDJ and CEJ shape.....	44
<b>Figure 7</b> – PCA plots of EDJ shape.....	46
<b>Figure 8</b> – Boxplot of natural logarithm of centroid size.....	48
<b>Figure 9</b> – Wireframe models of four early Homo specimens.....	49
<b>Figure 10</b> – Protoconid variation.....	54
<b>Figure 11</b> – EDJ and OES images.....	62

# Introduction to the thesis

The aim of this thesis is to characterise the evolution of the mandibular third premolar of fossil hominins, as well as non-hominin apes. The enamel-dentine junction morphology of a large sample of extant and fossil hominoid specimens will be examined using geometric morphometric analyses, as well as discrete trait analysis, with three main aims:

1. Evaluate the taxonomic potential of the P<sub>3</sub> EDJ using 3D geometric morphometrics, and evaluate the taxonomic affiliation of any specimens which have not been reliably assigned to a taxonomic group
2. Summarise the major transitions in P<sub>3</sub> morphology across hominin evolution, using extant non-hominin apes as an outgroup
3. Discuss the presence of a number of discrete traits at the EDJ and OES, and their potential importance both taxonomically and developmentally

The thesis is structured as follows: a literature review chapter, a chapter written as a stand-alone manuscript for journal submission, and supplementary information.

# Literature review

## 1. Teeth in the fossil record

Teeth are an important component of the fossil record; as highly mineralised and compact tissues, they are well preserved, and therefore extremely common in fossil deposits. In some cases, the majority of the fossil material available for a taxon comes from teeth, as is the case for *Gigantopithecus*, which was initially described on the basis of a single M<sub>3</sub> (von Koenigswald, 1952), and which even now is known exclusively from teeth and a few mandibles (Zhang *et al.* 2016). All the information known about this genus therefore has to come from this limited sample; however, this limited source of data does not stop us from making specific predictions about their diet, ecology and phylogenetic position (White, 1975; Ciochon *et al.* 1990; Daegling and Grine; 1994). The frequency of teeth in the fossil record is not the only reason they are so widely studied, however; they also contain vast quantities of information. For example, researchers commonly study the isotopic signature of tooth enamel diet (Lee-Thorp *et al.* 1994; Sponheimer and Lee-Thorp, 1999; Richards *et al.* 2001), as well as patterns of tooth wear on both a macro- (Kay, 1977; Dean and Beynon, 1991; Ungar, 2004) and micro- (Walker *et al.* 1978; Grine, 1986; Grine *et al.* 2012) scale, in order to reveal aspects of hominin diet.

An advantage of teeth is that, unlike bones, they are not remodelled throughout an organism's lifetime (Schour and Massler, 1940a, 1940b; Linde, 1984; Nanci, 2008); once fully developed they can only be modified by external factors such as breakage or disease, the effects of which are preserved for study in fossil teeth. Furthermore, the lack of lifetime remodelling of teeth means that the morphology of unworn dental specimens is highly genetically controlled, and this, combined with a high level of character richness, means that teeth are particularly useful in reconstructing evolutionary relationships, for example through phylogenetic analyses. Such analyses have been used in a number of extinct mammal groups such as the Hyaenodontidae, a highly successful group of carnivores which went extinct in the late Miocene (Zack, 2011), and the Taeniodonta, a group of 'archaic' mammals present around the Cretaceous-Paleogene mass extinction (Rook and Hunter,

2014), as well as in fossil hominins (Irish *et al.* 2013). Phylogenetic studies, including those centred on hominin systematics, often employ a wider suite of characters, either expanding to include cranial (Strait and Grine, 2004; Danilo *et al.* 2013; Dembo *et al.* 2015), or cranial and postcranial characters (Ni *et al.* 2013; O'Leary *et al.* 2013; Argue *et al.* 2017); however, even in these cases there is often a disproportionately large number of dental characters included.

There are a number of issues with cladistic analyses, however, including problems with homoplasy (Lieberman *et al.* 1996; Springer *et al.*, 2007), non-independence of characters (Kluge, 1989; Strait *et al.* 1997; McCollum, 1999) and choice of outgroup taxa (Curnoe 2003; Bjarnason *et al.* 2010), with some researchers even suggesting that these analyses are not suitable for determining evolutionary relationships in hominins (Collard and Wood 2000; Curnoe 2003).

### *Development*

These issues are not only important when building cladograms; any character-based method of utilising morphology for phylogenetic purposes faces similar problems. However, many of these issues can be alleviated through careful choice of characters for analysis. Two of the most prominent issues are homology, and non-independence of characters. Both issues are particularly relevant to the present study. For example, it has been demonstrated that for a number of common dental traits, features which appear to be homologous from the external morphology of the tooth may have multiple distinct morphologies at the enamel-dentine junction (EDJ), indicating that they represent multiple distinct, non-homologous traits (Skinner *et al.* 2008b; Anemone *et al.* 2012). Furthermore, there is evidence to suggest that certain crown features of the tooth may be strongly co-dependent. For example, the presence of an accessory cusp (C6) in chimpanzee molars has been shown to be correlated with the size of the tooth, as well as size and location of other cusps (Skinner and Gunz, 2010), whilst the spacing of cusps in human molars shows some correlation with the presence of the Carabelli trait, a cusp on the lingual side of the protocone (Hunter *et al.* 2010). Therefore, when studying the morphology of hominin P<sub>3</sub>S with the aim of discussing phylogenetic

hypotheses, it is important to consider whether the characters used are independent of one another, and that homoplasy is not mistaken for homology.

One method of tackling this issue is to consider the developmental processes which go into forming the observed morphology. This method allows us to identify traits which are developmentally linked, and allow us to assess whether they are independent. Equally, considering development allows us to identify when traits shared between groups have different developmental origins, suggesting homoplasy. For this purpose, the dentition is particularly useful; their lack of remodelling allows the teeth of individuals of any age can be used in reconstructing the developmental processes that went into their construction.

The formation of teeth happens at the boundary between oral epithelial cells and ectomesenchyme (Huggins, 1934; Butler, 1967; Thesleff, 2003; Nanci, 2008). A band of epithelium thickens in sites corresponding to the future dental arches and forms the dental lamina, which is the only place that tooth buds are able to form. The deciduous dentition forms first, as a series of thickenings on the lamina, with the permanent dentition forming later in a similar fashion (Reif, 1976; Jernvall and Thesleff, 2000; Nanci, 2008). Tooth development proceeds in three main stages; the bud, cap and bell stages. The bud stage is marked by the first intrusion of the epithelial cells into the ectomesenchyme, forming an epithelial bud. During the cap stage, the ectomesenchymal cells increase in density and the epithelial cells continue to proliferate. The epithelial cells will go on to form the enamel of the tooth, and as such, are referred to as the enamel organ, whilst ectomesenchymal cells, which condense into balls, will go on to form pulp and dentine, and are referred to as dental papilla. This is called the cap stage because enamel organs sit on top of dental papillae like a cap (Kollar and Baird, 1969; Reif, 1982; Miletich and Sharpe, 2003; Nanci, 2008).

As the germ continues to grow, it enters the bell stage, during which the inner and outer enamel epithelium form. These are continuous with one another, forming around the edge of the enamel organ; the inner enamel epithelium marks the boundary between the enamel organ and the dental

papilla, whilst the outer enamel epithelium marks the boundary between the enamel organ and the remaining ectomesenchyme. Cells at the tip of the future cusps differentiate into enamel forming cells (ameloblasts) and dentine forming cells (odontoblasts) in a process called histodifferentiation. These begin to deposit enamel and dentine on either side of the inner enamel epithelium, before a wave of cell differentiation sweeps down the sides of the cusps (Nanci, 2008). Dentinogenesis consists of two main stages; organic matrix secretion, and mineralisation (Linde, 1984; Linde and Goldberg, 1993). Odontoblasts are present in tubercles running from the EDJ to the pulp chamber and remain capable of producing dentine throughout their lives. The process of enamel formation by ameloblasts is called Amelogenesis. Ameloblasts are initiated to produce enamel matrix almost immediately after the odontoblasts secrete predentine, and this proceeds in a similar pattern of secretion and mineralisation (Goldberg *et al.*, 1995; Nanci, 2008).

The form of the outer enamel surface (OES), and the cusp patterning observed, is largely determined by the shape of the inner enamel epithelium after folding (Butler, 1956; Ruch, 1987). It is therefore important to understand the developmental processes that direct the folding of this surface. Of particular importance to this process are enamel knots; clusters of nondividing epithelial cells that occur at the boundary with the inner enamel epithelium (Jernvall *et al.* 1994). They are transient structures, eventually disappearing through apoptosis; however they have a controlling role in cusp development. Primary enamel knots, visible from the cap stage, are non-proliferative, but produce growth factors that stimulate mitosis in surrounding mesenchymal and epithelial cells. This process creates unequal growth in the inner enamel epithelium, causing it to buckle, and stimulate the growth of the cusp (Jernvall *et al.* 1994). Secondary enamel knots begin to form in the bell stage, immediately after apoptosis of the primary enamel knots (Keranen *et al.* 1998). These enamel knots occur at the site of extra cusps, and are thought to determine their form and size in a similar fashion (Jernvall *et al.* 1994; Jernvall and Thesleff, 2000), continuing until the final cusp pattern of the tooth is formed. The presence of enamel knots can adequately explain how cusps form, but they do not explain variation in their number, patterning and size, both within and between species. In hominins,

for example, accessory cusps C6 and C7 are common, and both are more common in some species than others. However, they are variable within species, as well as between species. Moreover, they can vary in their size, form and even frequency (Wood and Abbott, 1983). It could be expected that each individual enamel knot, and therefore each cusp, is determined individually. However, the same genes appear to be involved in initialising the development of each individual cusp, suggesting that they are instead formed through repeated use of the same developmental pathways (Keranen *et al.* 1998).

The patterning cascade model instead posits that the formation of enamel knots is an iterative process in which cusp patterning is determined by activators and inhibitors, ensuring that cusps will only form when there is enough space on the crown that the new cusp would be sufficiently far from existing cusps (Polly, 1998; Jernvall, 2000). In mice, a bone morphogenic protein inhibitor called *ectodin* has been shown to act as an inhibitor to cusp formation; it is expressed across developing molars, but not in regions containing primary and secondary enamel knots. Furthermore, *ectodin*-deficient mice have been shown to have enlarged enamel knots (Kasai *et al.* 2005). A study of human upper molars found that cusps which form later in development are more variable than those which form earlier, which would be expected under this model, given that the development of the later cusps depends on that of the earlier cusps (Kondo and Townsend, 2006). Equally, the patterning cascade model predicts that an important aspect controlling cusp number is the size of the tooth. Larger teeth would have larger regions between cusps in which there is no inhibition, allowing for the development of extra cusps. Equally, the size of the other cusps has to be considered, larger cusps would presumably have a larger associated zone of inhibition, preventing the development of cusps over a larger area. In this case, the timing of cusp formation would be particularly important, since this is one of the most important aspects of determining cusp size. A study looking into the prevalence of C6 in chimpanzee lower molars found that not only were molars possessing a C6 on average larger, but that they generally had smaller, more widely spaced dentine horns, supporting the predictions of the patterning cascade model (Skinner and Gunz, 2010).

It has also been shown that there is a relationship between crown size and Carabelli's trait, an accessory feature sometimes occurring on the mesiolingual side of upper molars. Teeth that displayed the trait were generally larger (Kondo and Townsend, 2006; Harris, 2007; Hunter *et al.* 2010). Furthermore, the spacing of early forming cusps is important; Carabelli's trait was more frequent, and generally larger, in teeth with low intercusp distance relative to tooth size. This is indicative of more closely spaced primary enamel knots because this presents a better opportunity for the formation of a secondary enamel knot at the future site of the Carabelli's trait (Hunter *et al.* 2010). Another interesting point to note is that dentine horns appear only to form on EDJ crests. The mechanism behind this is unclear, however it is very rare for accessory cusps to form in the occlusal basin, for example, so it seems that cusp growth is inhibited, or not activated, in these regions (Skinner and Gunz, 2010).

The results of these studies are particularly important for the use of dentition in studies of phylogeny. If cusps are not individually determined, as the patterning cascade model suggests, traits previously assumed to be developmentally homologous among taxa may instead be the result of homoplasy. For example, upper molars in two closely related Eocene adapid primate groups both display a distolingual cusp (Anemone *et al.* 2012). However, it has long been suspected that this cusp is not homologous between the two groups, with the cusp being termed a 'pseudo-hypocone' in one of the groups. In fact, when looking at the EDJ surface, it is clear that there is a different developmental origin for the cusp in the two groups, meaning they are not strictly homologous traits. The authors suggest that this lack of homology is the norm rather than the exception however, and that terms such as 'pseudo-hypocone' are not necessary as long as it is acknowledged that naming does not imply homology (Anemone *et al.* 2012).

The development cascade model presents a much more complex interpretation of cusp development; cusp spacing is determined through a series of epigenetic events such that small changes in the early spacing of cusps may have dramatic downstream effects. The model is particularly important for the present study because it suggests that, when considering discrete

crown features, inferences of homology should be cautiously. Moreover, when novel crown features arise, caution should be applied when inferring function, since apparently novel traits may be the result of small upstream changes in overall tooth size, or cusp size and spacing.

### *Hominin dental evolution*

There are a number of overall patterns which are apparent when looking at the dentition across hominin evolution. For example, when considering overall tooth size, the genus *Homo* can in general be characterized by postcanine reduction (Leakey *et al.* 1964; Brace, 1967; Bermudez de Castro and Nicolas, 1995), whilst *Paranthropus* are most easily identified by small anterior and large postcanine teeth (Robinson, 1956; Tobias, 1967; Ungar and Grine, 1991). There are also notable patterns in enamel thickness; it has long been noted that modern humans have relatively thicker enamel than living African apes (Molnar and Gantt, 1977; Martin, 1985; Schwartz, 2000; Skinner *et al.* 2015), whilst members of *Australopithecus*, and particularly *Paranthropus*, have especially thick enamel (Beynon and Wood, 1986; Grine and Martin, 1988; Skinner *et al.* 2015). Especially thick enamel is maintained in early members of the genus *Homo*, but lost in later *Homo* members, who show thinner enamel than earlier hominins (Smith *et al.* 2012; Skinner *et al.* 2015).

Equally, a number of authors have aimed to characterise the changes in crown morphology for individual hominin teeth (Wood *et al.* 1983; Wood and Uyttershaut, 1987; Bailey, 2002; Bailey and Lynch, 2005; Benazzi *et al.* 2011; Bailey *et al.* 2014; Gomez-Robles *et al.* 2015), identifying distinctive crown features such as talonid extension in *Paranthropus* premolars (Robinson, 1956; Wood and Uyttershaut, 1986) and expression of Carabelli's trait in human upper molars (Scott and Turner, 1997; Ortiz *et al.* 2012). Dental evolution can also be viewed in terms of function complexes; almost all anthropoids display a canine honing complex in which the mandibular canine and mesial mandibular premolar are adapted for a role in sharpening the upper canine during occlusion (Zingesser, 1969; Walker, 1984; Swindler, 2002; Delezene, 2015). However this condition is lost in modern humans, who have smaller, less dimorphic canines, and non-sectorial mandibular premolars

(Greenfield, 1992). It seems these changes began early in hominin evolution, with Mio-Pliocene hominins such as *Ardipithecus ramidus*, *Ardipithecus kadabba*, *Orrorin tugenensis* and *Sahelanthropus* all showing a reduction in canine size (White *et al.* 1994; Haile-Selassie, 2001; Senut *et al.* 2001; Brunet *et al.* 2002; Haile-Selassie, 2004; Suwa *et al.* 2009; White *et al.* 2009), with further changes in crown and root shape continuing in the *Australopithecus* lineage (Ward *et al.* 1999; Ward *et al.* 2001; Manthi *et al.* 2012).

## 2. Premolars

In general, dental analyses use molar teeth since they are the most complex and tend to be the most distinctive. Canines and incisors, by contrast, are assumed to have much simpler, less distinctive, morphologies. Premolars can show a range of morphologies; some mammals have caniform premolars, such as members of *Megalonychidae*, the two-toed sloths, whose anterior premolars resemble canines, and occlude with each other to retain sharp shearing edges (Feldhamer *et al.* 2015). Conversely, a number of species have premolars which are described as molariform or molarised. These terms can be used to describe a range of traits which have the effect of making premolar morphology resemble that of molars; in hominins it usually refers to an expanded talonid and the presence of accessory cusps (Wood and Uytterschaut, 1987). Therians have up to five premolars in each quadrant, although there is a debate over whether four or five represents the primitive condition (Cifelli, 2000; O'Leary *et al.* 2013; Averianov and Archibald, 2015). Catarrhines, including hominins, have two premolars, labelled P3 and P4 for the purpose of homology. This study is focusing on mandibular premolars, and as such, maxillary premolars will not be discussed here.

In a number of primate taxa the mesial premolar (which may be the P<sub>3</sub> or P<sub>2</sub>) is adapted for its role in a honing complex with the canines. This function often causes the mesial premolar to show a markedly distinct morphology from the distal premolars; a state which is described as premolar heteromorphy (Greenfield and Washburn, 1992; Deleuzene, 2015). The honing premolar tends to have a single, particularly tall cusp, along with a broad sloping mesial surface that hones the upper

canine, acting in a scissor motion (Swindler, 2002; Deleuzene, 2015). The complex appears to have been lost early in hominin evolution (Brunet *et al.* 2002); however members of *Ardipithecus*, and early *Australopithecus* retain some associated plesiomorphic features such as an open anterior fovea and a tall protoconid, and these features appear to be lost in a mosaic fashion (Ward *et al.*, 2001; Kimbel and Deleuzene, 2009; Deleuzene and Kimbel, 2011; Manthi, 2012; Deleuzene, 2015).

Hominin lower premolars consistently display a buccal cusp, the protoconid, which is well developed. The lingual cusp, the metaconid, is much more variable. It can be approximately equal in size to the buccal cusp, as in *H. naledi* (Berger *et al.* 2015), or it may be much less well-developed, as often seen in modern humans and Neanderthals. It also varies in its position on the crown; it is often rotated mesially in australopiths compared with later hominins. The lingual side can display multiple cusps, especially on the P<sub>4</sub>. Kraus and Furr (1953) described 17 discrete variables for modern human P<sub>3</sub>s, including the presence of extra lingual cusps, the form of the central occlusal ridge, and the position of the protoconid. For human P<sub>4</sub>s, Ludwig (1957) described seven variable traits including the number and position of lingual cusp(s). In both cases, a selection of these variables are applicable to earlier hominins, and have been used in describing variation in premolar from amongst Plio-Pleistocene hominins (Wood and Uytterschaut, 1987).

#### *For taxonomy*

The simplest use of teeth for testing evolutionary affinities involves simple measurements of the tooth crown such as mesiodistal and buccolingual diameters (Johanson and White, 1979; Stefan and Trinkaus, 1998), as well as measurements of crown area (Wood and Abbott, 1983). 'Crown shape index', a measure which expresses buccolingual diameter as a percentage of mesiodistal diameter, has also been used to attempt to distinguish among taxa on the basis of overall tooth diameters (Wood and Abbott, 1983; Wood and Uytterschaut, 1987). In premolars, some trends can be observed; for example *P. boisei* has relatively narrower P<sub>4</sub>s than *P. robustus*; however, these measures are not reliable in distinguishing among taxa (Wood and Uytterschaut, 1987). Therefore,

more complex methods are required in order to capture more of the shape and size variation present.

A number of more complex methods have been used. For example, cusp area measurements, as well as analysis of fissure patterns and cross sectional shape have been shown to contain some level of taxonomically distinctive information, often varying with tooth position and performing better for identifying certain taxa (Wood and Abbott, 1983; Wood *et al.* 1983; Suwa *et al.* 1994). Moreover, the enamel thickness can be studied in fossil teeth. For example, the 'robust' australopiths are characterised as having particularly thick enamel (Conroy, 1991; Grine and Martin, 1988). There are problems with this method however; enamel thickness is often homoplasious, and it seems that 2D measures of enamel thickness are not effective in discriminating among taxa (Smith *et al.* 2012; Skinner *et al.* 2015). 3D measures of enamel thickness and distribution perform better, but there is still often significant overlap among taxa (Olejniczak *et al.* 2008). Root morphology can also be considered. Mandibular premolar roots are extremely variable in hominins, and there is some indication that this may be useful for taxonomic identification (Wood *et al.* 1988; Moore *et al.* 2016), however it seems unlikely that root morphology carries as much information as the crown morphology, and thus may be limited in its ability to discriminate among taxa in the absence of other information.

Equally, qualitative trait analysis is a useful tool for distinguishing among taxa. This can include, for example, the number of main cusps, the presence of accessory cusps and the presence of further additional features such as extra ridges. Features that are common in one species might be rare in others, and they are often used, as part of a wider suite of characters, to identify a taxon. For example, an accessory cusp, C6, is commonly found in the M<sub>1</sub> of robust australopiths, but rare in *Australopithecus africanus*, whilst a second accessory cusp, C7, shows the opposite trend (Wood and Abbott, 1983). Premolar morphology is important in distinguishing early African *H. erectus* from later forms; both premolars have a more complex crown morphology, whilst the roots of the P<sub>3</sub> often

show an accessory mesiobuccal root, both of which are primitive traits not seen in later Asian *H. erectus* (Wood and Boyle, 2016).

For premolars, Wood and Uytterschaut (1987) analysed a sample of 91 hominid P<sub>3</sub> and P<sub>4</sub>s to investigate their taxonomic distinctiveness. They scored morphological traits based on a selection of the variables identified by Kraus and Furr (1953) and Ludwig (1957), as well as recording absolute and relative areas for the whole crown, the main cusps, and the talonid. They found that, in many of the measured traits, there were clear differences among taxa. In particular, they found that the 'robust' australopiths, especially *Paranthropus boisei*, could be distinguished from other taxa, most notably in terms of the size of the talonid relative to the crown. They furthermore investigated the claim that this talonid expansion was an allometric phenomenon, meaning that the change in shape observed was a direct result of the larger size of the premolars in these taxa, and found no evidence for this (Wood and Uytterschaut, 1987). They found these results variably useful in identifying the taxonomic affiliation of unknown specimens; some taxa, particularly *Paranthropus* species, could be identified on the basis of large talonids, as well as the presence of additional cusps and a more deeply incised median longitudinal fissure, whilst the lingual cusp in *P. boisei* is distinctive in its distal placement. Overall, absolute cusp area and talonid area performed best at discriminating among taxa, and the authors were able to determine the taxonomic affiliation of some isolated specimens (Wood and Uytterschaut, 1987).

Neanderthals can be distinguished from modern humans and other hominins based on a number of P<sub>4</sub> traits. In particular, the combination of a strong transverse crest, a large mesially placed metaconid, and crown asymmetry appear to be distinctive of the species (Bailey, 2002). Crown shape is particularly useful in identifying Neanderthal P<sub>4</sub>s; Bailey and Lynch (2005) used elliptic Fourier analysis to quantitatively assess the shape of the occlusal outline in the P<sub>4</sub>s of a number of late *Homo* species. They found that not only were Neanderthal P<sub>4</sub>s symmetrical, but that this was significantly different to the shape observed in modern humans. Attempts to use the differences in

occlusal outline shape to classify specimens was only partially successful, however. Whilst 98.1% of modern humans were classified correctly, only 65% of Neanderthals were correctly identified (Bailey and Lynch, 2005).

The Arizona State University Dental Anthropology System (ASUDAS) is a standardised method of scoring variation in modern human teeth. The system includes a number of variable traits and scores not just their presence/absence, but also their form or degree of expression, and in a form that is replicable between studies (Turner II *et al.* 1991). This system has also been used in studies of hominin dental variation (Irish, 1997; Irish, 1998; Bailey, 2000; Bailey, 2002; Irish and Guatelli-Steinberg, 2003; Irish *et al.* 2013), which is beneficial because the traits used are well-defined, easily and reliably identifiable, and are often highly heritable (Irish *et al.* 2013). However, the ASUDAS system was designed to capture the variation in modern human populations, and as such, does not capture all of the variation present in fossil hominin teeth (Bailey, 2002; Irish and Guatelli-Steinberg, 2003). This problem can be alleviated to some extent by using characters in addition to those in ASUDAS (Bailey, 2002), although this loses the benefit of standardisation unless the new characters are also widely adopted. For lower premolars, the ASUDAS focuses on lingual cusps, outlining 11 categories with which to score the number and form of any lingual cusps present (Turner II *et al.* 1991). The present study will look at a range of discrete traits in premolars at the EDJ which are found to be variable among fossil hominins and extant non-human apes. Where these EDJ traits overlap with ASUDAS traits, this will be discussed.

### 3. Geometric morphometrics

One method that can be used to capture detailed shape information is geometric morphometrics. This method is based on the comparison, in 2D or 3D, of the coordinates of landmarks placed on homologous structures in different specimens. One advantage of the method is the use of Procrustes superimposition, a least squares technique which rotates, translates and scales specimens in order to minimise the distances between landmarks, removing problems associated

with aligning specimens (Gower, 1975; Rohlf and Slice, 1990; Goodall, 1991; Dryden and Mardia, 1998).

A series of 2D geometric morphometric studies on hominin postcanine dentition revealed a number of morphological trends, especially in Pleistocene *Homo* (Gómez-Robles *et al.* 2007, 2008, 2011, 2012, 2015; Martín-Torres *et al.* 2006). These studies each focused on an individual tooth, or group of teeth, identifying patterns in their occlusal outline and cusp patterning, as well as assessing their use in taxonomic identification. This methodology has clear advantages; it effectively identifies patterns that are typical of particular species, or other groups, for specific teeth. For example, in upper first molars, a derived pattern can be seen in Neanderthals that consists of a rhomboidal occlusal polygon and an external occlusal outline that is skewed by the protrusion of the hypocone. This morphology is distinctive of Neanderthals when compared with modern humans, but is also present to a lesser extent in *H. heidelbergensis* (Gómez-Robles *et al.* 2007). Similarly, in upper premolars, *H. sapiens* can be distinguished from *H. neanderthalensis* through the former's reduction of the lingual cusp and a shortened interfoveal length (Gómez-Robles *et al.* 2011).

Two studies in this series focused on premolars (Gómez-Robles *et al.* 2008; Martín-Torres *et al.* 2006). Geometric morphometric analysis of hominin P<sub>4</sub>s (Martín-Torres *et al.* 2006) supported Bailey and Lynch (2005)'s conclusion that crown asymmetry is a distinctive trait of Neanderthal P<sub>4</sub>s, although this arrangement was also seen in *Australopithecus* taxa, suggesting it is not a derived morphology as suggested (Bailey and Lynch, 2005). However, it does contrast with the more circular occlusal outline seen in *H. sapiens*. The occlusal polygon, the shape formed by joining the four main occlusal landmarks (Morris, 1986), is large in *Australopithecus* and early *Homo*, but is reduced in later taxa. Although it is reduced in size in both *H. sapiens* and Neanderthals, the polygon is more lingually placed in modern humans. It is suggested that in Neanderthals and *H. heidelbergensis*, the reduced occlusal polygon is compensated for by enlargement of the talonid and the addition of lingual accessory cusps, retaining the crown asymmetry. In modern humans, the reduction in overall

size is accompanied by a reduction in talonid size, hence the crown symmetry (Martín-Torres *et al.* 2006).

In P<sub>3</sub>s, a number of patterns were apparent. The sample included early and later members of the genus *Homo*, as well as a number of australopith taxa. The primitive australopith morphology in this sample was characterised by an asymmetrical occlusal outline, largely driven by the presence of a large talonid. The occlusal polygon is also relatively large in the primitive condition. From here, there appears to be two main derived morphologies, one for modern humans, and one for Neanderthals and *H. heidelbergensis*. Modern humans have a symmetrical, circular occlusal outline, driven mostly by the absence, or weak expression, of the talonid. The tip of the protoconid is buccally placed, which shifts the occlusal polygon centrally within the occlusal outline. In Neanderthals and *H. heidelbergensis*, the occlusal outline is also symmetrical (the talonid is small when present), however the protoconid has moved more centrally, creating a smaller, more lingually placed occlusal outline (Gómez-Robles *et al.* 2008). They also found evidence of allometric effects in the observed shape changes. There is an overall pattern of reduction in P<sub>3</sub> size in more modern taxa, which is accompanied by an allometric reduction in crown size and protoconid-metaconid distance.

It is interesting to note that Neanderthal P<sub>4</sub> morphology appears to be primitive (Martín-Torres *et al.* 2006) whilst P<sub>3</sub> morphology is derived (Gómez-Robles *et al.* 2008) which could suggest that the two tooth positions are not controlled through the same mechanisms. This conclusion could lend support to previous suggestions that the third and fourth premolars belong to different evolutionary units (Bermúdez de Castro, 1993). Rather than the more common suggestion of strong associations among the post-canine (molars and premolars) and anterior (incisors and canines) dental units, the boundary would instead be placed between the third and fourth premolars. This is supported by evidence in the Gran Dolina sample that suggests P<sub>3</sub> size co-varies with incisors and canines, whilst the P<sub>4</sub> co-varies with the molars (Bermúdez de Castro, 1993; Bermúdez de Castro *et al.* 1999).

However, whilst 2D geometric morphometrics studies of hominin dentition are useful in characterising taxon specific patterns, they appear to show limited ability to assign taxonomic affiliations. This varies among taxa; mandibular molars, as well as  $M^2$ ,  $M^3$ ,  $P^3$  and  $P^4$  show a moderate to low ability to distinguish Neanderthals among European Pleistocene taxa (Gómez-Robles *et al.* 2011, 2012, 2015). In upper second molars, for example, just 16.7% of Neanderthal specimens were correctly assigned when measured using a cross-validation technique in which the specimen was considered 'unknown' before classification was attempted using a canonical variates analysis (CVA) (Gómez-Robles *et al.* 2012). This varied with tooth position, and overall classification accuracy was often much better (Gómez-Robles *et al.* 2012; Gómez-Robles *et al.* 2015); however this still limits the use of these results for applying taxonomic affiliations.

The limited ability to distinguish among taxa in these studies could be due to the amount of shape variability captured; the studies discussed so far mostly deal with 2D analyses of the occlusal basin. One method of improving on this would be to use analyses that capture 3D shape variation. Logically, this would capture significantly more of the shape variation present in the sample, increasing our ability to distinguish among taxa. In particular, this would be useful in capturing information about cusp height, which is known to differ between fossil hominin taxa, and is one of the distinctive features of the *H. naledi*  $P_3$ s, for example (Berger *et al.* 2015).

This is well demonstrated by a 3D geometric morphometric study of the OES in *Pan* mandibular molars that was able to distinguish between species and tooth position accurately (Singleton *et al.* 2011). Using both  $M_1$ s and  $M_2$ s, *Pan paniscus* molars could be distinguished from those of *Pan troglodytes* with 100% accuracy, whilst, when both species were pooled, specimens could be assigned to molar position with 95% accuracy.

#### 4. Enamel-Dentine Junction

The methods outlined above generally involve assessment of features in the OES. There are issues with such analyses, however, the most prominent of which is tooth wear. Teeth in the hominin fossil

record are often heavily worn, which can degrade the distinctive features of the OES (Burnett *et al.* 2013). Therefore, analyses that do not rely on preservation of the enamel surface can be extremely useful.

Another option is to instead look at the EDJ, the boundary between enamel and the underlying dentine. Since the EDJ lies beneath the enamel cap, it can be well preserved in teeth with moderate wear. The EDJ preserves the form of the basement membrane of the inner enamel epithelium. As the surface on which enamel is deposited, many of the distinctive features of the OES originate from the form of the inner enamel epithelium. However, the contribution of the process of non-uniform enamel deposition should also be considered as it can create disparities between the EDJ and OES. For example, enamel deposition begins at the tip of cusps, meaning that it is more thickly deposited here than at the cervix (Swindler, 2002). Moreover, the majority of hominin species have been shown to have thicker enamel in the occlusal basin of mandibular molar than on the lingual or buccal faces (Skinner *et al.* 2015).

Numerous studies have investigated the degree of correspondence between the OES and the EDJ (Bailey *et al.* 2011; Guy *et al.* 2015; Martínez de Pinillos *et al.* 2014; Nager, 1960; Ortiz *et al.* 2012; Skinner *et al.* 2010). Nager (1960) suggested three categories for dental traits. 'Primary definitive' traits are present at the EDJ and the OES, with only minor differences in morphology. 'Primary temporary' traits are present at the EDJ, but not at the OES, whilst 'Secondary traits' are present at the OES but not the EDJ. Primary definitive traits are most common (Nager, 1960; Skinner *et al.* 2008b; Skinner *et al.* 2010); for example, primary molar cusps are present at both the EDJ and OES, although they are generally sharper and less rounded at the EDJ (Guy *et al.* 2015). However, there are also examples of primary temporary and secondary traits (Corruccini, 1987; Nager, 1960; Skinner *et al.* 2010).

Studies of trigonid crest patterns in modern humans and Neanderthals (Bailey *et al.* 2011), as well as in *H. heidelbergensis* (Martínez de Pinillos *et al.* 2014) showed general correspondence between the

OES and EDJ, and similar results were found when looking at the expression of Carabelli's trait in chimpanzee and modern human maxillary molars (Ortiz *et al.* 2012). Equally, a study of the relative contributions of the EDJ and the enamel cap to crown complexity in primate molars found that, for the most part, the complexity of the OES derives from the EDJ (Skinner *et al.* 2010). However, they also found that the enamel cap can contribute to complexity in teeth with extensive surface crenulations. In two taxa, *Pongo* and *Pan*, these crenulations are present at the EDJ, but exaggerated at the OES, a pattern that was most notable in *Pongo*. In *Chiropotes*, the crenulations are absent at the EDJ, meaning they are driven entirely by enamel deposition (Skinner *et al.* 2010). Looking at the EDJ in *Pan* mandibular molars, Skinner *et al.* (2009a) found that M<sub>2</sub>s had smaller more centrally located mesial dentine horns than M<sub>1</sub>s, however this pattern was not replicated when Singleton *et al.* (2011) completed a similar study of the OES. This difference could be due to enamel deposition or specific patterns of wear at the OES.

Overall, there does seem to be a general pattern of concordance between the OES and EDJ (Morita, 2016; Skinner *et al.* 2008b; Skinner *et al.* 2010), especially in the case of major features such as cusps. However, there are a number of examples of non-concordance (Kono, 2004; Kraus, 1952; Olejniczak *et al.* 2004), and enamel deposition can also play a role (Morita *et al.* 2014). It therefore seems that the morphology of the EDJ and OES are useful in different scenarios. The OES is often more useful in studies of dietary reconstruction since this provides the occlusal surface used in processing food items. This was demonstrated in a geometric morphometric study of occlusal morphology in extinct Platyrrhine primates that reconstructed dietary adaptations of various groups (Cooke, 2011). In this case, groups of specimens clustered together in shape space due to similar dietary adaptations that may often be due to homoplasy rather than close phylogenetic relationships. This effect of homoplasious clustering in shape space is likely to be less notable at the EDJ since this surface is not the surface directly used for processing food; however, this is something that should be considered nonetheless, given the generally close concordance between the two structures.

Alternatively, the EDJ is more useful in studies of tooth development. Given that this is where the majority of distinctive dental traits are initially determined; this provides a clearer indication of the underlying developmental processes. This is also true of studies of phylogeny. The EDJ is useful because it provides us with a clearer indication of homology; it is easier to misinterpret homoplasious traits as homologous at the OES because the features are less sharp, and therefore less distinctive. The morphology of the EDJ has been shown to effectively distinguish between extant and extinct primate taxa (Crevecoeur *et al.* 2013; Skinner *et al.* 2008a; Skinner *et al.* 2009), and was recently used, among other measures, to identify two isolated deciduous Neanderthal teeth (Arnaud *et al.* 2016). Equally, a geometric morphometric study of hominin M<sup>2</sup>s found that, whilst there was a high level of covariation between the EDJ and the OES, the EDJ provided better separation of taxonomic groups (Fornai *et al.* 2015).

A 3D geometric morphometric analysis of the EDJ surface of lower molars was carried out for species and subspecies of *Pan* (Skinner *et al.* 2009a). Cross-validation analysis gave the correct species identification in 100% of instances, whilst for subspecies 87–100% of molars were correctly identified. Furthermore, these methods proved to be promising when looking at lower molars in *A. africanus* and *P. robustus* (Skinner *et al.* 2008a). Three landmark sets were used, one containing landmarks for 8 points on the EDJ surface, including the tips of each major dentine horn (called the 'MAIN' set), one set of landmarks along the ridges that connect the main dentine horns (called the 'RIDGE' set) and another running around the cementum-enamel junction (CEJ) of the tooth (called the 'CERVIX' set). Classification was better when the MAIN and RIDGE landmark sets were included, either alone or as well as the CERVIX set, and was in general better when considering size as well as shape (form space). Classification is 74-91% accurate when using both sets in form space, and 79–93% accurate when using only the RIDGE set in form space (Skinner *et al.* 2008a).

Geometric morphometric study of the EDJ surface in 3D was recently used in assessing the taxonomic affinity a partial mandible (BH-1) found at Balanica in Serbia (Roksandic *et al.* 2011;

Skinner *et al.* 2016), dated to a minimum age of 397-525 Ka (Rink *et al.* 2013). The EDJ morphology supported previous assertions that the specimen is not Neanderthal, nor does it show the degree of Neanderthal features seen in Sima de los Huesos specimens, and would be better assigned to *H. heidelbergensis* sensu lato (Skinner *et al.* 2016). A similar study used 3D geometric morphometrics of the EDJ surface to assess the taxonomic affinities of an isolated upper molar (#Ish25) from the site of Ishango, Democratic Republic of Congo (Crevecoeur *et al.* 2013). Although a species definition was not possible, it was clear that #Ish25 clustered with australopiths and early *Homo*, rather than later *Homo* species. These results suggest that 3D geometric morphometrics of EDJ morphology is extremely useful in assigning taxonomic designations to hominin molars. Previous studies have identified taxon-specific morphologies in mandibular premolars, but have had only limited success in assigning isolated specimens to species (Bailey and Lynch, 2005; Gómez-Robles *et al.* 2008; Martín-Torres *et al.* 2006). Therefore, this study will utilise the 3D geometric morphometric methodology in order to further investigate the taxonomic distinctiveness of mandibular premolars in hominins.

Only a limited amount of work has been done in this area. One small study used geometric morphometric analysis to investigate premolar EDJ morphology in hominins (Pan *et al.* 2016). They found clear separation of australopiths and *Homo*, and were able to distinguish *A. africanus* from *P. robustus*. They found that, for P<sub>3</sub>s, modern humans and an early *Homo* specimen were characterised by an oval shaped EDJ outline and an elevated protoconid, whilst *P. robustus* specimens showed a more trapezoid outline and more centrally placed dentine horns. However, more detailed analysis of morphological patterns was hindered by the restricted sample; no Neanderthal specimens, and only two early *Homo* premolars (one P<sub>3</sub> and one P<sub>4</sub>), were included.

This study will utilise a larger sample and cover a wider selection of hominoids. Furthermore, the Pan *et al.* (2016) study only used landmarks on the occlusal surface of the tooth, whereas in this study, landmarks will also be placed on the CEJ. This will allow for more of the shape variation

present in the sample to be captured, and possibly more importantly, will allow the inclusion of extremely worn specimens, in which the EDJ crown is not preserved.

# Manuscript

## 1. Introduction

Teeth are an important component of the fossil record; as highly mineralised and compact tissues, they are well-preserved, and therefore common in fossil deposits. They also contain large quantities of information regarding taxonomy, diet, and environment, amongst other factors (Walker *et al.* 1978; Sponheimer and Lee-Thorp, 1999; Richards *et al.* 2001; Lee-Thorp *et al.* 2003; Grine *et al.* 2012). Unlike bones, the external morphology of the tooth crown is not remodelled throughout an organism's lifetime; once fully developed they are only modified by external factors such as breakage or wear. This means that the morphology of unworn dental specimens is highly genetically controlled, and this, combined with a high level of character richness, means that teeth are particularly useful in reconstructing taxonomic affinities and developing phylogenetic hypotheses (Wood and Abbott, 1983, Wood *et al.* 1983; Suwa *et al.* 1996; Irish and Guatelli-Steinberg, 2003; Skinner *et al.* 2008a).

In general, studies of hominin dentition focus on molars since they are the most complex, whilst premolars are considered transitional teeth between the simple, single cusped canines, and the more complex, multi-cusped molars (Butler, 1939; Dahlberg, 1945; Townsend *et al.* 2009). Premolars are extremely variable however, and even within hominoids can show a variety of morphologies. This is especially true of the mandibular third premolar, which performs a different function in modern humans than in non-human apes. In non-human apes, the P<sub>3</sub> is involved in the canine honing complex whereby the upper canine occludes with the broad mesiobuccal surface of the P<sub>3</sub> in order to maintain the canine's sharp shearing crest (Walker 1984, Swindler, 2002; Delezene, 2015). The honing canine appears to have been lost early in hominin evolution (Brunet *et al.* 2002; Haile-Selassie, 2004; Suwa *et al.* 2009; White *et al.* 2009), allowing the tooth to be fully adapted for its role in mastication. In later hominins, the P<sub>3</sub> may be molarised (Robinson, 1956; Wood and Uytterschaut, 1978; Leonard and Hegmon, 1987), which is usually defined as the expansion of the talonid, and the possible addition of extra cusps (Wood and Uytterschaut, 1978). This condition is most extreme in

members of the genus *Paranthropus*, where it is accompanied by a range of unique dental adaptations (Robinson, 1956; Tobias, 1967; Grine and Martin, 1988).

A number of studies have investigated the taxonomic potential of the P<sub>3</sub>, with promising results. Wood and Uytterschaut (1978) scored hominid premolars on a number of traits (mostly based on those identified by Kraus & Furr (1953) and Ludwig (1957) in their studies of modern human premolars) such as cusp number and metaconid position, as well as absolute and relative crown proportions. They found a number of distinguishing features in hominin premolars, particularly amongst the robust australopiths. Suwa (1990) identified a number of premolar traits which could be used to identify P<sub>3</sub>s of *Australopithecus africanus* and early *Homo*, as well as a number of traits unique to early *Homo*. Later, Gómez-Robles *et al.* (2008) used 2D geometric morphometric analysis to investigate patterns in hominin P<sub>3</sub> morphology, finding clear differences between early hominins (*Australopithecus* and early *Homo*) and later *Homo* specimens. The earlier species display an asymmetrical occlusal outline and an expanded talonid, whilst the later taxa tend towards a more symmetrical occlusal outline and a reduced talonid. They also found differences between late *Homo* species such as the placement of the protoconid (Gómez-Robles *et al.* 2008). A number of studies have used 3D geometric morphometrics for studying hominoid dentition (Skinner *et al.* 2008a; Skinner *et al.* 2009a; Singleton *et al.* 2011; Pan *et al.* 2017; Martin *et al.* 2017), finding that this method can successfully distinguish hominoid species, and even subspecies (Skinner *et al.* 2009a).

A number of these studies look at the enamel-dentine junction (EDJ) rather than the outer-enamel surface (OES). The EDJ preserves the form of the inner enamel epithelium, the layer on which the enamel is deposited. The majority of the distinctive features of the OES originate at the EDJ, and the two surfaces are thought to have a high level of correspondence (Nager, 1960; Skinner *et al.* 2010; Ortiz *et al.* 2012; Guy *et al.* 2015). Studying the EDJ rather than the OES has a number of advantages. Firstly, the EDJ is often preserved in specimens showing moderate levels of wear, allowing for specimens which would otherwise be undiagnostic to be included in the analyses. Secondly, features

at the EDJ are typically sharper and more distinctive. Hominin species may have relatively thick enamel (Beynon and Wood, 1986; Macho and Thackeray, 1992; Smith *et al.* 2012; Skinner *et al.* 2015), meaning some small crown features may be difficult to distinguish. The sharper appearance of the EDJ allows for reliable placement of landmarks in geometric morphometric analyses (Skinner, 2008; Skinner *et al.* 2009a; Martin *et al.* 2017), as well as facilitating the precise assessment of a number of small discrete traits, such as accessory cusps and crests. Analysis of these traits at the EDJ may allow for a better understanding of the developmental processes which went into forming these features (see Skinner and Gunz, 2010; Anemone *et al.* 2012).

This study will evaluate the mandibular third premolar EDJ morphology in a number of extant and fossil hominoid taxa, with three main aims:

1. Evaluate the taxonomic potential of the P<sub>3</sub> EDJ using 3D geometric morphometrics, and evaluate the taxonomic affiliation of any specimens for which this is uncertain
2. Summarise the major transitions in P<sub>3</sub> morphology across hominin evolution, using extant non-hominin apes as an outgroup
3. Discuss the presence of a number of discrete traits at the EDJ and OES, and their potential importance both taxonomically and developmentally

## 2. Materials and methods

### 2.1. Study sample

The study sample is summarised in Table 1 (a full list of specimens can be found in Supplementary Table 1), and consists of 123 mandibular third premolars, mostly assigned to well established hominoid taxa, but also including nine specimens designated as *Homo* sp., and four specimens considered here to be of unknown taxonomic affiliation. These include KNM-WT 8556, a fragmentary mandible which has been previously assigned to both *Australopithecus afarensis* (Brown *et al.* 2001) and *Kenyanthropus platyops* (Leakey *et al.* 2001), KNM-ER 5431E, which has been suggested to represent early *Homo*, but was cautiously assigned as Hominidae gen. et sp.

**Table 1**

Study sample summary. The extant and fossil taxa included in the sample are listed, along with their locality, and the sample size for each of the four different geometric morphometric analyses. Full specimen list can be found in Supplementary Table 1

Taxa	Locality	Full	CEJ+ Med	CEJ only	EDJ only
Hylobates	South East Asia	4	4	4	4
Pongo	Borneo; Sumatra	6	6	6	6
Gorilla	Cameroon; Congo	5	5	5	5
Pan	Côte d'Ivoire	5	5	5	5
A. anamensis	Kanapoi, Kenya	3	3	3	3
A. afarensis	Hadar + Omo, Ethiopia	5	7	10	5
A. africanus	Sterkfontein + Taung, South Africa	5	8	9	9
P. robustus	Drimolen, South Africa; Swartkrans, South Africa	5	6	8	9
P. boisei	Koobi Fora + West Turkana, Kenya; Omo, Ethiopia	2	2	3	4
Homo sp.	Baringo, Kenya; Koobi Fora, Kenya; Swartkrans, South Africa	3	3	6	3
H. rudolfensis	Uraha, Malawi	0	0	1	0
H. ergaster	Koobi Fora, Kenya; West Turkana, Kenya	0	1	3	0
H. erectus	Sangiran, Indonesia	1	1	2	1
H. naledi	Rising Star, South Africa	4	5	8	4
H. heidelbergensis	Mauer, Germany	0	1	1	0
H. neanderthalensis	Combe Grenal, France; Krapina, Croatia; Scladina, Belgium	10	15	15	10
<i>Fossil H. sapiens</i>	Qafzeh, Israel; Jebel Irhoud, Morocco	2	3	3	2
<i>Recent H. sapiens*</i>	Anatomical collection, various localities	8	12	12	8
<i>Unknown**</i>	West Turkana + Koobi Fora, Kenya; Makapansgat + Swartkrans + Sterkfontein, South Africa	5	5	5	5

\* Further details on the modern human sample can be found in Supplementary Table 2

\*\*Unknown specimens are KNM-WT 8556, KNM-ER 5431E, Cave of Hearths mandible, SK 96 and STW 151

indet. by Wood (1991), and a Late-Pleistocene mandibular fragment from the Cave of Hearths, Makapansgat.

STW 151 represents a number of cranial and dental fragments of a juvenile individual from Sterkfontein which has been suggested to share a number of features with *A. africanus*, but which may be more derived towards the early *Homo* condition (Moggi-Cecci *et al.* 1998). The specimen has therefore been separated from the main *A. africanus* sample in this study, and the P<sub>3</sub> EDJ morphology will be discussed.

The final specimen considered unknown here is SK 96, a mandibular fragment, lower canine and P<sub>3</sub> from Swartkrans member 1 which has traditionally been assigned to *Paranthropus robustus* (Robinson, 1956). In the initial description of the specimen, Robinson (1956) noted that the premolar differed from the typical *P. robustus* form, but suggested that this was due to incomplete crown development. In initial analyses, it became clear that the P<sub>3</sub> was in fact crown-complete, and therefore this could not account for the unusual morphology.

Specimens from Qafzeh and Jebel Irhoud are included here, but will be separated from the recent *Homo sapiens* sample. From here, when discussing modern humans or *H. sapiens*, this excludes Qafzeh and Jebel Irhoud, unless otherwise stated. The recent *H. sapiens* sample is derived from the University of Leipzig Anatomical Collection (ULAC). Relatively little information is available on this sample, but the information which is available is presented in Supplementary Table 2.

## 2.2 Microtomography

Microtomographic scans of the premolar sample were obtained using either a SkyScan 1173 at 100-130 kv and 90-130 microA, a BIR ACTIS 225/300 scanner at 130 kV and 100-120 microA, or a Dicono d3 at 100-140kv and 100-140 microA and reconstructed as 16-bit tiff stacks (isometric voxel resolutions ranging from 13-45 microns).

### 2.3 Image filtering

The image stacks for each premolar were filtered using a three-dimensional median filter, followed by a mean of least variance filter, both with a kernel size of either one or three, implemented using MIA open source software (Wollny *et al.* 2013). This process facilitates the segmentation of enamel from dentine by improving the homogeneity of the grey-scale values for the enamel and dentine, and by sharpening the boundaries at the interface between tissue types (Schulze and Pearce, 1994). The kernel size was decided by manually assessing the level of contrast between enamel and dentine; a kernel size of three was used on those scans with low contrast. The effect of filtering on the morphology of the EDJ has previously been shown to be minimal (Skinner, 2008).

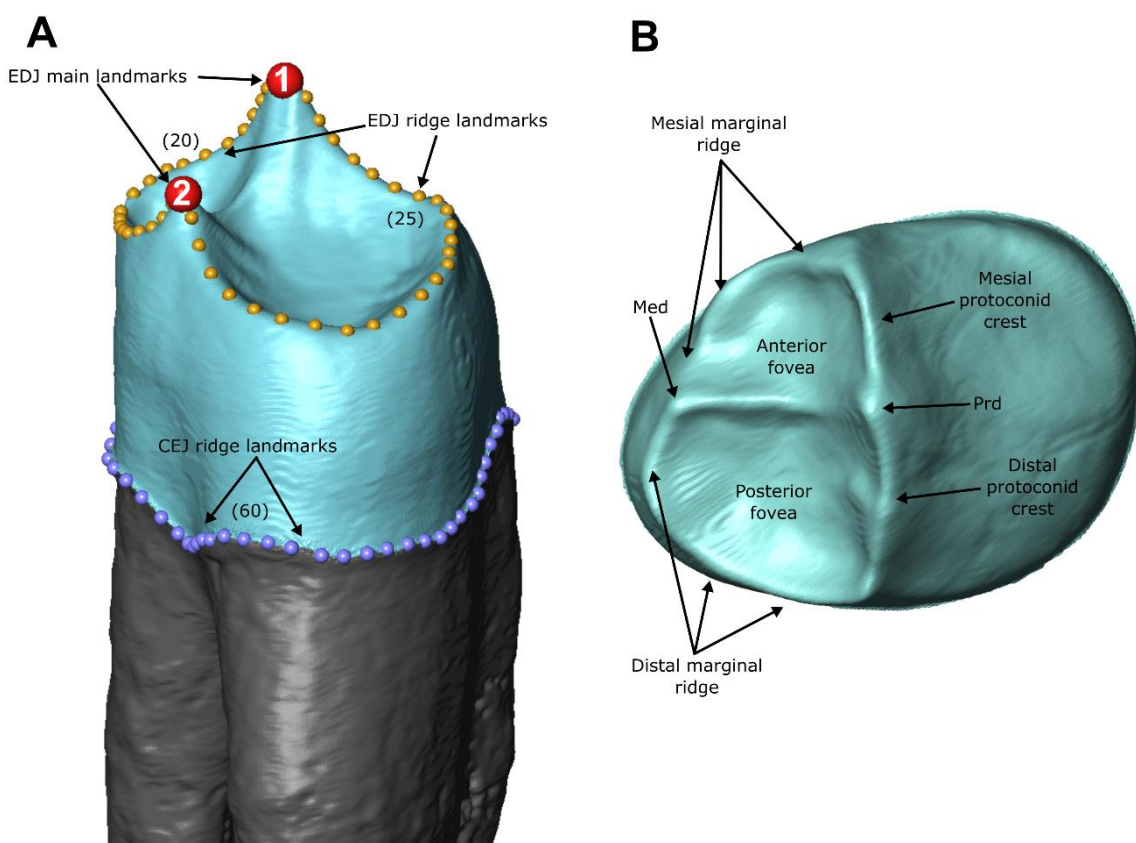


**Figure 1.** Landmarking protocol and P<sub>3</sub> terminology guide. Left: Example of the landmarking protocol for all three landmark sets. Numbers in brackets indicate the number of landmarks placed in each set, with the EDJ ridge set split into two sections. 1 – Protoconid landmark, 2 – Metaconid (or equivalent point – see text) landmark. Right: Neanderthal right P<sub>3</sub> illustrating the major morphological features present in hominoid P<sub>3</sub>s. Prd – Protoconid, Med – Metaconid.

## 2.4 Tissue segmentation

The filtered image stacks were processed using Avizo 6.3 ([www.vsg3D.com](http://www.vsg3D.com)) in order to produce surface models of the EDJ. Enamel and dentine were segmented semi-automatically using grey-scale values in the 3D voxel value histogram. In some cases, less distinct tissue classes made segmentation through this method not possible, and instead a seed growing algorithm was employed to segment enamel from dentine, before being checked manually. A triangle-based surface model of the EDJ was produced using in .ply format, using the unconstrained smoothing parameter in Avizo.

In some specimens, dental wear had removed the tips of dentine horns. In the case of specimens with minimal wear, the missing portion of the dentine horn was reconstructed following the procedure of Skinner (2008); Skinner *et al.* (2008a) and Skinner *et al.* (2009a). This procedure is similar to correcting for interstitial wear, and involves inferring the structure of the dentine horn tip from the preserved anatomy of the dentine horn. An example can be seen in AL 266-1 (shown in Figure 11 - the reconstructed portion of the protoconid is visualised in blue). This procedure was restricted to specimens for which less than a quarter of the dentine horn was missing, which was assessed through viewing the EDJ in occlusal view where the proportion of missing dentine horn can be easily assessed. Specimens considered for reconstruction were restricted to those showing a wear level less than wear level 3 according to Molnar (1971). This procedure was also restricted to cases in which multiple observers were confident of the original position of the dentine horn using their experience, anatomical knowledge, and the preserved EDJ morphology. Dentine horns reconstruction was performed using the 'fill holes' function in Geomagic Studio 2014 ([www.geomagic.com](http://www.geomagic.com)) and reconstructed specimens are marked in Supplementary Table 1. One specimen (SK 96) showed a large crack which had caused a portion of the crown to move relative to the remainder of the crown. In this case, the EDJ was realigned using Geomagic Studio 2014. The crack ran diagonally across the mesial side of the crown, running directly through the protoconid. Four points on the crown were used as reference points for alignment; two points on the CEJ (one

on the buccolingual side of the crown and one on the mesiodistal side of the crown), one point on the mesial marginal ridge, and a final point at the tip of the protoconid.

## 2.5 *Landmark collection*

3D landmarks were collected in Avizo 6.3 in three distinct sets; 'EDJ main', 'EDJ ridge' and 'CEJ ridge'. EDJ main and EDJ ridge landmarks were placed on the EDJ surface model produced, often assisted by the unfiltered image stack. EDJ main consists of two landmarks, the first placed on the tip of the protoconid, and the second placed on the metaconid where present. For specimens where a metaconid was not present, the landmark was placed on the equivalent position, where transverse crest meets the marginal ridge (Fig. 1). In non-hominin apes, the transverse crest often does not reach the marginal ridge, so for these specimens, the second EDJ main landmark was placed on the lingual margin of the crown, mesiodistally level with the transverse crest. EDJ ridge landmarks were placed around the marginal and protoconid ridges encircling the basin of the tooth, beginning at the protoconid landmark, and running mesially, eventually returning to the protoconid (Fig. 1). Some specimens display an interrupted marginal ridge, and in these cases landmarks were placed along the equivalent points along the flattened EDJ surface.

CEJ ridge landmarks were placed on an isosurface rendering of the surface morphology of the tooth, sometimes assisted by the unfiltered image stack when the CEJ was otherwise unreachable due to matrix build-up or the presence of an adjacent tooth. The first landmark was placed on the CEJ at the midpoint of the buccal face of the tooth, then landmarks were placed mesially around the CEJ. In cases where part of the CEJ was missing, the location of these landmarks was estimated if the observer was confident of the CEJ's original position. For some specimens, it was not possible to place all landmarks, either due to dental wear beyond the level that could be reconstructed (as described above), poor tissue contrast prohibiting the placement of EDJ landmarks, or in some cases, the tooth may not be fully crown complete, meaning the CEJ has yet to form. In these instances, analyses were completed on subsets of landmarks, depending on the areas of morphology

preserved. Ultimately, analyses were conducted in four groups, each utilising different combinations of landmarks, to allow analysis of as many specimens as possible, and to assess the utility of these landmark sets for taxonomic

**Table 2**

*Geometric morphometric analyses. Summary of the four analyses and the landmarks included*

Analysis	Description
EDJ+CEJ	Uses all landmarks, from both the EDJ and CEJ
CEJ+Med	Uses the landmarks placed on the CEJ, as well as a single fixed landmark on the metaconid (or equivalent point)
CEJ only	Uses only the landmarks placed on the CEJ
EDJ only	Uses only the landmarks placed on the EDJ

distinctions. The analyses are summarised in Table 2, and the specimens included in each of the analyses are summarised in Supplementary Table 1.

## 2.6 Derivation of homologous landmark sets

Geometrically homologous semilandmarks were derived using a software routine written by Philipp Gunz (Gunz et al. 2005; Gunz and Mitteroecker, 2013) implemented in Mathematica 8.0 ([www.wolfram.com](http://www.wolfram.com)). A smooth curve was fit through the landmarks of the EDJ ridge and CEJ ridge

landmark sets using a cubic-spline function. For the EDJ ridge set, the EDJ main landmarks were projected on to the curve, dividing the curve into mesial and distal portions. A fixed number of equally spaced landmarks were placed along the curve; the EDJ has 20 landmarks in the mesial portion and 25 in the distal, whilst the CEJ has 60 landmarks. Landmarks in the EDJ main set were fixed whilst those in the EDJ ridge and CEJ ridge were treated as semilandmarks. These landmarks were allowed to slide along their curves so as to reduce the bending energy of the thin-plate spline interpolation function calculated between each specimen and the Procrustes average for the sample (Gunz et al. 2005; Gunz and Mitteroecker, 2013). The sliding operation was performed twice, after which the landmarks were considered to be geometrically homologous. The landmarks were then converted into shape coordinates using generalized least squares Procrustes superimposition which

removes scale, location, and orientation information from the coordinates (Gower, 1975; Rohlf and Slice, 1990; Goodall, 1991; Dryden and Mardia, 1998).

### 2.7 Analysis of EDJ and CEJ shape and size

A principal components analysis (PCA) was carried out using the Procrustes coordinates of each specimen in both shape and form space, the latter of which includes, as an additional variable, the natural logarithm of the centroid size of the specimen. This process was completed for all four analyses. The natural logarithm of centroid size for the EDJ+CEJ analysis was also analysed separately using a Kruskal-Wallis one-way analysis of variance test, followed by a post-hoc pairwise Wilcoxon rank sum test, with Bonferroni correction to correct for multiple comparisons. This method was used to test for differences in the centroid sizes between pairwise combinations of taxon groups. Both the Kruskal-Wallis test and Wilcoxon rank sum test were performed in R ([www.r-project.org](http://www.r-project.org)), using the functions 'kruskal.test' and 'pairwise.wilcox.test' in the 'stats' package.

For the purpose of assessing classification accuracy, a canonical-variates analysis (CVA) was used. A CVA creates a linear combination of variables such that the variation between pre-determined groups is maximised, relative to the variation within the groups. In this case, the groups are the taxa to which the specimens have been assigned. The CVA was carried out separately for each dataset (EDJ+CEJ, CEJ+Med, CEJ only and EDJ only) including all specimens which have been reliably assigned to a taxa which contains four or more specimens, which excludes *P.boisei*, *A. anamensis* and early *Homo* taxa from all analyses. The specimens were assigned to groups using a leave-one-out cross validation approach in which each specimen is assumed to be unknown before being assigned to a group using the remaining dataset. Cross-validation reduces the likelihood of 'over fitting' the model to the data (Kovarovic et al. 2011). Ordinarily, a CVA requires that the number of variables be less than the number of specimens, however this is rarely achievable in GM analysis of fossil material (Mitteroecker and Bookstein, 2011). Therefore, the number of variables has been reduced by performing the CVA on limited numbers of principal components (PCs). This analysis was completed

using sets of PCs up to PC 15, each starting at PC 1 and consisting of at least 3 PCs (e.g. PCs 1:3, 1:4, 1:5 etc.). A specimen was considered to be correctly classified if it was placed into the correct group in more than 80% of these sets, following the protocol of Skinner *et al.* (2008a), Skinner *et al.* (2009a) and Martin *et al.* (2017). The PCA and CVA, as well as the classification accuracy analysis, were conducted in R ([www.r-project.org](http://www.r-project.org)).

### 2.8 *Visualisation of EDJ shape variation*

Three-dimensional PCA plots of the first three PCs were generated for the purpose of visualising the variation in P<sub>3</sub> EDJ shape across the study sample. For this analysis, specimens were split into three groups; non-hominin apes, Plio-Pleistocene hominins, and late-Pleistocene hominins. Wire-frame models were also used in order to visualise the mean landmark configuration for each well-represented taxonomic group included in the full analysis. 3D PCA plots and wireframe models were generated in Mathematica 8.0 using code written by Philipp Gunz.

### 2.9 *Classification of additional specimens*

A number of specimens were included for which the taxonomic affiliation is unknown or uncertain. Some have been assigned to *Homo* sp., however given that the sample used here does not include Olduvai *Homo habilis* (and the sample of other early *Homo* specimens is quite limited), This study will not attempt to assess their taxonomic affiliations. Specimens which have been suggested to belong to one of the included taxa will be discussed.

### 2.10 *Discrete traits*

Examination of the EDJ surfaces of hominoid P<sub>3</sub>s revealed a number of interesting and potentially important discrete traits. Many of these features are small EDJ features which may not be recognised at the OES (particularly in worn specimens). Each of these traits were analysed on a subset of the sample depending on the preservation of the region of interest so as to include as many specimens as possible. However, specimens were only included in the trait type could be fully assessed.

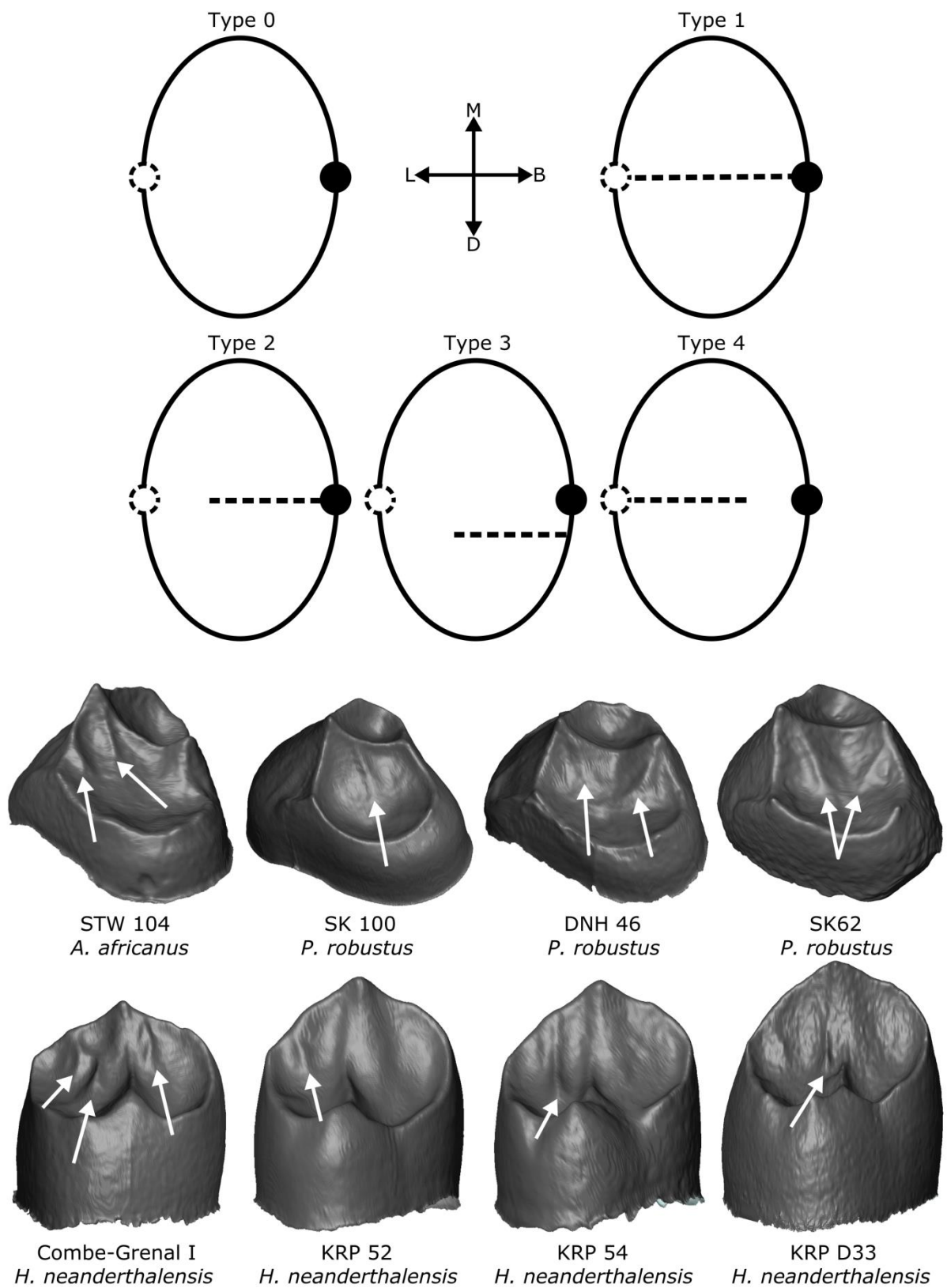


**Figure 2.** Transverse crest variation. Top: Diagram illustrating the 6 main transverse crest forms seen in hominoid  $P_3$ s. Represents the tooth in occlusal view. Filled black circle indicates the protoconid, dashed circle indicates the metaconid (or equivalent point on the crown, when a metaconid is not present).

Bottom: Examples of accessory crests, marked with white arrows. The images of SK 100, DNH46 and Combe-Grenal I have been flipped such that all specimens appear left sided

**Transverse crest.** A number of authors have considered aspects of premolar transverse crest form at the OES (Suwa, 1990; Leonard and Hegmon, 1987; Delezene and Kimbel, 2011; Bailey, 2002). Some focussed on the prominence of the transverse crest (Suwa, 1990; Bailey, 2002), while others instead preferred to score the orientation of the transverse crest (Delezene and Kimbel, 2011). Leonard and Hegmon (1987) previously scored a number of *A. afarensis* P<sub>3</sub>s 'Transverse ridge development', using a 5 point typology which attempted to score both the form and prominence of the P<sub>3</sub> transverse crest. When studying the transverse crest at the EDJ, it is apparent that the relationship between this crest and other crown structures, particularly the main premolar cusps, is highly variable. Therefore the typology used here focusses on the position of the transverse crest relative to other crown structures, and is based on the range of variation observed within the present sample. Unlike previous studies, the scoring system does not aim to characterise how strongly developed the transverse crest is (beyond presence/absence), however this will be discussed separately.

The scoring procedure is as follows (Fig. 2):

0. Transverse crest is absent, or only small incipient crests are present
1. Transverse crest is present, and connects the protoconid to the metaconid (or equivalent point on the marginal ridge, when a clear metaconid is not present)
2. Transverse crest connects to the protoconid, but is either deflected distally, or flattens before reaching the marginal ridge on the lingual side of the tooth
3. Transverse crest connects to the protoconid crest distal to the dentine horn tip and, as in type two, is either deflected distally or flattens before reaching the marginal ridge on the lingual side of the tooth
4. Transverse crest connects to the lingual margin of the tooth, but is either deflected or flattened before reaching the protoconid.

It should be noted that in some specimens, particularly those with tall well-developed dentine horns, the transverse crest may appear to flatten before it reaches the dentine horn tip or adjacent crest. Here, the transverse crest was considered to connect to the dentine horn provided that the crest reaches at least 2/3 of the height of the dentine horn. Therefore, type 4 is reserved for specimens in which the transverse crest is flattened for more than 2/3 of the height of the protoconid. The distinction between types 2 and 3, in the case of a partly flattened transverse crest, was made by judging whether the remaining portion of the crest is angled such that, were it to be present for the full length of the crown, it would make contact with the tip of the protoconid or with the adjacent crests.

Partially reconstructed specimens have been included in this analysis where the form of the transverse crest is preserved. The expression of any additional crests present in the occlusal basin of the tooth will also be discussed.

**Marginal ridge form.** One difference between the P<sub>3</sub> of hominin and non-hominin apes is that hominins typically have more strongly developed distal and mesial marginal ridges (Suwa, 1990). However, there is variation among hominins in terms of the prominence and form of the marginal ridge, which has been considered at the OES by a number of authors (Suwa, 1990; Ward *et al.* 2001; Delezene and Kimbel, 2011).

Further, Sakai (1967) noted the presence of a 'trigonid notch' at the EDJ of modern human P<sub>3</sub>s, which was defined as a clear indentation in the mesial marginal ridge. This is a feature which is also seen in fossil hominins, as well as an equivalent feature on the distal marginal ridge. However, we also find that a number of specimens show overall poorly developed, or absent, marginal ridges. Since the difference between a 'notched' marginal ridge and one that is poorly developed may be very slight, the grading system used here instead scores marginal ridge continuity or discontinuity, where a discontinuous marginal ridge is one which is entirely flattened to the level of the occlusal

basin for some portion of its length, therefore including absent, poorly developed and notched marginal ridges. Specimens were therefore scored according to the following system (Fig. 3):

**C** – Continuous marginal ridges – the distal marginal ridge runs from the distal protoconid crest to the metaconid (or equivalent point on the crown), and the mesial marginal ridge runs from this point, to the mesial protoconid crest.

**M** – The mesial marginal ridge is discontinuous

**D** – The distal marginal ridge discontinuous

**MD** – The mesial and distal marginal ridges are both discontinuous

This analysis was only completed on hominin specimens, excluding the extant nonhuman-apes, since the mesial and distal marginal ridges are generally poorly developed in extant apes.

Marginal ridges may appear to flatten at the base of the metaconid dentine horn, an example of which can be seen in Figure 1B, where the mesial marginal ridge appears flattened next to the metaconid. However this

was only counted as discontinuous if the flattened section clearly continued beyond the base of the metaconid.

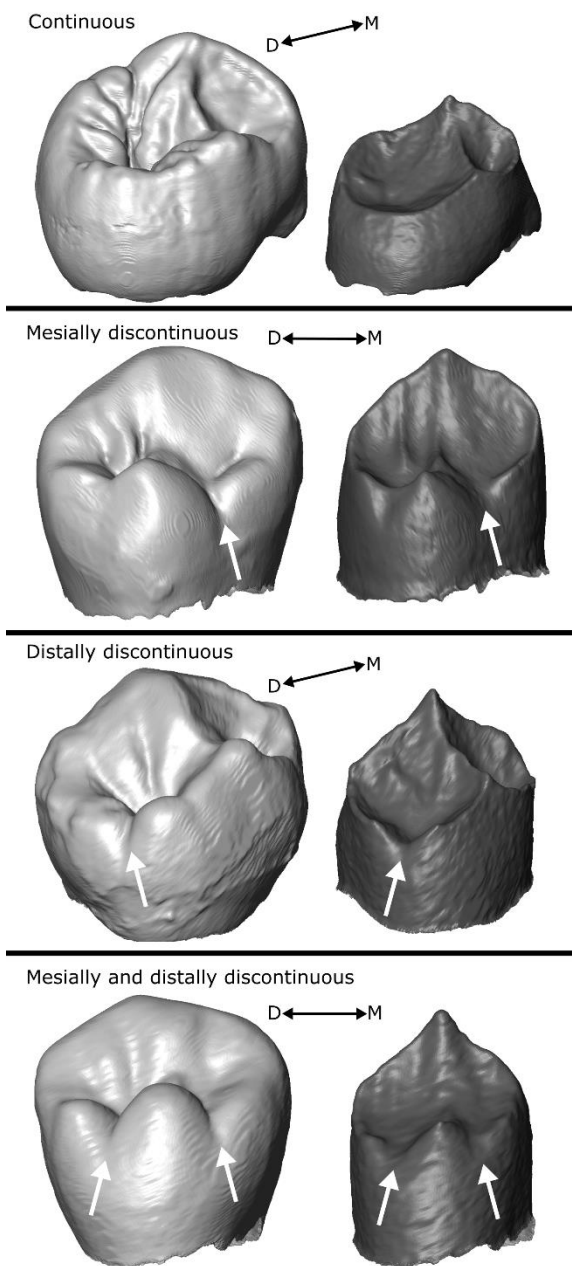


**Figure 3.** Marginal ridge form. Four specimens in lingual view illustrating the forms of marginal ridge interruption seen in hominin  $P_3$ s. Specimens used are (top to bottom) DNH 107, KRP 54, ULAC 801 and ULAC 806. All specimens are left sided.

**Buccal grooves.**

Kraus and Furr (1953), in their description of the morphology of the modern human P<sub>3</sub>, describe the occasional presence of “a ridge and accompanying shallow vertical groove” on both the mesial and distal margins of the buccal face, but specify that these features are more often absent than present. Typically termed ‘buccal grooves’, this feature appears to be more common in some fossil hominin groups (Robinson, 1956; Wood and Uytterschaut, 1987; Suwa, 1990). Suwa (1990) scored the degree of expression of buccal grooves at the OES for a number of hominin P<sub>3</sub>s; distal buccal grooves were scored

as “strong”, “moderate” or “trace/lacking”, whilst a fourth category of “ill-defined but with a significant triangular depression” was included for mesial buccal grooves. Similarly, Sakai (1967)

scored the presence of ‘buccal ridges’ at the EDJ in a sample of modern human P<sub>3</sub>s using three categories; ‘Pronounced’, ‘Weak’ or ‘No ridge’.

Here specimens were scored using a similar system to these two studies, although the fourth category used by Suwa (1990) for mesial buccal grooves was not included. Therefore, specimens were scored separately for mesial and distal EDJ buccal grooves, but using the same scoring procedure (Fig. 4):

***Absent/Trace (0):*** The EDJ buccal face shows no distinct grooves. The crown corner may show a slight vertical ridge, but it is not associated with a clear concavity on the buccal surface

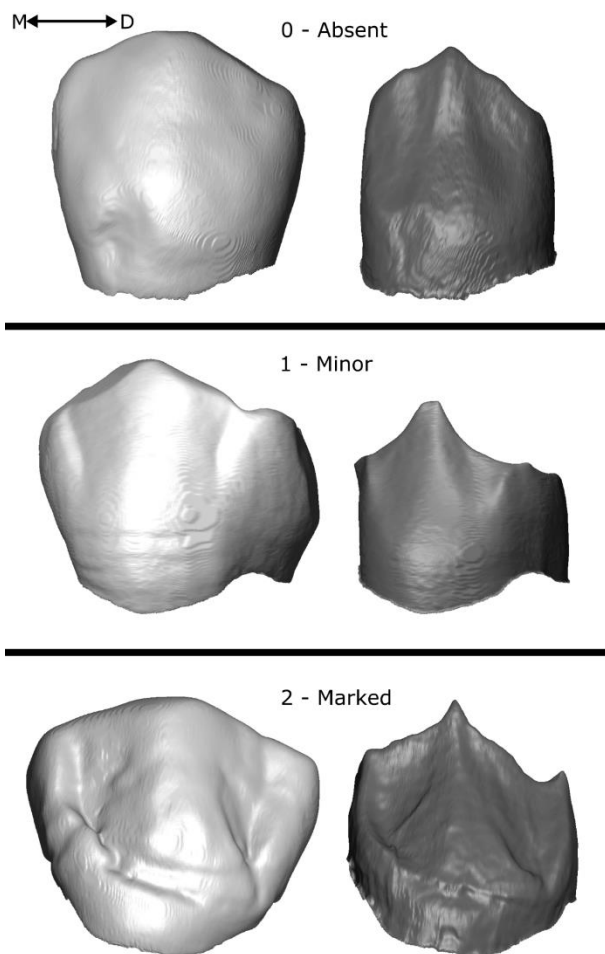


**Figure 4.** Buccal groove variation. Three specimens in buccal view illustrating the range in buccal groove expression, and the scoring system used. Examples used are those which display the same score for their mesial and distal buccal grooves. Specimens used are (top to bottom) KRP 54, UW101 889 and STW 213. The image of STW 213 is reversed such that all specimens appear left sided

**Minor (1):** A vertical ridge is present on the EDJ surface, and is associated with a small but distinct concavity

**Marked (2):** The EDJ buccal surface shows a clear extended vertical ridge associated with a marked concavity

**Cusp form and frequency.** The protoconid is universally present in hominoid  $P_3$ s, and in the majority of cases, consists of a single raised, conic dentine horn. However, there are a limited number of cases in which the protoconid departs from this form, and these examples will be discussed. The variable presence of a second cusp, the metaconid, will also be discussed within the hominoid species included in the sample. Lastly, the presence of accessory cusps will be discussed briefly; however the frequency of these cusps will not be scored since accessory cusps can often be very small at the EDJ, and a number of specimens do not have a sufficiently high scan resolution to accurately assess this feature.

**Observer error** For each of the four traits which were formally examined (transverse crest form, marginal ridge form, mesial buccal grooves and distal buccal grooves) a test for inter-observer error was carried out. A second observer was given the trait descriptions outlined below and asked to score the entire sample independently of the primary observer. Further, intra-observer error was assessed through the primary observer returning to rescore the sample one month later. The intra- and inter-observer test results were analysed through counting percent agreement for each trait.

### 3. Results

#### 3.1 *Changes in $P_3$ morphology through time*

Here, the patterns and differences in  $P_3$  shape among hominoid taxa are described, with reference to the mean EDJ and CEJ ridge wireframe models (Fig. 5), as well as PCAs of the shape variation in all analyses (Figs. 6, 7 and Supplementary Figure 1). Furthermore, differences in centroid size between groups are considered (Fig. 8), for which the results of the Wilcoxon rank sum test are summarised in Table 3.

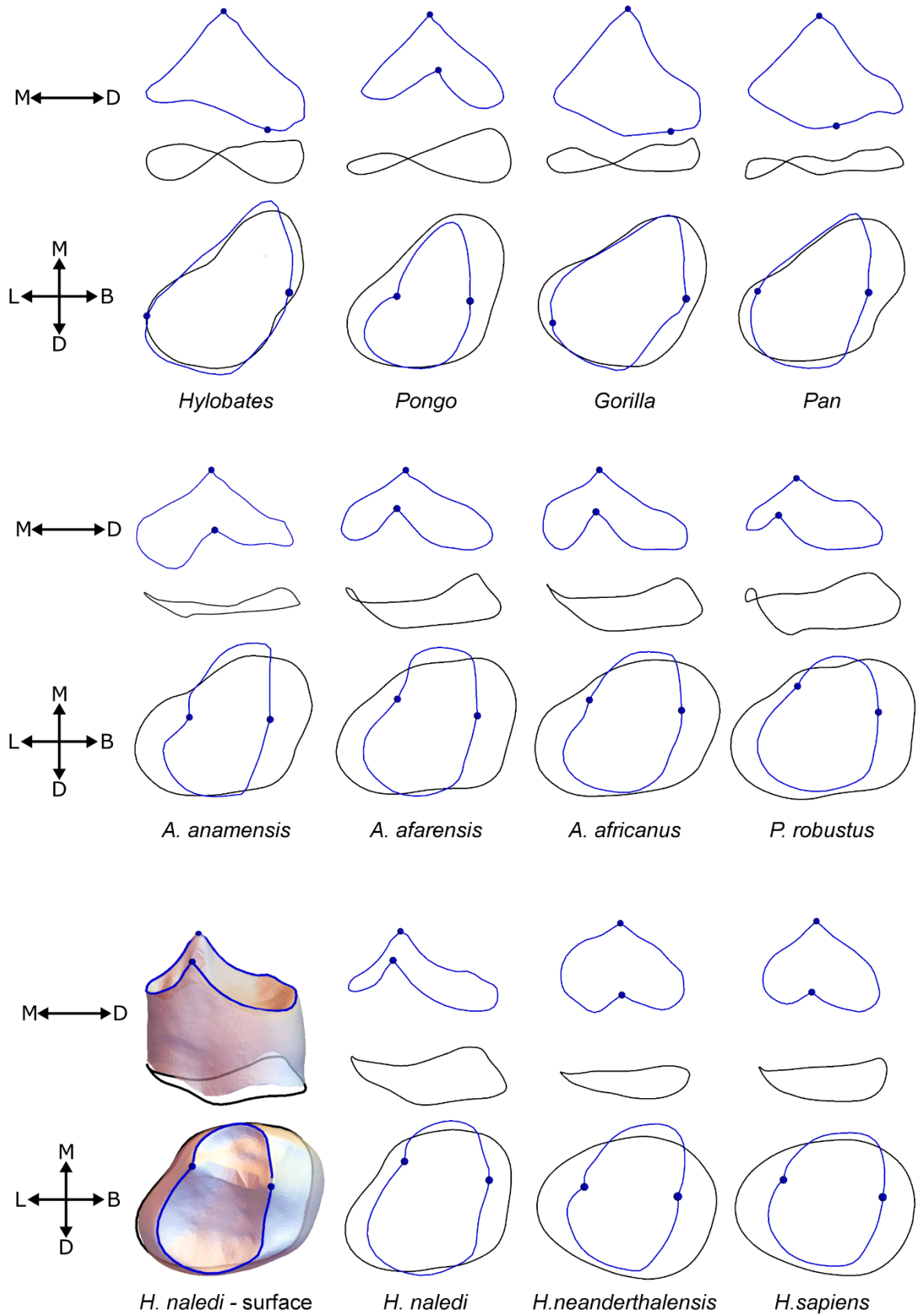


**Figure 5.** Wireframe images for each well-represented hominoid species included in the sample, showing the mean shape for the EDJ ridge landmark set (blue lines) and CEJ ridge landmark set (black lines), and the mean position of the EDJ main landmarks (blue circles). For each species, the top image is in lingual view, and the bottom image is in occlusal view.

**Extant non-hominin apes.** The non-hominin apes display a tall protoconid, a low crown height, and a CEJ which is expanded mesiobuccally compared with hominins. The mesiobuccal expansion of the CEJ also extends apically, giving the CEJ a sinusoidal shape, which, when viewed from the lingual direction as in the wireframe models (Fig. 5), appears as a figure of 8.

The PCAs show clear separation among taxa in all three analyses (Figs. 6, 7 and Supplementary Figure 2), although this analysis is more marked in the analyses which include the EDJ ridge, compared with the CEJ only analysis. *Pongo* is distinct from the other apes due to a peak in the midpoint of the lingual side of the marginal ridge. This peak is caused by the extension of the transverse crest to the lingual margin of the tooth where it meets the marginal ridge, a feature which is near-universal in hominins, but among the non-hominin apes, is unique to *Pongo*. By contrast, in other extant apes, particularly *Gorilla*, the marginal ridge is much lower, and therefore closer to the CEJ, which results in a lower crown height. This feature is the main driver of the first principal component (PC1) for the non-hominin apes in Figures 6 and 7.

*Hylobates* P<sub>3</sub>s are by far the smallest in the sample, whilst *Gorilla* were the largest (Fig. 8). *Hylobates* P<sub>3</sub>s are relatively mesiodistally longer, and buccolingually narrower, than the other non-hominin ape species, however this is particularly variable in *Gorilla*; this can be seen in Figure 6, where PC2 for the non-hominin apes is largely driven by this feature.

**Australopithecus anamensis.** This is the earliest hominin species in the sample, which is reflected in a number of symplesiomorphic features of the crown shape, including weak development of the mesial marginal ridge, and a mesiobuccal extension of the CEJ. The CEJ is not lowered on the mesiobuccal side as in apes, which means the characteristic sinusoidal shape is not present. Also, the transverse crest extends to the marginal ridge meaning that, although a metaconid is not present, there is a raising of the marginal ridge at this point relative to the condition seen in *Pan*, *Gorilla* and *Hylobates*.

**Table 3**

Pairwise comparisons of  $P_3$  centroid size. p-values were calculated using a Wilcoxon rank sum test.

	Hy	Pongo	Gor	P. tv	A. ana	A. afa	A. afri	P. rob	H. nal	H. nea
Pongo	<b>0.026</b>	-	-	-	-	-	-	-	-	-
Gor	<b>0.029</b>	<b>0.026</b>	-	-	-	-	-	-	-	-
P. tv	<b>0.029</b>	0.119	<b>0.026</b>	-	-	-	-	-	-	-
A. ana	0.085	0.199	0.060	0.847	-	-	-	-	-	-
A. afa	<b>0.029</b>	0.082	<b>0.026</b>	1.000	0.847	-	-	-	-	-
A. afri	<b>0.029</b>	0.082	<b>0.026</b>	0.873	1.000	0.873	-	-	-	-
P. rob	<b>0.029</b>	0.165	<b>0.026</b>	0.134	0.293	0.184	0.184	-	-	-
H. nal	0.051	<b>0.026</b>	<b>0.029</b>	<b>0.029</b>	<b>0.085</b>	<b>0.029</b>	<b>0.055</b>	<b>0.029</b>	-	-
H. nea	<b>0.012</b>	<b>0.020</b>	<b>0.011</b>	0.165	0.329	0.165	0.165	<b>0.020</b>	0.341	-
H. sap	<b>0.020</b>	<b>0.011</b>	<b>0.011</b>	<b>0.011</b>	<b>0.029</b>	<b>0.011</b>	<b>0.011</b>	<b>0.011</b>	<b>0.020</b>	<b>0.003</b>

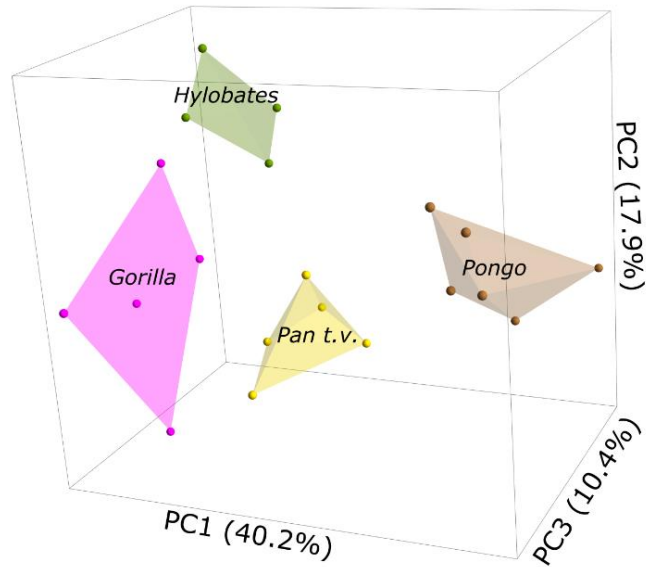
Bold indicates  $p < 0.05$ .

Hy = Hylobates, Gor = Gorilla, P. tv = Pan troglodytes verus, Australopithecus anamensis, A. afa = A. afarensis, A. afri = Australopithecus africanus, P. rob = Paranthropus robustus, H. nal = Homo naledi, H. nea = Homo neanderthalensis, H. sap = Homo sapiens.

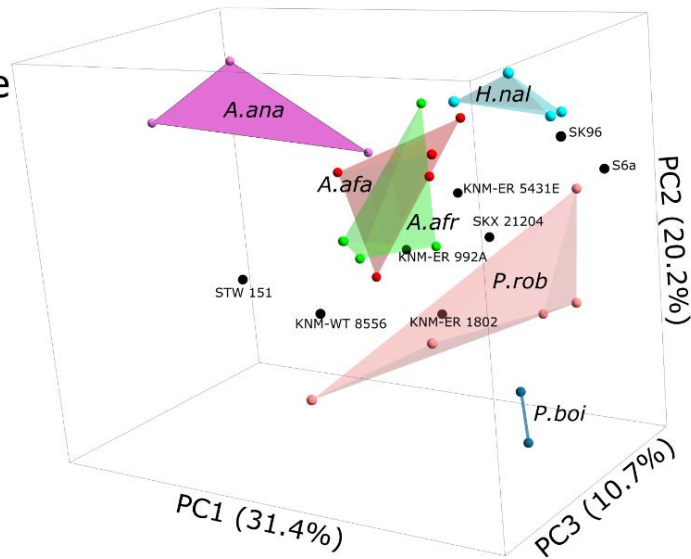
**Australopithecus afarensis.** The *A. afarensis* hypodigm is variable, with some specimens more similar to *A. anamensis* than others. Specimens such as AL 128-23 and AL 266-1 display little mesial marginal ridge development and no metaconid, similar to *A. anamensis*, whilst others such as W8-978 and AL 333w-1c both display a well-developed metaconid and mesial marginal ridge, similar to later *Australopithecus* and *Paranthropus* specimens. In the mean wireframe model (Fig. 5), the anterior fovea makes up a smaller proportion of the occlusal surface in *A. afarensis* than *A. anamensis* or *A. africanus*, as the transverse crest meets the marginal ridge more mesially.

At the OES, a longitudinal groove is variably present, which at the EDJ appears to derive from the presence of a well-developed metaconid which is well separated from the protoconid, as well as a lowered, convex transverse crest. This combination of features can be seen in AL333w-1c and its

Non-hominin apes



Plio-Pleistocene hominins



Late-Pleistocene hominins

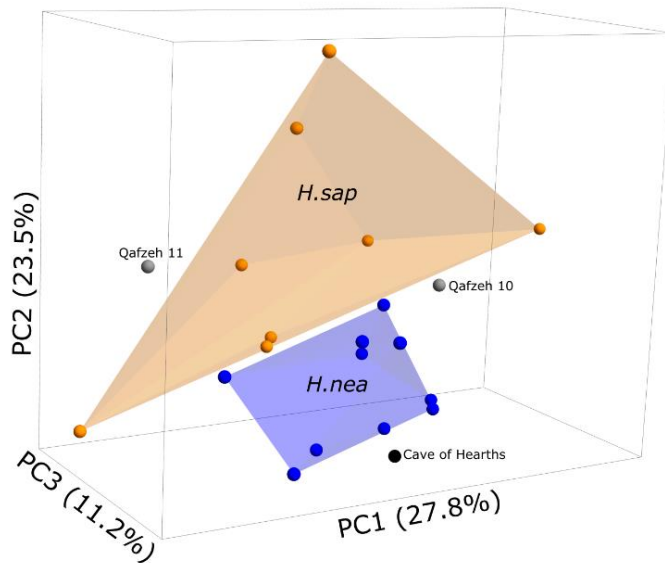


**Figure 6.** PCA plots of EDJ and CEJ shape. Percentages in brackets indicate the proportion of the total variation in the sample which is explained by each principle component. Abbreviations: PC = Principal Component, *Pan t.v.* = *Pan troglodytes verus*; *A.ana* = *Australopithecus anamensis*; *A.afa* = *Australopithecus afarensis*; *A.afr* = *Australopithecus africanus*; *H.nal* = *Homo naledi*; *P.rob* = *Paranthropus robustus*; *P.boi* = *Paranthropus boisei*; *H.sap* = Extant *Homo sapiens*; *H.nea* = *Homo neanderthalensis*

antimere, as well as W8-978 and potential *A. afarensis* specimen KNM-WT 8556.

*A. afarensis* also has a taller crown than *A. anamensis*, which is particularly marked on the mesial side, and is associated with the development of the mesial marginal ridge in some specimens. The CEJ is raised on the mesial and distal sides, which is characteristic of *Australopithecus* and *Paranthropus* species (except *A. anamensis*) and is also seen in *Homo naledi*. The raising of the CEJ is generally more prominent on the mesial side, particularly in *P. robustus*, in which the mesial side of the CEJ shows a marked upward protrusion.

***Australopithecus africanus***. In terms of centroid size, *A. africanus* specimens overlap greatly with specimens of *A. afarensis*, and the two species were not significantly different in the Wilcoxon rank sum test ( $p = 0.873$ ). In fact, size alone is not useful in distinguishing the P<sub>3</sub>s of *Australopithecus* species (Table 3), and the classification accuracy of *A. africanus* specimens is reduced by the inclusion of size as a variable. The *A. africanus* sample shows significant overlap with *A. afarensis* in shape space in the EDJ+CEJ and CEJ only analyses (Fig. 6 and Supplementary Figure 2). However, when only the EDJ is considered, the two species are clearly separated. Moreover, the *A. africanus* specimens are largely classified correctly in the EDJ+CEJ analysis in shape space, suggesting that they are distinguishable from *A. afarensis* specimens in PCs above PC3.

*A. africanus* specimens display a crown outline which is buccolingually expanded compared to *A. afarensis*. In particular, the anterior fovea is wider than temporally older *Australopithecus*, and the metaconid is placed more lingually. The mesial marginal ridge is relatively lower in *A. africanus* than *A. afarensis*, which is likely reflecting that in some specimens (e.g. STW 213, STW 401) the ridge is interrupted mesial to the metaconid. The CEJ is buccolingually wider, and compared to earlier *Australopithecus* species, more closely resembles the Late-Pleistocene *Homo* state in which the CEJ is oval shaped in occlusal view. However, in *A. africanus*, as in earlier *Australopithecus*, the lingual

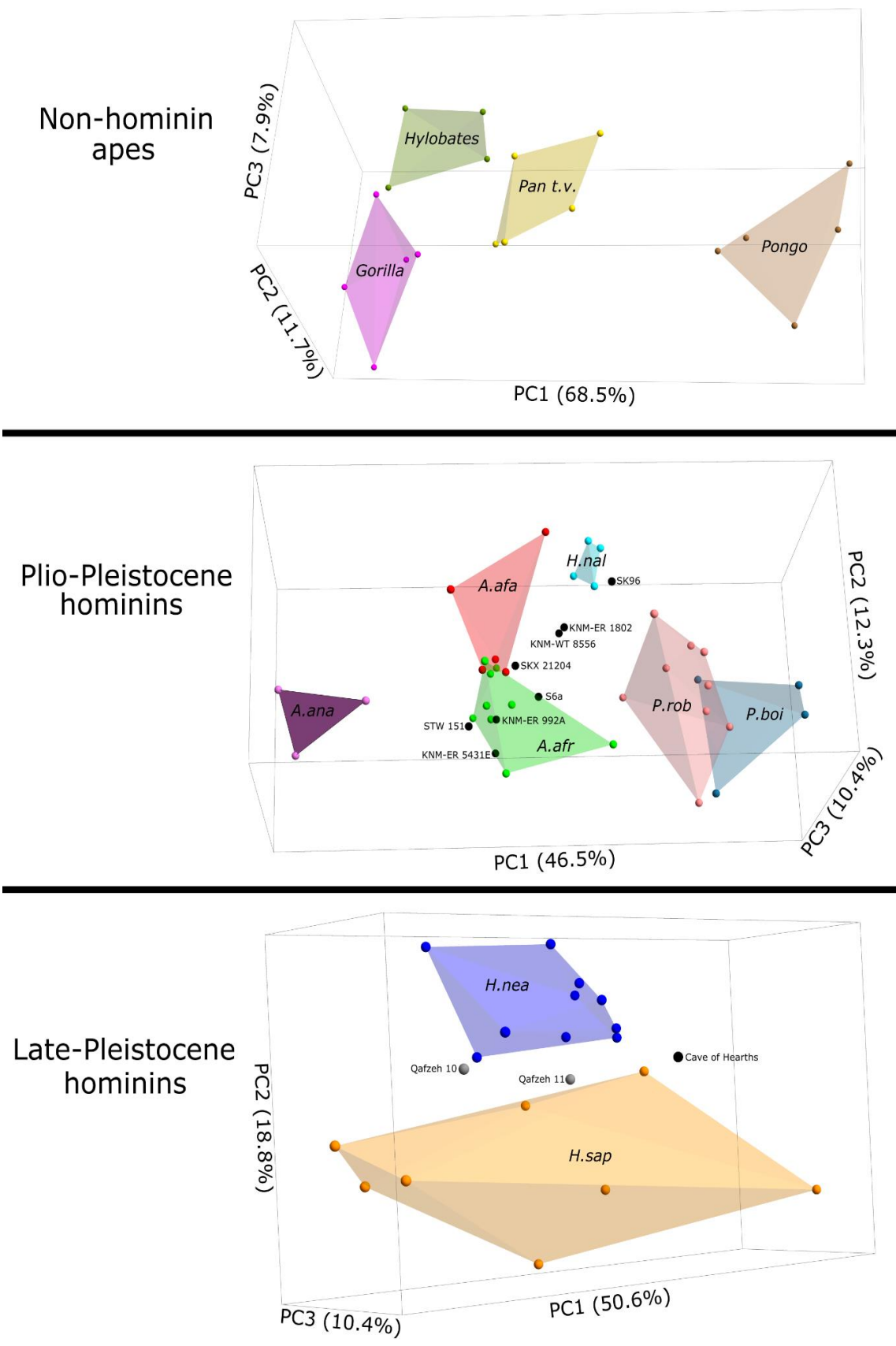
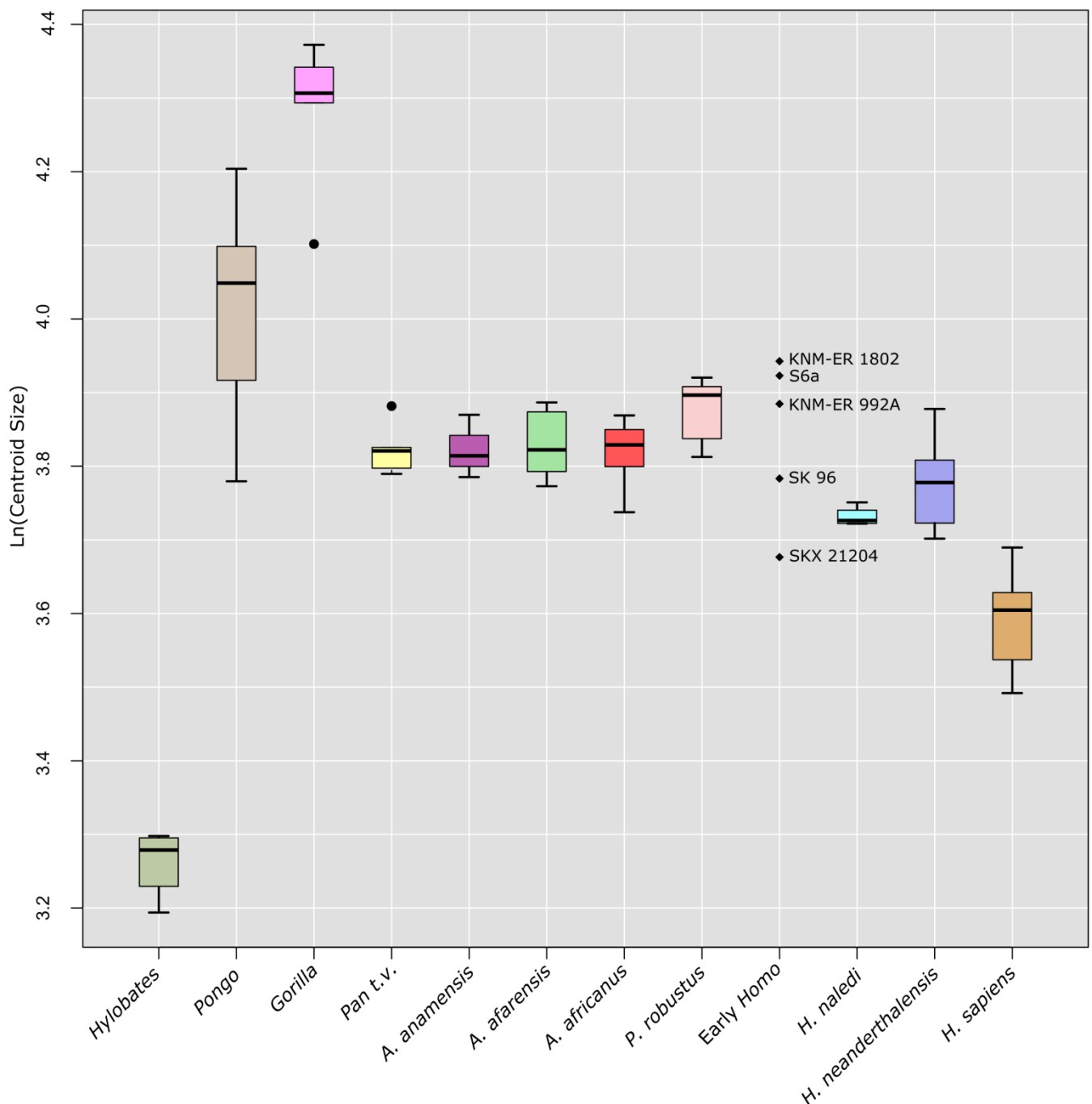


**Figure 7.** PCA plots of EDJ shape. Percentages in brackets indicate the proportion of the total variation in the sample which is explained by each principle component. Abbreviations: PC = Principal Component, *Pan t.v.* = *Pan troglodytes verus*; *A.ana* = *Australopithecus anamensis*; *A.afa* = *Australopithecus afarensis*; *A.afr* = *Australopithecus africanus*; *H.nal* = *Homo naledi*; *P.rob* = *Paranthropus robustus*; *P.boi* = *Paranthropus boisei*; *H.sap* = Extant *Homo sapiens*; *H.nea* = *Homo*

and distal sides of the CEJ are raised, and the long axis of the CEJ is rotated mesially, relative to Late-Pleistocene *Homo*.

STW 213 is separated from the other *A. africanus* specimens in the EDJ+CEJ analysis in PC2 (Fig. 6). In this specimen, the distal marginal ridge appears 'pinched' distal to the metaconid, and is interrupted on the lingual side, only beginning again at on the lingual margin of the tooth. The specimen is also



51 **Figure 8.** Boxplot of natural logarithm of centroid size for each taxon, as well as four early *Homo* taxa

the smallest of the *A. africanus* sample (in fact, it is the smallest *Australopithecus* specimen in the EDJ+CEJ sample), and has a particularly tall protoconid. The buccal ridges which are common in the *A. africanus* hypodigm are especially prominent in this specimen, as is a distobuccal accessory cusp. In the classification analysis, the specimen is often misclassified as *A. afarensis*, or occasionally *H. naledi*, and this is more common in the form analysis than the shape analysis, underlining the contribution of the small size.

**Paranthropus.** Although *P. robustus* specimens have the largest mean centroid size of any of the hominin species included here (excluding *Paranthropus boisei*, for which only two specimens were able to be included in the EDJ+CEJ analysis), no significant difference between the size of *P. robustus* and any of the *Australopithecus* species was found (Table 3). *P. robustus* P<sub>3</sub>s display a posterior fovea which is larger than that of *Australopithecus* specimens due to an expansion of the talonid region, as well shifting of the metaconid mesially, which leads to the transverse crest projecting mesiolingually from the protoconid, as opposed to *Australopithecus* specimens in which the transverse crest is angled more lingually. The CEJ is expanded, particularly on the buccal side, which leads to a more squared buccal cervix face. *P. robustus* specimens display a raised section of the CEJ on the mesial side which begins at the mesiobuccal corner of the tooth and ends just beyond the midpoint of the mesial face of the tooth. In general, *A. afarensis* and *A. africanus* specimens also display CEJs which are raised on the mesial side, however the condition in *P. robustus* is more pronounced.

In Figure 6, *P. robustus* specimens can be seen to occupy a large area across PC3, with Drimolen specimens on one extreme and Swartkrans specimens on the other, suggesting there may be distinct shape differences between the two sites. The two Drimolen specimens in the CEJ+EDJ analysis display an EDJ ridge which is larger, relative to the size of the CEJ, than the Swartkrans specimens in this analysis, as well as a relatively lower crown height. However, since this is only based on two Drimolen and three Swartkrans specimens, this pattern would require further investigation. Only

two *P. boisei* specimens were included in the EDJ+CEJ analysis, however they occupy a distinct space in Figure 6, largely due to an enlarged talonid, even relative to *P. robustus*.

### Early *Homo* specimens.

Wireframe models for early *Homo* specimens are presented in Figure 9. KNM-ER 1802 has a particularly large P<sub>3</sub>; the centroid size is greater than all *P. robustus* specimens in this sample, although a similarly large size is also seen in Sangiran *Homo erectus* specimen S6a. Equally, in the PCA of EDJ+CEJ shape, KNM-ER 1802 falls close to the *P. robustus* range of variation (Fig. 6). This is likely due to the well-developed talonid, large mesially-placed metaconid, and well-developed mesial marginal ridge, although the fact that the specimen is better separated from *P. robustus* in the EDJ only analysis suggests that the crown height is also an important factor in this placement. The CEJ is also raised on the mesial and distal sides, as seen in *A. afarensis*, *A. africanus* and *P. robustus*. SKX 21204 has a number of derived features, relative to *Australopithecus* specimens. The crown is tall, with a shortened metaconid and a small talonid. Compared to *A. afarensis* and *A. africanus*, it has a flatter, more oval shaped CEJ. The specimen is also very small; the centroid size is within the range of modern *H. sapiens*. KNM-ER 992 is larger, with a centroid size within the range of *A. afarensis*, and

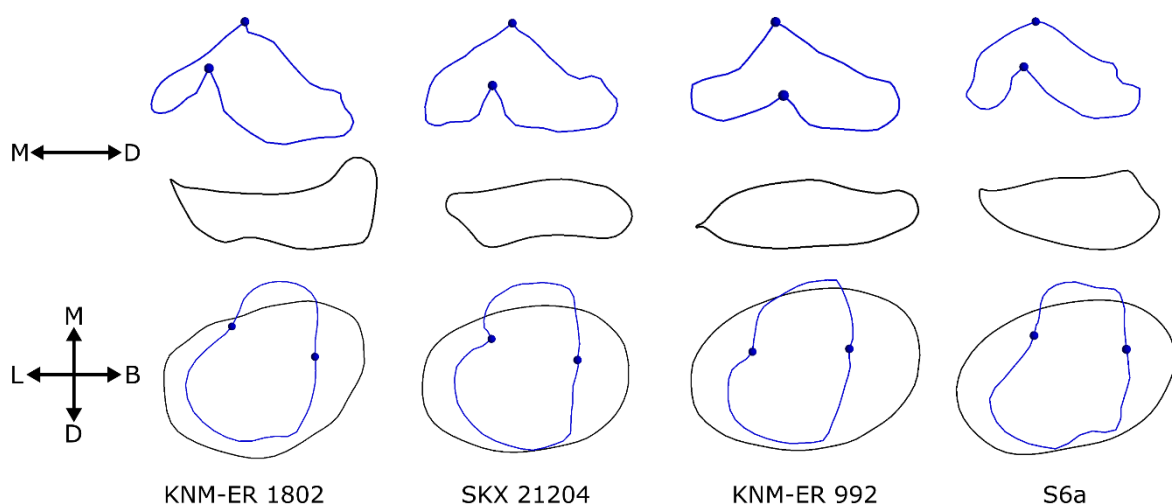


**Figure 9.** Wireframe models for four early *Homo* specimens showing the shape of the EDJ ridge landmark set (blue lines) and CEJ landmark set (black lines), and the position of the EDJ main landmarks (blue circles). Top row is in lingual view, bottom row is in occlusal view

only slightly smaller than Sangiran *H. erectus* specimen S6a. As in SKX 21204 and S6a, the metaconid is smaller than the majority of *A. africanus* specimens, and more distally placed than in *P. robustus*. The talonid is also relatively small. However, in both the EDJ+CEJ and the EDJ only analyses, the specimen falls close to the *A. africanus* range of variation (Figs. 6 and 7).

Sangiran *H. erectus* specimen S6a has a relatively tall crown, and a blunted protoconid. The talonid is reasonably well-developed, but the metaconid is located more buccally than in *Australopithecus* taxa, which causes the middle and mesial aspect of the EDJ ridge to appear buccolingually pinched. The CEJ is apicocervically flattened and oval shaped, relative to *Australopithecus* specimens. S6a is large (within the range of *Paranthropus*), however this appears to be highly variable within the Sangiran sample given that S7-25 is far smaller (the EDJ could not be assessed for this specimen, but the CEJ is within the size range of modern humans). In the PCA of all specimens for the EDJ+CEJ analysis (Supplementary Figure 2), S6a is placed more closely to the late *Homo* cluster than any other early *Homo* specimen, which is driven in part by the crown height of the specimen.

A number of early *Homo* specimens could only be included in the CEJ only analysis. The main distinguishing feature of the CEJ is the transition from an asymmetrical shape when viewed occlusally (with a mesiobuccal expansion) in earlier hominin taxa, mostly *Australopithecus*, to a roughly oval shaped CEJ in late-Pleistocene hominins. This morphology is present in Sangiran *H. erectus*, as well as *Homo neanderthalensis* and *H. sapiens*. This is also evident in the placement of *H. erectus* and *H. ergaster* specimens in the PCA of the CEJ only analysis (Supplementary Figure 1). African *H. ergaster* specimens KNM-ER 992A, KNM-ER 806E and KNM-WT 15000 cluster particularly closely, and are quite close to KNM-ER 1507, as well as South African early *Homo* specimens SKX 21204 and SK 18a.

**Homo naledi.** *H. naledi* P<sub>3</sub>S occupy a distinct area in shape space from all other hominins in all except the CEJ only analysis in which they overlap with *P. robustus*. The teeth are significantly smaller than those of all *Australopithecus* species (Table 3), and sit in the lower end of the size range

**Table 4**

The classification accuracies for hominoid  $P_3s$  per analysis. Those higher than 80% are in bold

Analysis	Shape/Form	Accuracy (%)
EDJ+CEJ	Shape	<b>89.5</b>
	Form	<b>94.7</b>
CEJ+Med	Shape	72.6
	Form	<b>82.1</b>
CEJ only	Shape	64.6
	Form	79.3
EDJ only	Shape	<b>90.7</b>
	Form	<b>89.2</b>

of *H. neanderthalensis* (Figure 8). They are significantly larger than the  $P_3s$  of modern humans ( $p = 0.02$ ). South African specimens which have been suggested as belonging to early *Homo* (SKX 21204 and SK 96 – this paper) also occupy a similar size range (Supplementary Table 1). As at the outer enamel surface, one of the most striking features of the *H. naledi*  $P_3$  is the

metaconid, which is uniformly well developed, and only marginally shorter than the protoconid. Compared to *Australopithecus* specimens, the crown is higher, especially on the mesial side, with a well-developed mesial marginal ridge. The talonid region is reduced compared to *A. africanus*, leading to a more symmetrical EDJ occlusal outline. The CEJ is relatively narrower, BL, than *Australopithecus* specimens, and the buccal face is flattened, as is seen in *P. robustus*, and, to an extent, *A. afarensis*. The *H. naledi* CEJ resembles the condition seen in *Australopithecus* and *Paranthropus* more than later *Homo* condition as there are no signs of the derived oval shape, and the mesial side is raised as in *Australopithecus*. In Figure 6, the *H. naledi* group can be seen to sit closely to S6a, Sangiran *H. erectus*, although this is not repeated in the EDJ only analysis (Fig. 7). In both cases, SK 96 clusters closely to *H. naledi*.

#### **Late-Pleistocene Homo.**

Late-Pleistocene *Homo* specimens display an oval shaped CEJ, when viewed occlusally. The anterior fovea is reduced in size through reduction of the talonid region, when compared with earlier hominins in the sample. They also have a tall crown height, a tall protoconid, and display very little metaconid development. This morphology can be seen in Neanderthals and recent modern humans, as well as fossil modern humans from Qafzeh, and the

Cave of Hearths P<sub>3</sub>. Although the Mauer P<sub>3</sub> was too worn to include in analyses considering the entire EDJ ridge, its placement in the CEJ+Med analysis, as well as the preserved EDJ morphology, strongly suggest that it fits the late *Homo* condition.

Modern humans and Neanderthals are separated the EDJ+CEJ analysis (Fig 6). This separation mainly pertains to the shape of the EDJ ridge. Neanderthals frequently display a transverse crest which intersects with the marginal ridge more distally than in recent modern humans. The Neanderthal EDJ ridge is relatively longer, mesiodistally, whilst the modern human EDJ ridge is mesiodistally shortened, and therefore more circular. Neanderthal specimens frequently display a protoconid tip which protrudes lingually, towards the basin of the tooth, a feature which is much less common in modern humans. Also, the Neanderthal CEJ is flattened apicocervically, whereas the modern human CEJ appears convex when viewed mesially or distally. This shape results from a combination lowered CEJ on the buccal side, and a raised CEJ on the mesial and buccal sides. Neither of these features are present in all specimens, and can sometimes be seen in Neanderthal specimens, but the differences in frequency are enough for this to be picked up in the wireframe models. Further, the two Qafzeh specimens more closely approximate the modern human condition, whilst Irhoud 11 is intermediate (although given the variability of these traits within modern humans and Neanderthals, caution should be exercised in inferring general trends from just one or two specimens). Furthermore, the Neanderthal P<sub>3</sub>s are significantly larger than those of modern *H. sapiens* ( $p = 0.003$ ).

### 3.2 Classification accuracies

The classification accuracies from the CVA analysis are shown in Table 4, and the full classification results for each specimen can be found in Supplementary Tables 3-10. The accuracies are reported for each of the GM analyses in both shape and form space. The form space analyses generally performed better than the shape analyses, except in the EDJ only analysis, and the best performing analysis overall was the EDJ+CEJ analysis in form space, followed by the EDJ only analysis in shape

space. The CEJ only analysis performed poorest overall, with a slight improvement when the metaconid landmark was included.

### 3.3 *Specimens of uncertain taxonomic affinity*

The P<sub>3</sub> of KNM-WT 8556 does not fall within the variation of *A. afarensis* within the EDJ+CEJ or EDJ only analyses. In the EDJ+CEJ analysis, the specimen does not cluster clearly with any one taxon. It is separated from *A. afarensis* and *A. africanus* in PC3, which seems to reflect the relatively low crown height, amongst other factors. Similarly, KNM-ER 5431E does not fall within the variation of any of group included here, although it is close to the *A. africanus* group in the EDJ only analysis (Fig. 7). While STW 151 falls close to the *A. africanus* range of variation in the EDJ only analysis (Fig. 7), the specimen plots far from all other specimens in the EDJ+CEJ analysis (Fig. 6), which is likely due to the particularly low crown height of this specimen, when compared with other *A. africanus* specimens.

The Cave of Hearths P<sub>3</sub> has a morphology similar to that of other Late-Pleistocene *Homo*, and is close to the Neanderthal range of variation in the Figure 6. SK 96 is outside of the *P. robustus* range of variation in all analyses, in shape and form space. When placed into the leave-one-out classification test based on the CVA, SK 96 is consistently classified as *H. naledi* in both shape and form space for the EDJ+CEJ analysis. Further, in Figure 6, SK 96 can be seen to cluster closely with *H. naledi*, and Sangiran *H. erectus* specimen S6a. In the EDJ only analysis (Fig. 7) *H. naledi* and SK 96 cluster closely together, but S6 is much further away. SK 96 is slightly larger than the observed size range for *H. naledi*, and much smaller than that of S6a.

### 3.4 *Discrete traits*

Full results of the discrete trait analysis can be found in Supplementary Table 11.

**Transverse crest.** There were 73 specimens for which the form of the transverse crest was assessed. The majority of specimens display a type 1 transverse crest (48/73), however this type is less common when looking only at the extant ape specimens, and is in fact only seen in *Pongo*.

*Hylobates* specimens all show deflected transverse crests, with some connecting to the protoconid

(type 2) and others connecting to the distal protoconid ridge (type 3). *Gorilla* specimens also show a deflected transverse crest, but all connect to the protoconid (type 2). All five *Pan* specimens display a transverse crest which is deflected (or otherwise fails to reach the lingual margin of the tooth); of these, three connect to the protoconid (type 3), and two do not (type 5).

Type 3 is only present among the non-hominin apes, and only one hominin specimen displays a type 2 transverse crest. 79% of hominin specimens display a transverse crest which runs from the protoconid to the metaconid (or the equivalent point on the marginal ridge) (type 1), and all hominin species represented here by multiple specimens show a type 1 transverse crest in at least one specimen. Type 4, in which the transverse crest connects to the marginal ridge but does not reach the protoconid, is seen exclusively in Neanderthal specimens, for which 44% of specimens (4/9) display this type (the rest are type 1).

A special case is the modern human specimen ULAC 790 (seen in Fig. 10B) which has poorly developed mesial and distal marginal ridges, and has no metaconid or clear apex to the protoconid, which makes it difficult to assign the specimen to a transverse crest type. In this specimen, the transverse crest extends lingually from the protoconid to meet a small ridge, which may or may not be a section of distal marginal ridge, but is very poorly developed (the main portion of the distal marginal ridge is situated on the distal edge of the crown, and does not connect to the transverse crest at any point).

A number of specimens also display crests in addition to the main transverse crest. For example, *A. africanus* and *P. robustus* specimens frequently display small/incipient crests which run distolingually towards the centre of the posterior fovea. These crests typically meet the transverse crest at the protoconid, however, they may also meet partway across the transverse crest, lingual to the protoconid (e.g. SK 61 and SK 100 – Fig. 2). Accessory crests are sometimes present on the lingual side of the tooth. For example, DNH46 displays a crest originating at the metaconid and running towards the centre of the posterior fovea, whilst SK 62 displays a similar crest on the lingual side of

the tooth, but which appears to originate at the distal marginal ridge (Fig 2). Moreover, Neanderthal specimens frequently display accessory crests either mesial or distal to the main transverse crest, on the face of the tall protoconid ridge (Fig. 2). These are variable in number, size and position, and are also seen, albeit less frequently, in modern human specimens.

**Marginal ridge.** There were 72 hominin specimens for which the form of the marginal ridge was able to be scored. Of these, 69% (50/72) displayed a continuous marginal ridge (Fig. 3). All major hominin species represented in the sample by more than three specimens have at least one specimen displaying a continuous marginal ridge, except *A. anamensis*, for which all three specimens display a mesially poorly developed mesial marginal ridge, which is scored here as mesially discontinuous. Four *A. afarensis* specimens were scored, of which two displayed a discontinuous mesial marginal ridge, and two displayed an entirely continuous marginal ridge. KNM-WT 8556 also displays a continuous marginal ridge.

*A. africanus* displays a range of marginal ridge forms, although the majority are continuous (nine continuous, two mesially discontinuous and one distally discontinuous), whilst continuous marginal ridges are seen in all specimens of *Paranthropus*, *H. naledi*, as well as probable early *Homo* specimen SKX 21204. Overall, continuous marginal ridges are the most common form amongst *Australopithecus*, *Paranthropus* and early *Homo* specimens. When looking at later *Homo*, however, nearly half of the P<sub>3</sub>s in the sample display a discontinuous mesial and/or distal marginal ridge (14/30 = 47%). Discontinuous mesial marginal ridges are common in Neanderthal specimens (4/13 = 31%), and modern humans show a range of marginal ridge forms (only 7/15 are continuous, whilst four specimens show mesial and distal discontinuity). The P<sub>3</sub> of the Mauer mandible also shows both mesial and distal discontinuity. In some cases (e.g. ULAC 171), the marginal ridge is mostly absent, with only small lingual deflections from the mesial and distal protoconid crests. Finally, this trait is not always consistent between antimeres – ULAC 58 displays a discontinuous mesial marginal ridge on the left P<sub>3</sub>, but not the right.

*A. africanus* specimen STW 401 is the only example within this sample of a discontinuous distal marginal ridge in an *Australopithecus* P<sub>3</sub>, and is particularly interesting because the form of this trait appears to be different to that seen in later hominin specimens, and different to that often seen in the mesial marginal ridge in *Australopithecus*. In most cases, discontinuities in the marginal ridge appear either side of the metaconid; the marginal ridge lowers and flattens before reaching the dentine horn. In this case however, there are two portions of the distal marginal ridge present which overlap one another, but do not meet.

**Buccal grooves.** Overall, 98 specimens were able to be scored for buccal groove expression. Of these, 67% show some level of buccal groove expression (mesial and/or distal). Buccal grooves are less common in the extant ape specimens; no ape specimen showed marked buccal grooves, mesial or distal, although all *Gorilla* and *Pan* specimens show minor distal buccal grooves (minor mesial buccal grooves are also present in half of these specimens). Conversely, all 20 *Australopithecus* specimens that were able to be scored showed either minor or marked buccal grooves on both the distal and mesial sides, and where the mesial and distal buccal grooves are not equal, it is always the mesial buccal groove which is more strongly expressed.

The opposite pattern is evident in *Paranthropus*, where the distal buccal grooves are generally better developed, and in fact mesial buccal grooves are absent in 12/14 specimens. SXX 21204 shows marked mesial and minor distal buccal grooves. *H. naledi* specimens show minor or absent buccal grooves on both mesial and distal sides. Among later *Homo*, buccal grooves are less common; no specimen showed marked mesial or distal buccal grooves. Neither the Mauer P<sub>3</sub> nor the Cave of hearths P<sub>3</sub> show any buccal grooves, whilst 6/14 Neanderthal and 12/15 *H. sapiens* P<sub>3</sub>s exhibit no buccal grooves at all.

**Protoconid form.** The variation observed in the form of the protoconid is shown in Figure 10, and the full results are found Supplementary Table 12. The vast majority of specimens display a single, conic dentine horn underlying the protoconid (Fig. 10A). In Neanderthals and modern humans, this dentine horn may be less pronounced due to the strong development of the mesial and distal protoconid ridge, however there is a clear apex to the dentine horn in all specimens except one specimen, modern human ULAC 790. In this specimen, there is no clear protoconid tip, only a well-developed ridge (Fig. 10B).

The protoconid may also be longitudinally expanded (Fig. 10C). This feature is seen in two *H. naledi* specimens; UW 101-144 and UW 101-889, and their probable antimeres (UW 101-506 and UW 101-377, respectively), as well as one *Pan* specimen, ZMB 11800. In some cases, such as UW101-377, it is clear that the expanded dentine horn actually consists of two semi-distinct tips. In other cases, the tip simply appears as a flattened ridge, however since this structure is very small, it is possible that the resolution of the scans may be insufficient to discern two individual peaks.

In one modern human specimen, ULAC 58, the tip of the protoconid is transversely expanded (Fig. 10D). The protoconid ridge meets the protoconid on the buccal side of the tip, whilst the transverse

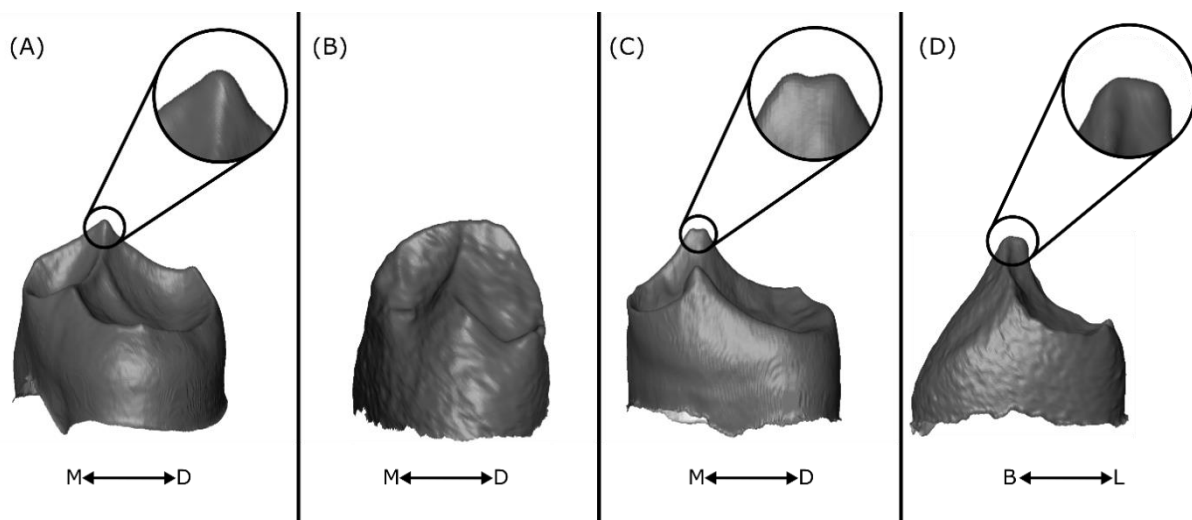


**Figure 10.** Protoconid variation. Four specimens showing variation in protoconid form are displayed. (A) ‘Standard’ simple conic dentine horn – SK 100 (*P. robustus*). (B) Flat ridge – ULAC 790 (*H. sapiens* – image flipped). (C) ‘Double’ dentine – UW101 377 (*H. naledi*). (D) Transversely expanded dentine horn – ULAC 58 (*H. sapiens*). A-C in lingual view, D in distal view

crest meets it on the lingual side of the tip, but these two points are not coincident, and are connected by a short ridge. This feature is present in both antimeres, but is not present in any other P<sub>3</sub>s within the sample.

**Metaconid presence.** Of the hominin species included in this sample, *A. africanus*, *P. robustus*, *P. boisei* and *H. naledi* P<sub>3</sub>s most regularly display a well-developed metaconid at the EDJ. Early *Homo* and *H. erectus* specimens variably display a metaconid, whilst later *Homo* specimens generally lack a well-developed metaconid. Apes typically display unicuspid P<sub>3</sub>s, however, two *Pan* specimens in the sample (ZMB 13437, and ZMB 1180) display what could be potentially interpreted as a second cusp at the OES. These appear to differ from the typical hominin metaconid, however, since in these specimens, the transverse crest does not intersect with the marginal ridge, which is where the hominin metaconid forms. Instead, the metaconid forms as an upwards extension of the transverse crest. The developmental homology of this feature to a metaconid in hominins is uncertain.

**Accessory cusps.** Poor tissue contrast in a number of specimens inhibits proper characterization of the frequency and detailed morphology of small accessory cusps. However, a number of general observations can be made.

Many hominin P<sub>3</sub>s display small cusps beyond the protoconid and metaconid. These may be present at multiple locations along the distal and mesial marginal ridges. There is commonly a small dentine horn at the distobuccal corner of the tooth, at the intersection between the distal marginal ridge and the distal protoconid ridge. This cusp can be seen in various hominin species, although it appears to be less common in later *Homo*, and may be related to the presence of distal buccal grooves since the tip of the dentine horn is often contiguous with a raised ridge of dentine on the buccal face, whilst the concavity seen on the buccal face, immediately mesial to this ridge, is somewhat contiguous with the base of the dentine horn, on the protoconid ridge. A particularly pronounced example of this can be seen in STW 213 (Fig. 4).

Accessory cusps are also found along the distal and mesial marginal ridges, and in some cases they can be nearly as large as the metaconid. Other specimens, such as STW 151, display multiple accessory cusps, in this case along the distal marginal ridge.

### **Observer error**

The full results of the inter- and intra-observer error tests can be found in Supplementary Table 11.

The inter-observer error test found mostly low levels of difference between observer scores, although this differed between traits. For the marginal ridge, observers agreed on 97% of specimens, while for the transverse crest, agreement was 85%. For mesial and distal buccal grooves, agreement was slightly lower (79% for mesial and 75% for distal), although the disagreements were always between adjacent categories.

Intra-observer error was also low; the marginal ridge and transverse crest scores agreed on 97% and 99% of scores, respectively, whilst the buccal groove agreement was again lower, at 76% for mesial buccal grooves and 79% for distal buccal grooves. Again, disagreements were always between adjacent categories.

## **4. Discussion**

### *4.1 Premolar morphology for taxonomy*

The best performing analysis was the EDJ+CEJ analysis in form space (Table 4), which contains the maximum amount of information, suggesting that a combination of size and shape of both the EDJ and CEJ provides the most accurate method of assessing taxonomic questions. When looking only at the EDJ landmarks, the shape analysis performs better than the form analysis, however the difference is marginal, and is mostly driven by the form analysis performing worse in differentiating *A. afarensis* specimens, which have been previously noted to be highly variable in size (Deleuzene and Kimbel 2011) and *A. africanus* specimens, which occupy a similar size range to both *A. afarensis* and *P. robustus* (Fig. 8). The CEJ only analysis did not perform as well, particularly in the shape analysis. The addition of the metaconid landmark improved the classification accuracy somewhat, with the

form analysis correctly classifying over 80% of specimens, however it still performed poorly at differentiating Plio-Pleistocene hominins. Ultimately, these analyses are more than sufficient for distinguishing between hominoid genera, and are able to distinguish between species of extant non-human apes, as well as between modern humans and Neanderthals. However, for distinguishing between Plio-Pleistocene hominin species, including the shape of the EDJ ridge is most appropriate.

#### 4.2 *Specimens of uncertain taxonomic affinity*

KNM-WT 8556 has previously been attributed to both *A. afarensis* (Brown *et al.* 2001) and *K. platyops* (Leakey *et al.* 2001). Here, the specimen does not closely cluster with *A. afarensis*, however it is well acknowledged that the *A. afarensis* hypodigm is variable (Leonard and Hegmon, 1987; Suwa, 1990), especially in P<sub>3</sub> morphology (Deleuzene and Kimbel, 2011), and it is likely that not all of this variation is covered in the sample used here. Unfortunately, until a larger sample of dental specimens which are clearly attributable to *K. platyops* are available, the taxonomic affiliation of KNM-WT 8556 will be difficult to resolve.

KNM-ER 5431 consists of associated mandibular teeth which have previously been assigned to *A. afarensis* (Leonard and Hegmon, 1987), whilst Wood (1991) suggested that the molars are more *Homo*-like, but did not assign the specimen to a species. Here, the P<sub>3</sub> groups with the *A. africanus* and *A. afarensis* specimens in the EDJ+CEJ analysis; however, it also falls close to some South African Early *Homo* specimens. The early *Homo* sample in this analysis is relatively fragmentary, so for specimens such as this one, a sample of *Homo habilis* would be helpful for comparison. Furthermore, the transverse crest in this specimen is different to other hominin in our sample; the crest appears to flatten before reaching the metaconid (type 2). Ultimately, the inclusion of all available tooth positions in the KNM-ER 5431 sample will be required to confidently assess its taxonomic affiliation.

The Cave of Hearths mandible is from Makapansgat, South Africa, found in a layer with late Achulean industry tools. The specimen has been frequently compared to Neanderthals (Dart, 1948; Tobias, 1971), and this is mirrored in the results here. In the EDJ+CEJ analysis, the specimen falls close to,

but not within, the Neanderthal range of shape variation (Fig. 6). This result would suggest that, on the basis of the P<sub>3</sub> morphology, the Cave of Hearths mandible likely represents late-Pleistocene *Homo* which is distinct from *H. sapiens*. Future analyses should compare this specimen to other African late-Pleistocene mandibular specimens such as those from Thomas Quarry.

SK 96 consists of a mandibular fragment, lower canine and lower first molar from Member 1 at Swartkrans, and has typically been assigned to *P. robustus* (Robinson, 1956). The P<sub>3</sub> was singled out by Robinson (1956) as having an unusual morphology; however this was attributed to the specimen's incomplete crown development. With the benefit of micro-CT imaging, it is clear that the specimen is in fact crown complete, so this cannot be the reason for its unusual morphology. In the geometric morphometric analyses, the specimen is clearly distinguishable from *Paranthropus*, and is smaller than any *Paranthropus* P<sub>3</sub>. Moreover, the P<sub>3</sub> occupies a similar position in shape space to both *H. naledi* and Sangiran *H. erectus* specimen S6a in the EDJ+CEJ analysis, although the shape of the EDJ alone is more similar to *H. naledi*. Visually, the EDJ does appear remarkably similar to *H. naledi*, displaying an occlusally symmetrical EDJ, a well-developed mesial marginal ridge and a prominent transverse crest, although the metaconid is less well-developed than in *H. naledi* (Fig. 11).

Robinson (1956 – pg. 47) suggested that the canine of this specimen is also modern in appearance, saying:

“...if this particular specimen had not been in its crypt in a fragment of mandible bearing a typical australopithecine P<sub>3</sub> it would probably have been classified as a *Telanthropus* tooth”

We therefore suggest that this specimen is better assigned to *Homo* sp. Further investigation, including analysis of the canine morphology in this specimen, as well as comparison of the P<sub>3</sub> to a wider early *Homo* sample including *H. habilis*, would help to further evaluate the taxonomic affinities of this specimen and whether it is perhaps evidence for the presence of *H. naledi* in Swartkrans much earlier than the material from Rising Star.

STS 151 was suggested by Moggi-Cecchi *et al.* (1998) to display a number of derived features compared with other Sterkfontein *A. africanus*. In terms of discrete traits, the mandibular premolar was said to lack any derived early *Homo* traits, however the shape clustered with the smaller *A. africanus* specimens, towards the range of *H. habilis*. The present analysis of the P<sub>3</sub> largely agrees with this assessment, with the specimen falling outside of the *A. africanus* range of variation, particularly in the EDJ+CEJ analysis (Fig. 6). The specimen does not cluster closely with other early *Homo* specimens, however a larger sample, particularly of *H. habilis*, would be required to fully assess the early *Homo* affinities of this specimen.

#### 4.3 Major EDJ shape trends

**Canine honing.** The observed P<sub>3</sub> morphology of the extant apes is driven largely by its function in the honing complex in which the upper canine occludes with the broad mesiobuccal face of the P<sub>3</sub>. This explains the presence of the tall protoconid, the lack of a metaconid, as well as the apical extension of the CEJ on the mesiobuccal side. Since the CEJ marks the limit of the tooth's enamel coverage, the CEJ likely extends further apically to provide an apicocervically long, as well as broad, sloping surface along which the upper canine can occlude. This condition is not seen in the earliest hominin in this study's sample, *A. anamensis*, having been presumably lost following the loss of the canine honing complex.

Since canine honing is observed in all extant catarrhines except humans, it is very likely that the last common ancestor of *Pan* and humans would have had a canine honing complex, and therefore would have likely had a P<sub>3</sub> which resembles that of the extant non-human apes (Delezenne, 2015).

Canine honing seems to have been lost early in hominin evolution (Brunet *et al.* 2002; Haile-Selassie *et al.* 2004; Suwa *et al.* 2009), although many of the associated P<sub>3</sub> features were retained for some time. For example, the earliest hominin species in the sample, 4.07-4.17Ma *A. anamensis* (Leakey *et al.* 1998, Ward *et al.* 1999), retains a tall protoconid, a small mesiobuccal expansion of the crown base, and no strong metaconid development.

**Mastication and molarisation.** The loss of the canine honing complex allowed for significant changes in P<sub>3</sub> morphology (Deleuzene and Kimbell 2011). No longer adaptively constrained by a dual role in canine honing and mastication, the P<sub>3</sub> was able to be fully adapted for its role in the latter. The vast majority of hominins have well developed marginal ridges which encircle the anterior and posterior foveae, creating an enclosed grinding or chewing surface for mastication. This is evident as early as *A. anamensis*, for which the distal (but not mesial) marginal ridge is well developed. The first hominins displaying well-developed mesial and distal marginal ridges appear with *A. afarensis*, and this feature is extremely common in later hominin species (although see section on marginal ridge form). Therein followed a suite of changes often referred to as ‘molarisation’. This includes the expansion of the talonid region, as well as the addition of extra cusps and/or cuspules. The talonid region is expanded in *A. afarensis* and *A. africanus* relative to *A. anamensis* (Fig. 5), and the metaconid is variably present in *A. afarensis*, and ubiquitous in *A. africanus*. Furthermore, *A. africanus* specimens frequently show accessory cusps. These adaptations served to improve the masticatory capabilities of the P<sub>3</sub>, providing a wider chewing surface and greater occlusal relief for processing food particles.

*Paranthropus* specimens display a suite of characters across the dentition that have been linked to forceful mastication using the postcanine dentition including thicker enamel (Conroy, 1991; Grine and Martin, 1988; Olejniczak *et al.* 2008), large post-canine teeth (Robinson, 1956; Tobias, 1967), small anterior teeth (Robinson, 1956; Tobias, 1967; Ungar and Grine, 1991), and robust mandibles (Robinson, 1956; Tobias, 1967; Wood and Aiello, 1998). These adaptations suggest a unique dietary scheme for *Paranthropus*, including increased levels of hard-object-feeding (Grine, 1986; Lucas *et al.* 1985; Scott *et al.* 2005) - although this not necessarily indicative dietary specialism (Wood and Strait, 2004). The results of the present study are consistent this interpretation with *Paranthropus* P<sub>3</sub>s exhibiting marked talonid expansion and the highest frequency of distal accessory cusps. (Fig. 5). Unfortunately, the majority of specimens of *P. boisei* (considered the most derived with respect to

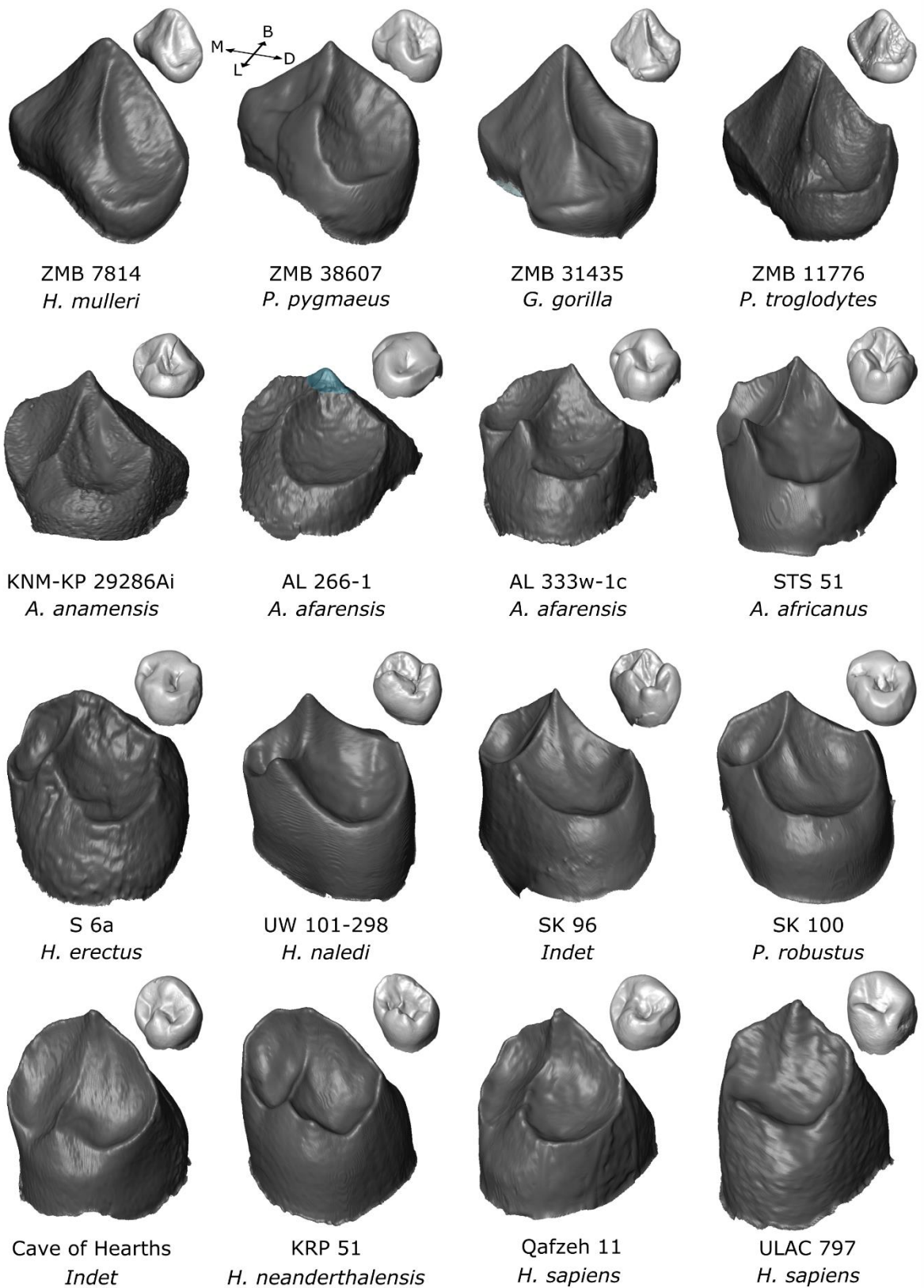


**Figure 11.** The EDJ and OES in oblique view for a number of hominoid species. Two specimens of *A. afarensis* are included, highlighting the variation in  $P_3$  EDJ morphology seen in this species. The protoconid of AL 266-1 is worn, and was reconstructed here for the purpose of GM analysis. The reconstructed section is shown in blue.

these masticatory changes) exhibit little to no tissue contrast, preventing detailed examination of the EDJ surface. Should it be possible to image this surface using synchrotron based imaging techniques (e.g., phase contrast) then it would be possible to assess the EDJ manifestation of outer enamel surface morphology that indicates quite extreme development of, for example, distal accessory cusps.

**Early Homo** The conclusions of this study with respect to early *Homo* are limited due to the limited sample. However, there are a number of specimens which can be discussed. KNM-ER 1802 has typically been suggested to represent early *Homo* species *H. habilis* or *H. rudolfensis* (Leakey, 1974; Groves, 1989; Wood, 1991; Wood, 1992; Spoor *et al.* 2015), but has also been previously suggested to share a number of premolar features with *Australopithecus* and *Paranthropus* taxa (Wood and Uytterschaut, 1987), which is supported here in the finding that at the EDJ, the P<sub>3</sub> of this specimen displays a well-developed talonid and a tall, mesially placed metaconid, and is close to the *P. robustus* range of variation in the EDJ+CEJ PCA (Fig. 6). This result is in contrast to KNM-ER 992, which displays a reduced talonid, a shorter metaconid approximately level with the protoconid, and a flattened, oval shaped CEJ. Some of these features are shared with *A. africanus*, as previously noted by Wood (1991). Although the specimen is thought to be closely aligned with African *H. erectus* (Howell, 1978; Wood, 1991), and was used by Groves and Mazák (1975) as the type specimen of *H. ergaster*, KNM-ER 992 does not here group closely with Sangiran *H. erectus* specimen S6a, potentially pointing to differences in P<sub>3</sub> morphology between African and Asian *H. erectus* (although larger samples are needed to better assess this).

SKX 21204 is from Swartkrans Member 1 and was attributed to *Homo* on the basis of a number of dental and mandibular features (Grine, 1989), although not on the basis of the P<sub>3</sub>, which was unerupted. The EDJ surface morphology of the specimen was analysed by Pan *et al.* (2016), and was found to be within the modern human range of variation. Here, the P<sub>3</sub> is found to display a number of derived features relative to *Australopithecus* specimens, however it is also clearly distinct from

modern humans. This is largely due to the relatively shorter crown height in this specimen, which appears to be one of the main drivers of the separation between late *Homo* specimens and earlier hominins. This can be seen in Supplementary Figure 2, where PC2 is largely driven by crown height. For PC2, SKX 21204 is within the range of *Australopithecus*, *Paranthropus* and other early *Homo* specimens, but distinct from later *Homo* specimens. As may be expected, Sangiran *H. erectus* specimen S6a shows a more derived condition than other early *Homo* specimens, including its position on PC2 which suggests a relatively taller crown, more similar to that of later *Homo* specimens.

**Late Homo** Modern human specimens appear to be highly variable in Figures 6 and 7. This is in part due to the scale of these figures (modern humans are only compared with Neanderthals, which are mostly from one site, Krapina). In Supplementary Figure 2, which includes all taxa in the same PCA, it can be seen that modern humans do show a high level of variation, but this is similar to that seen in *Gorilla* and *P. robustus*. Modern humans are found to be especially variable in the EDJ only analysis, and this is likely due to the variable presence of interrupted or absent marginal ridges. Given that the marginal ridge is the structure on which the landmarks are placed, the GM analysis is likely to be particularly sensitive to variation in the form of this structure.

Whilst *Paranthropus* specimens display frequent, and sometimes large accessory cusps, a number of other hominin taxa display cusps in addition to the protoconid and metaconid, including modern humans. The ASUDAS, a system which aims to characterise the variation in modern human dentition, scores mandibular premolars based on the number of lingual cusps, a trait which includes the metaconid, and varies between zero and three cusps (Turner II *et al.* 1991). There are no modern human specimens in the present analysis with two accessory cusps, but some of the ASUDAS variation may be specific to P<sub>4</sub>s. However, specimens with single accessory cusps can be found in the modern human sample, and moreover, since modern human specimens are found to be quite variable in general it is likely that not all of the variation in modern humans is captured within the

present sample. Another confounding factor is that, at the OES, specimens with a discontinuous marginal ridge may appear similar to those with an accessory cusp (Fig. 3), particularly in worn specimens.

Although modern humans are variable, later *Homo* can be characterised as displaying reduced metaconid development, and increased tendency to show discontinuous marginal ridges. In some ways, this could be viewed as a reversal to the non-human ape and early hominin state of no metaconid development and poorly developed marginal ridges. However, there is a range of considerable differences in, for example, crown height, crown base asymmetry, and the form of the marginal ridge discontinuity (apes and *A. anamensis* tend to show poorly developed marginal ridges, whereas late *Homo* specimens typically show well developed, but interrupted, marginal ridges). These features do not appear to be associated with the reduction in P<sub>3</sub> size seen in modern humans since a similar morphology is seen in the larger Neanderthal P<sub>3</sub>s, for which no significant size differences were found with any of the *Australopithecus* species (Table 3).

**CEJ morphology.** The shape of the CEJ relates to several features previously discussed in relation to P<sub>3</sub> morphology. The occlusal outline, or occlusal crown shape, refers to the 2D shape of the tooth in occlusal view, and has been discussed extensively for fossil hominin teeth (Wood and Uytterschaut, 1987; Asfaw *et al.* 1999; Bailey and Lynch, 2005; Martínón-Torres *et al.* 2006; Gómez-Robles *et al.* 2008). This feature typically pertains to the outward-most protrusion of the enamel on all sides of the tooth, which is likely to refer to the occlusal shape above the level of the CEJ, however the two features are likely to be related. Other studies have referred to the shape of the crown base, which is likely to be analogous to the shape of the CEJ. Specifically, a mesiobuccal protrusion in the crown base has been discussed with reference to early hominin taxa such as *Ar. ramidus* and *A. anamensis* (White *et al.* 1994; Leakey *et al.* 1995).

It has been suggested that the occlusal outline is a poor discriminator of taxa (Strait *et al.* 1997; Strait and Grine, 2004). This appears to also be the case for the shape of the crown base/CEJ given

that there is a large degree of intraspecific variation in CEJ shape within Plio-Pleistocene hominins (Supplementary Figure 1), as well as a relatively low classification accuracy in the CEJ only analysis (Table 4). However, broad patterns can be observed. Non-hominin apes typically have the most strongly asymmetrical CEJ due to the presence of a distinct mesiobuccal expansion of the crown base which helps to create a broad sloping surface along which the upper canine can be honed. In hominins, this mesiobuccal expansion is reduced, making the crown more symmetrical. Late Pleistocene *Homo* specimens have a more oval shaped CEJ relative to *Australopithecus* and *Paranthropus* specimens, and a number of early *Homo* and *H. erectus* specimens also show this oval form. The shape of the CEJ depends, to a large extent, on root formation, and it is likely that the single roots of modern human and Neanderthal P<sub>3</sub>s (Cleghorn *et al.* 2007; Shields, 2015) contribute to the oval shape. Earlier hominins, meanwhile, display a larger range of root morphologies; *A. africanus* and *P. robustus* have highly variable root morphologies (Moore *et al.* 2016), while *H. naledi* P<sub>3</sub>s are typically double-rooted (Berger *et al.* 2015), and *A. afarensis* P<sub>3</sub>s can be single or double rooted (Ward *et al.* 1982). Another feature seen in a number of hominin species, in which the CEJ is raised on the mesial and/or distal sides, also appears to be related to root structure as the CEJ curves over the base of the roots, sitting highest on the tooth crown when in line with the middle of the base of the root, and lowest when in line with inter-radicular grooves.

Modern humans and Neanderthals have a largely similar CEJ shape, however there is often a difference in that Neanderthals more often display an apicocervically flat CEJ, which appears to be a derived feature given that all included hominin species, including modern humans, show some degree of raising of the CEJ on the mesial and distal sides. The condition seen in modern humans is much less pronounced than in *A. africanus* and *P. robustus*, and the expression of this trait varies between specimens, however the difference between modern humans and Neanderthals can be seen in the wireframe models (Fig. 5). This difference may also relate to differences in root structure between the two groups; both groups mostly display single rooted P<sub>3</sub>s, however the expression of traits such as Tomes' root may also influence CEJ form. Given that the Neanderthal sample is derived

mostly from Krapina, it is also possible that an apicocervically flat CEJ is a derived feature of Krapina Neanderthals, specifically. A detailed study of modern human and Neanderthal root morphology, as well as its relation to CEJ shape, would help in further evaluating the difference seen here.

**A. anamensis to A. afarensis.** *A. anamensis* is thought to be the direct ancestor of *A. afarensis*, with the two species representing an anagenetically evolving lineage (Ward *et al.* 1999; Kimbel *et al.* 2006, White *et al.* 2006). The sample only included *A. anamensis* specimens from ~4.2Ma deposits at Kanapoi and *A. afarensis* specimens mostly from Hadar at ~3.2Ma (Johanson *et al.* 1982; Walter, 1994; Leakey *et al.* 1998), meaning there is a 1Myr gap between the samples. Only *A. anamensis* specimen KNM- KP 53160A clusters closely with the *A. afarensis* sample in the EDJ+CEJ analysis (Fig. 6), and given that this is not the case in the EDJ only analysis (Fig. 7), it is likely that this is mostly due to the taller crown in KNM-KP 53160A, compared with KNM-KP 29281 and KNM-KP 29286Ai. In order to better assess this theory using the method used here, a sample of Allia Bay *A. anamensis*, as well as *A. afarensis* from Laetoli, Dikika and Woranso-Mille would be required.

*A. afarensis* has a particularly variable hypodigm; for P<sub>3</sub>s, the crown size, metaconid expression and mesial marginal ridge development are all variable, often independently of one-another, and these features even vary within the same site (Leonard and Hegmon, 1987; Suwa, 1990; Deleuzene and Kimbel, 2011). Two Hadar *A. afarensis* specimens are shown in Figure EDJ, demonstrating some of the variation seen at this site. Moreover, the extent of variation is well demonstrated by the difference between specimens AL333w-1c and AL333-10, both of which are large specimens from the AL333 'first family' collection, but which are well separated in shape space when looking at the EDJ+CEJ analysis (Fig. 6). As previously noted for AL333 specimens (Deleuzene and Kimbel, 2011), both have a well-developed mesial marginal ridge, however AL333w-1c has an anterior fovea which is much narrower buccolingually than that of AL333w-1c, as well as displaying a well-developed metaconid. Despite this variability, it is clear that a number of the features which are common in

later hominins such as *A. africanus* and *P. robustus*, (such as a well-developed metaconid, an increase in talonid size, and a well-developed mesial marginal ridge) do appear first in *A. afarensis*.

#### 4.4 Discrete Traits

**Observer error** Inter- and intra-observer error for the transverse crest and marginal ridge scores is minimal, and is random where present. Error between and within observers is higher for the scoring of buccal grooves, and this is likely because the variation in this trait is essentially continuous, so we would expect to find some disagreement when categorising this variation into a small number of strict grades where the difference between grades may be very minor. It is important to note that the error observed was always between adjacent grades; in no case was there a disagreement between absent (0) and marked (2) buccal grooves. Nonetheless, this level of error is relatively high, and given that the error was present also in the intra-observer error test, future studies should seek to find more replicable category definitions for this trait. Alternatively, a method which directly measures the length and depth of the crest should be used.

**Transverse crest form.** In the majority of hominin P<sub>3</sub>s (79%), a single transverse crest extends lingually from the protoconid to meet the metaconid (or equivalent point on the marginal ridge) (Fig. 2). This is often not the case when looking at non-hominin apes; in *Hylobates*, *Gorilla* and *Pan*, the transverse crest does not typically reach the weakly developed marginal ridge, either ending mesial to the ridge, or deflecting distally. *Pongo* is an exception among the non-hominin apes, and shows the type 1 form in which the transverse crest extends to the lingual edge of the crown. This feature causes the EDJ ridge landmarks to be raised in the middle of the lingual face of the tooth, which can be seen in the wireframe models in Figure 5, and leads to the separation of *Pongo* from the other non-hominin apes in PC1 of the EDJ only analysis (Fig. 7). This feature leads to a superficial resemblance between *Pongo* and the hominins in the wireframe models, however this is not matched by the shape of the rest of the crown, and it seems likely that the presence of a type 1

transverse crest in *Pongo* and the hominins is homoplasious given its absence in all other non-hominins studied here.

The earliest hominin in the sample, *A. anamensis*, displays a type 1 transverse crest, suggesting that this feature evolved early in hominin evolution. Haile-Selassie *et al.* (2004 – pg. 1505) suggest that this is also the case in a 5.6-5.8Ma *Ar. kadabba* P<sub>3</sub>:

*“The transverse crest descends from the tip of the protoconid to the metaconid, which is hardly expressed as a distinct entity”.*

However, this observation would have been made at the OES, rather than the EDJ, meaning that small differences in the configuration of the transverse crest and marginal ridge may be less apparent.

Within hominins, there is relatively little variation in the form of the main transverse crest; excluding those with no transverse crest (type 0), only Neanderthals and KNM-ER 5431E display anything other than type 1. There is more variation in the expression of accessory crests, however (Fig. 2), which form in the occlusal basin either mesial or distal to the main transverse crest, and may connect to the protoconid ridge, marginal ridge, either of the main cusps, or to other accessory crests. In hominin lower molars, multiple crests may form between the protoconid and metaconid, in a feature which shows substantial variation but is generally termed trigonid crest patterning (Wu and Turner II, 1993; Skinner *et al.* 2008b; Bailey *et al.* 2011; Martínez de Pinillos *et al.* 2014). Given the location of these crests, it is possible that these features are homologous to the transverse crest (and accessory crests) discussed here for hominin P<sub>3</sub>s. Trigonid crests are particularly common in Neanderthal lower molars (Bailey *et al.* 2002; Bailey, 2006), which is interesting given the high frequency of accessory crests found here (and previously noted by Bailey, 2006) for Neanderthal P<sub>3</sub>s. Martínez de Pinillos *et al.* (2014) found substantial trigonid crest variation in the Sima de los Huesos population at the EDJ, broadly equivalent to that of Neanderthals. Interestingly, Martínón-Torres *et al.* (2012) report that a high proportion of Sima de los Huesos P<sub>3</sub>s show distal accessory crests, as

well as pronounced transverse crests, when compared with modern humans. This finding could suggest that the same pattern may exist in the Sima de los Huesos population as found here for Neanderthals, although this would require comparing the EDJ morphologies of the two samples.

In P<sub>3</sub>s, the formation of accessory crests seems to be dependent on the space available in the occlusal basin. Neanderthal P<sub>3</sub>s have a high protoconid ridge which creates a steep, almost vertical, lingual facing surface running from the top of the protoconid ridge to the bottom of the occlusal basin of the tooth. Accessory crests are frequently present on this face in Neanderthals. *A. africanus* and *P. robustus* far more often show accessory crests which connect to the main dentine horns, which are often particularly large, or to the transverse crest itself, which is also well developed. Given the level of variation seen in premolar accessory crests, as well as molar trigonid crests, it seems likely that these traits are not individually determined, but are instead the result of upstream developmental processes. There are a number of ways in which this could operate. Firstly, the formation of these crests could be genetically determined, but only able to form where there is sufficient space for them within the occlusal basin of the tooth. In this case, accessory crests could develop through some of the same developmental processes as other crests and ridges on the tooth crown (such as the protoconid crest, transverse crest, and marginal ridges in premolars), but would presumably form later in development than the main crests, which would explain their variability. This process would be analogous to the patterning cascade model of cusp development in which cusps form where there is space for them on the crown, and are prevented from forming too closely to each other by the presence of inhibitor proteins (Polly, 1998; Jernvall, 2000; Kassai *et al.* 2005), with later forming cusps generally smaller and more variable than earlier forming cusps (Kondo and Townsend, 2006; Skinner and Gunz, 2010). Crests are different to cusps in that they are often found in association with other crests. In fact, the accessory cusps identified here were invariably found to be associated with other crests or cusps on the tooth crown. However these features appear to be common in the relatively large posterior fovea of *A. africanus* and *P. robustus*, as well as along the

tall protoconid crest of *H. neanderthalensis*, suggesting that the available space on the crown is important.

Alternatively, these crests could arise as the result of biomechanical forces during the development of the tooth crown. The EDJ preserves the form of the basement membrane of the inner enamel epithelium, the morphology of which is determined by folding driven by differential cell division in structures called enamel knots (Jernvall *et al.* 1994). Since the accessory crests are most common on relatively tall crown structures (dentine horns of *P. robustus*, and the protoconid ridge of Neanderthals), it is possible that during the formation of these structures, the inner enamel epithelium is 'pulled' in such a way that small buckles and folds form, which go on to become the accessory ridges seen. It is important to note that no specimens in the sample displayed accessory crests running parallel to the protoconid ridge or the dentine horn tip; all run towards the crest/ridge. In this case accessory crests would likely be developmentally distinct from the main crests and ridges of the tooth crown, which are far less variable within species.

**Marginal ridge.** This trait was only scored for hominin specimens since non-hominin apes have poorly developed marginal ridges. Marginal ridge discontinuity is present in the earliest hominins in our sample, appearing in all three *A. anamensis* specimens, and 2/4 *A. afarensis* specimens. Subsequently, the majority of *A. africanus* specimens (9/12), and all *Paranthropus* specimens display a continuous marginal ridge. If the inferred ancestral condition is considered to be non-human ape-like in nature, then the 'discontinuity' seen in early *Australopithecus* may in fact represent the initial stages of the development of the P<sub>3</sub> occlusal surface for improved mastication. In this sense, the discontinuity may be more properly interpreted as a lack of complete development of an enclosing marginal ridge. In later *Australopithecus* and *Paranthropus*, the marginal ridge is well-developed and largely continuous, reflecting the increased masticatory ability of the P<sub>3</sub>. Discontinuity of the marginal ridge appears much more often among Late Pleistocene *Homo* P<sub>3</sub>s, where they are present in nearly half of all specimens (14/30 = 47%). Along with the single *Homo*

*heidelbergensis* P<sub>3</sub> included here, modern humans are the only hominin species in this sample to have specimens which display mesial and distal marginal ridge interruption. In this case, this is likely due to the secondarily reduced metaconid development in these Late Pleistocene *Homo* species, and is likely to reflect changing masticatory demands of the P<sub>3</sub> in these taxa.

Sakai (1976) recorded the presence of a 'trigonid notch' when looking at the EDJ of modern human P<sub>3</sub>s, a feature which is equivalent to the mesial marginal ridge interruption noted here. They found the feature in roughly a quarter of specimens in their sample, but did not discuss any presence of a similar feature on the distal marginal ridge (although this feature is rarer in the present sample). This trait is much clearer at the EDJ than at the OES as the interruptions can be small, and are often located immediately next to the metaconid where the enamel of the cusp may obscure visibility of the interruption at the OES. In fact, Sakai (1976) only found the trigonid notch at the EDJ, and stated that the feature was entirely absent at the OES in all specimens.

**Buccal grooves.** Within the sample used here, buccal grooves are universally present (minor or marked) in all *Australopithecus* specimens on both the mesial and distal sides of the crown. They are much less common in non-hominin apes, *Paranthropus*, and late-Pleistocene *Homo* P<sub>3</sub>s, but are still occasionally seen. It seems that they are more commonly seen in those specimens which show a straight protoconid ridge, which tends to be a feature of *Australopithecus* P<sub>3</sub>s. When the protoconid ridge is straight, there is a more angled intersection between the protoconid ridge and the mesial/distal marginal ridge, often marked by a small accessory cusp. The buccal ridge is visible as a vertical crest on the buccal surface, as well as a slight concavity next to the ridge (towards the centre of the crown), which could be considered an extension of the marginal ridge on the buccal surface. Sakai (1967) scored the presence of buccal grooves in modern human P<sub>3</sub>s at the EDJ, where they were considered to be a primitive feature. The results support this assumption, with buccal grooves seen far less in modern humans (as well as other Late-Pleistocene *Homo*) than in *Australopithecus* P<sub>3</sub>s. Suwa (1996) suggested that weak or absent distal buccal grooves are a unique derived feature of

early *Homo P<sub>3</sub>s*. Only a small number of early *Homo P<sub>3</sub>s* were able to be scored for this trait at the EDJ, however KNM-ER 806E displayed no distal buccal groove, while KNM-ER 992 and KNM-WT 15000 display very little sign of distal buccal grooves at the OES (although this could not be assessed at the EDJ). SKX 21204, on the other hand, does show a minor distal buccal groove at the EDJ, and STW 151 displays a marked distal buccal groove.

Based on their analysis of the EDJ of mandibular molars, Skinner and colleagues (2009b) suggested that crests on the buccal face of the protoconid and hypoconulid should be considered part of the protostylid dental trait in mandibular molars. It should be considered whether the buccal grooves present on *P<sub>3</sub>s* are developmentally homologous to these features in mandibular molars. For example, STW 213 (Fig. 4) exhibits strong buccal grooves in addition to protostylid-like crests running diagonally across the buccal face towards the protoconid. In this case, the buccal groove and possible protostylid appear to be separate features, but it is interesting to note that this was present on the *P<sub>3</sub>* with the most well defined buccal grooves of any specimen within the sample. Ultimately, further investigation is required to assess the developmental basis of both of these traits.

**Protoconid form.** The transversely expanded dentine horn seen in ULAC 58 may be related to the 'internally placed cusps' identified at the OES of Neanderthal molars (Tattersall and Schwartz, 1999; Bailey, 2004), as well as the 'centrally placed dentine horn tips' identified by Martin *et al.* (2017) for Neanderthal and modern human molars at the EDJ. In fact, the modern human mandible, ULAC 58, for which the present study observed the longitudinally expanded dentine horn tip (Fig. 10D), was also included in the sample for Martin *et al.* (2017), where they found that the *M<sub>1</sub>* and *M<sub>3</sub>* displayed a centrally placed entoconid dentine horn.

Martin *et al.* (2017) found that centrally located dentine horns were common in Neanderthals. Although this study did not find any longitudinally expanded dentine horns in Neanderthal specimens, it was found that in a number of Neanderthal *P<sub>3</sub>s*, the apex of the protoconid ridge and the tip of the protoconid are angled lingually, resulting in a more centrally located protoconid. This

can be seen in the occlusal view of the Neanderthal wireframe model (Fig. 5). This condition has been previously suggested to be distinctive of the P<sub>3</sub>s of both Neanderthals and *H. heidelbergensis*, and may also be related to the centrally placed molar dentine horns identified by Martin *et al.* (2017).

Another trait discussed here, namely the longitudinally expanded dentine horn (Fig. 10C), also relates to a feature discussed by Martin *et al.* (2017); twinned dentine horns. This study did not find this trait in any modern human or Neanderthal specimens, but it was found in a high proportion of *H. naledi* P<sub>3</sub>s, as well as a single *Pan* specimen. In some cases, the *H. naledi* P<sub>3</sub> protoconid appears to be simply expanded, rather than twinned, although it is possible that the separate apices of the twinned dentine horns are too small to be visible in the scans. Martin *et al.* (2017) also found specimens which showed 'unusually wide' dentine horns, and suggested this may be a diminutive form of the twinned dentine horn trait. These traits are particularly interesting since they are difficult to reconcile with the currently well-accepted patterning cascade model of cuspal development (Polly, 1998; Jernvall 2000; Kondo and Townsend, 2006; Skinner and Gunz, 2010), in which cusps develop iteratively across the crown, and that a zone of inhibition during crown development prevents the formation of cusps in close proximity to one-another. Neither of the protoconid traits described here were seen on P<sub>3</sub> metaconids, although this may be due a combination of the rarity of the features, and the reduced number of specimens displaying a well-developed metaconid.

## 5. Conclusion

This study suggests that mandibular third premolars hold a wealth of taxonomically important information, and that geometric morphometric analysis of P<sub>3</sub> EDJ shape is able to accurately distinguish between hominoid taxa.

The non-hominin apes have a P<sub>3</sub> morphology which is specialised for its role in honing the large upper canine. The wireframe models show a tall crown, and a mesiobuccally expanded CEJ which is

lowered, apically, in order to provide a long, broad sloping surface for the upper canine. Features related to mastication, such as the presence of strong marginal ridges and additional cusps, are mostly absent. Early hominin evolution can be characterised by the gradual loss of features relating to canine honing such as reduction of the protoconid and the mesiobuccal expansion of the crown base. Moreover, we see the gradual accumulation of features related to improved masticatory abilities such as the enclosing of the occlusal surface of the tooth through the development of a continuous marginal ridge, and the development of a large metaconid. The earliest members of *Homo* appear to have a morphology largely similar to that of a number of *Australopithecus* specimens, although there are differences, which require further investigation though looking at the EDJ of a larger sample of early *Homo* specimens. Late-Pleistocene *Homo* taxa have a distinct morphology which includes a tall crown and increased frequency of marginal ridge discontinuity associated with a reduction of the metaconid. The morphology of the P<sub>3</sub> in these taxa likely reflects the altered dietary adaptations in late-*Homo* taxa related to their increased geographical range, differing climates and increased dietary specialisms.

Studies of the EDJ in fossil hominins remain important in improving the amount of morphological information that can be gained from worn dental specimens. This allows the study of larger samples and the utilisation of as much fossil material as possible. It also allows us to study aspects of dental morphology which may not be obvious at the OES, such as the presence of discontinuous marginal ridges, which may point to important details on tooth development and assist in our understanding of dental homology.

## Reference List

- Anemone, R.L., Skinner, M.M., and Dirks, W., 2012. Are there two distinct types of hypocone in Eocene primates? The 'pseudohypocone' of notharctines revisited. *Palaeontol. Electron.* 15, 1-13.
- Anton, S.C., Potts, R., and Aiello, L.C., 2014. Evolution of early Homo: An integrated biological perspective. *Science* 345, 45.
- Argue, D., Groves, C.P., Lee, M.S.Y., and Jungers, W.L., 2017. The affinities of *Homo floresiensis* based on phylogenetic analyses of cranial, dental, and postcranial characters. *J. Hum. Evol.* 107, 107-133.
- Arnaud, J., Peretto, C., Panetta, D., Tripodi, M., Fontana, F., Arzarello, M., Thun Hohenstein, U., Berto, C., Sala, B., Oxilia, G., Salvadori, P.A., and Benazzi, S., 2016. A reexamination of the Middle Paleolithic human remains from Riparo Tagliente, Italy. *Quat. Int.* 425, 437-444.
- Asfaw, B., White, T., Lovejoy, O., Latimer, B., Simpson, S., and Suwa, G., 1999. *Australopithecus garhi*: a new species of early hominid from Ethiopia. *Science* 284, 629-635.
- Averianov, A.O., and Archibald, J.D., 2015. Evolutionary transition of dental formula in Late Cretaceous eutherian mammals. *Sci. Nat.* 102, 56.
- Bailey, S.E., 2000. Dental morphological affinities among late Pleistocene and recent humans. *Dent. Anth.* 14, 1-8.
- Bailey, S.E., 2002. A closer look at Neanderthal postcanine dental morphology: the mandibular dentition. *Anat. Rec.* 269, 148-156.
- Bailey SE. 2006. Beyond shovel shaped incisors: Neanderthal dental morphology in a comparative context. *Period. Biol.* 108, 253–267.
- Bailey, S.E., and Lynch, J.M., 2005. Diagnostic differences in mandibular P4 shape between Neanderthals and anatomically modern humans. *Am. J. Phys. Anth.* 126, 268-277.
- Bailey, S.E., Skinner, M.M., and Hublin, J., 2011. What lies beneath? An evaluation of lower molar trigonid crest patterns based on both dentine and enamel expression. *Am. J. Phys. Anth.* 145, 505-518.
- Bailey, S.E., Benazzi, S., Souday, C., Astorino, C., Paul, K., and Hublin, J., 2014. Taxonomic differences in deciduous upper second molar crown outlines of *Homo sapiens*, *Homo neanderthalensis* and *Homo erectus*. *J. Hum. Evol.* 72, 1-9.
- Benazzi, S., Fornai, C., Bayle, P., Coquerelle, M., Kullmer, O., Mallegni, F., and Weber, G.W., 2011. Comparison of dental measurement systems for taxonomic assignment of Neanderthal and modern human lower second deciduous molars. *J. Hum. Evol.* 61, 320-326.
- Berger, L.R., Hawks, J., de Ruiter, D.J., Churchill, S.E., Schmid, P., Delezene, L.K., Kivell, T.L., Garvin, H.M., Williams, S.A., DeSilva, J.M., Skinner, M.M., Musiba, C.M., Cameron, N., Holliday, T.W., Harcourt-Smith, W., Ackermann, R.R., Bastir, M., Bogin, B., Bolter, D., Brophy, J., Cofran, Z.D., Congdon, K.A., Deane, A.S., Dembo, M., Drapeau, M., Elliott, M.C., Feuerriegel, E.M., Garcia-Martinez, D., Green, D.J., Gurtov, A., Irish, J.D., Kruger, A., Laird, M.F., Marchi, D., Meyer, M.R., Nalla,

S., Negash, E.W., Orr, C.M., Radovic, D., Schroeder, L., Scott, J.E., Throckmorton, Z., Tocheri, M.W., Vansickle, C., Walker, C.S., Wei, P., and Zipfel, B., 2015. *Homo naledi*, a new species of the genus *Homo* from the Dinaledi Chamber, South Africa. *eLife* 4, e09560.

Bermúdez de Castro, J.M., 1993. The Atapuerca dental remains. New evidence (1987-1991 excavations) and interpretations. *J. Hum. Evol.* 24, 339-371.

Bermúdez de Castro, J.M., and Nicolas, M.E., 1995. Posterior dental size reduction in hominids: the Atapuerca evidence. *Am. J. Phys. Anth.* 96, 335-356.

Bermúdez de Castro, J.M., Rosas, A., and Nicolas, M.E., 1999. Dental remains from Atapuerca-TD6 (Gran Dolina site, Burgos, Spain). *J. Hum. Evol.* 37, 523-566.

Beynon, A.D., and Wood, B.A., 1986. Variations in enamel thickness and structure in East African hominids. *Am. J. Phys. Anth.* 70, 177-193.

Bjarnason, A., Chamberlain, A.T., and Lockwood, C.A., 2011. A methodological investigation of hominoid craniodental morphology and phylogenetics. *J. H. Evol.* 60, 47-57.

Brace, C.L., 1967. Environment, tooth form, and size in the Pleistocene. *J. Dent. Res.* 46, 809-816.

Brown, B., Brown, F.H., and Walker, A., 2001. New hominids from the Lake Turkana basin, Kenya. *J. Hum. Evol.* 41, 29-44.

Brunet, M., Guy, F., Pilbeam, D., Mackaye, H.T., Likius, A., Ahounta, D., Beauvilain, A., Blondel, C., Bocherens, H., Boisserie, J. De Bonis, L., Coppens, Y., Dejax, J., Denys, C., Dourner, P., Eisenmann, V., Fanone, G., Fronty, P., Geraads, D., Lehmann, T., Lihoreau, F., Louchart, A., Mahamat, A., Merceron, G., Mouchelin, G., Otero, O., Campomanes, P.P., De Leon, M.P., Rage, J., Sapanet, M., Schuster, M., Sudre, J., Tassy, P., Valentin, X., Vignaud, P., Viriot, L., Zazzo, A., and Zollikofer, C., 2002. A new hominid from the Upper Miocene of Chad, Central Africa. *Nature* 418, 145-151.

Burnett, S.E., Irish, J.D., and Fong, M.R., 2013. Wear's the problem? Examining the effect of dental wear on studies of crown morphology. In: Scott, R.S., and Irish, J.D. (Eds.), *Anthropological Perspectives on Tooth Morphology: Genetics, Evolution, Variation*, Cambridge University Press, Cambridge, pp. 535-545.

Butler, P.M., 1939. Studies of the mammalian dentition. Differentiation of the post-canine dentition. *Proc. Zool. Soc. Lond. B.* 109, 1-36

Butler, P.M., 1956. The ontogeny of molar pattern. *Biol. Rev.* 31, 30-69.

Butler, P. M., 1967. Dental merism and tooth development. *J. Dent. R.* 46, 845-50.

Cifelli, R., 2000. Counting premolars in early eutherian mammals. *Acta Palaeontol. Pol.* 45, 195-198.

Ciochon, R.L., Piperno, D.R., and Thompson, R.G., 1990. Opal phytoliths found on the teeth of the extinct ape *Gigantopithecus blacki*: implications for paleodietary studies. *PNAS* 87, 8120-8124.

Collard, M., and Wood, B., 2000. How reliable are human phylogenetic hypotheses? *Proc. Nat. Acad. Sci.* 97, 5003-5006.

Conroy, G.C., 1991. Enamel thickness in South African australopithecines: noninvasive evaluation by computed tomography. *Palaeont. Afr.* 28, 53-59.

Cooke, S.B., 2011. Paleodiet of extinct platyrrhines with emphasis on the Caribbean forms: three-dimensional geometric morphometrics of mandibular second molars. *Anat. Rec. (Hoboken)* 294, 2073-2091.

Corruccini, R.S., 1987. The dentinoenamel junction in primates. *Int. J. Primatol.* 8, 99-114.

Crevecoeur, I., Skinner, M.M., Bailey, S.E., Gunz, P., Bortoluzzi, S., Brooks, A.S., Burlet, C., Cornelissen, E., De Clerck, N., Maureille, B., Semal, P., Vanbrabant, Y., and Wood, B., 2013. First Early Hominin from Central Africa (Ishango, Democratic Republic of Congo). *PLoS ONE* 9, e84652.

Curnoe, D., 2003. Problems with the use of cladistic analysis in palaeoanthropology. *HOMO – J. Comp. Hum. Biol.* 53, 225-234.

Daegling, D.J., and Grine, F.E., 1994. Bamboo feeding, dental microwear, and diet of the Pleistocene ape *Gigantopithecus blacki*. *S. Af. J. Sci.* 90, 527-532.

Dahlberg, A.A., 1945. The changing of dentition of man. *JADA.* 32, 676-690.

Danilo, L., Remy, J.A., Vianey-Liaud, M., Marandat, B., Sudre, J., and Lihoreau, F., 2013. A new Eocene locality in southern France sheds light on the basal radiation of Palaeotheriidae (Mammalia, Perissodactyla, Equoidea). *J. Vert. Pal.* 33, 195-215.

Dart, R.A., 1948. The first human mandible from the Cave of Hearths, Makapansgat. *S. Af. Arch. Bul.* 3, 96-98.

Dean, M.C., and Beynon, A.D., 1991. Tooth crown heights, tooth wear, sexual dimorphism and jaw growth in hominoids. *Zeitsch. Morph. Anth.* 78, 425-440.

Deleuzene, L.K., 2015. Modularity of the anthropoid dentition: Implications for the evolution of the hominin canine honing complex. *J. Hum. Evol.* 86, 1-12.

Deleuzene, L.K., and Kimbel, W.H., 2011. Evolution of the mandibular third premolar crown in early australopithecus. *J. Hum. Evol.* 60, 711-730.

Dembo, M., Matzke, N.J., Mooers, A.Å., and Collard, M., 2015. Bayesian analysis of a morphological supermatrix sheds light on controversial fossil hominin relationships. *Proc. Biol. Sci.* 282, 20150943.

Dembo, M., Radovčić, D., Garvin, H.M., Laird, M.F., Schroeder, L., Scott, J.E., Brophy, J., Ackermann, R.R., Musiba, C.M., and de Ruiter, D.J., 2016. The evolutionary relationships and age of *Homo naledi*: An assessment using dated Bayesian phylogenetic methods. *J. Hum. Evol.* 97, 17-26.

Dryden, I., and Mardia, K.V., 1998. *Statistical Shape Analysis*. John Wiley and Sons, New York.

Feldhamer, G.A., Drickamer, L.C., Vessey, S.H., Merritt, J.F., and Krajewski, C., 2015. *Mammalogy: Adaptation, Diversity, Ecology*. Johns Hopkins University Press.

Fornai, C., Bookstein, F.L., and Weber, G.W., 2015. Variability of *Australopithecus* second maxillary molars from Sterkfontein Member 4. *J. Hum. Evol.* 85, 181-192.

- Goldberg, M., Septier, D., Lecolle, S., Chardin, H., Quintana, M.A., Acevedo, A.C., Gafni, G., Dillouya, D., Vermelin, L. and Thonemann, B., 1995. Dental mineralization. *Int. J. Dev. Biol.* 9, 93-110.
- Gómez-Robles, A., Martínón-Torres, M., Bermúdez de Castro, J.M., Margvelashvili, A., Batir, M., Arsuaga, J.L., Perez-perez, A., Estebaranz, F., and Martínez, L.M., 2007. A geometric morphometric analysis of hominin upper first molar shape. *J. Hum. Evol.* 53, 272-285.
- Gómez-Robles, A., Martínón-Torres, M., Bermúdez de Castro, J.M., Prado, L., Sarmiento, S., and Arsuaga, J.L., 2008. Geometric morphometric analysis of the crown morphology of the lower first premolar of hominins, with special attention to Pleistocene Homo. *J. Hum. Evol.* 55, 627-638.
- Gómez-Robles, A., Martínón-Torres, M., Bermúdez de Castro, J.M., Prado-Simón, L., and Arsuaga, J.L., 2011. A geometric morphometric analysis of hominin upper premolars. Shape variation and morphological integration. *J. Hum. Evol.* 61, 688-702.
- Gómez-Robles, A., Bermúdez de Castro, J.M., Martínón-Torres, M., Prado-Simón, L., and Arsuaga, J.L., 2012. A geometric morphometric analysis of hominin upper second and third molars, with particular emphasis on European Pleistocene populations. *J. Hum. Evol.* 63, 512-526.
- Gómez-Robles, A., Bermúdez de Castro, J.M., Martínón-Torres, M., Prado-Simón, L., and Arsuaga, J.L., 2015. A geometric morphometric analysis of hominin lower molars: Evolutionary implications and overview of postcanine dental variation. *J. Hum. Evol.* 82, 34-50.
- Goodall, C., 1991. Procrustes methods in the statistical analysis of shape. *J. R. Stat. Soc. Series. B. Stat. Methodol.* 53, 285-339.
- Gower, J.C., 1975. Generalized Procrustes analysis. *Psychometrika* 40, 33-51.
- Greenfield, L.O., 1992. Origin of the human canine: A new solution to an old enigma. *Am. J. Phys. Anth.* 35, 153-185.
- Greenfield, L.O., and Washburn, A., 1992. Polymorphic aspects of male anthropoid honing premolars. *Am. J. Phys. Anth.* 87, 173-186.
- Grine, F.E., 1986. Dental evidence for dietary differences in Australopithecus and Paranthropus: a quantitative analysis of permanent molar microwear. *J. Hum. Evol.* 15, 783-822.
- Grine, F.E., 1989. New hominid fossils from the Swartkrans Formation (1979–1986 excavations): craniodental specimens. *Am. J. Phys. Anth.* 79, 409-449.
- Grine, F.E., and Martin, L., 1988. Enamel thickness and development in Australopithecus and Paranthropus. In: *Evolutionary History of the Robust Australopithecines*, Grine, F. E. (Ed.), (New York: Aldine de Gruyter) pp. 3-42.
- Grine, F.E., Sponheimer, M., Ungar, P.S., Lee-Thorp, J., and Teaford, M.F., 2012. Dental microwear and stable isotopes inform the paleoecology of extinct hominins. *Am. J. Phys. Anth.* 148, 285-317.
- Groves, C. P., 1989. *A Theory of Human and Primate Evolution*. Clarendon Press
- Groves, C.P., and Mazák, V., 1975. An approach to the taxonomy of the Hominidae: gracile Villafranchian hominids of Africa. *Cas. Min. Geol.* 20, 225–247.

Guy, F., Lazzari, V., Gilissen, E., and Thiery, G., 2015. To What Extent is Primate Second Molar Enamel Occlusal Morphology Shaped by the Enamel-Dentine Junction? *PLoS One* 10, e0138802.

Haile-Selassie, Y., 2001. Late Miocene hominids from the Middle Awash, Ethiopia. *Nature* 412, 178-181.

Haile-Selassie, Y., Suwa, G., White, T.D., 2004. Late Miocene teeth from Middle Awash, Ethiopia, and early hominid dental evolution. *Science* 303, 1503-1505.

Harris, E.F., 2007. Carabelli's trait and tooth size of human maxillary first molars. *Am. J. Phys. Anth.* 132, 238-246.

Howell, F. C., 1978. Hominidae. In: VJ Maglio and HBS Cooke (Eds), *Evolution of African Mammals*. Cambridge, Harvard University Press.

Huggins, C.B., McCarroll, H.R., and Dahlberg, A.A., 1934. Transplantation of tooth germ elements and the experimental heterotopic formation of dentin and enamel. *J. Exp. Med.* 60, 199-210.

Hunter, J.P., Guatelli-Steinberg, D., Weston, T.C., Durner, R., and Betsinger, T.K., 2010. Model of tooth morphogenesis predicts carabelli cusp expression, size, and symmetry in humans. *PLoS One* 5, e11844.

Irish, J.D., 1997. Characteristic high- and low-frequency dental traits in sub-Saharan African populations. *Am. J. Phys. Anth.* 102, 455-467.

Irish, J.D., 1998. Ancestral dental traits in recent Sub-Saharan Africans and the origins of modern humans. *J. Hum. Evol.* 34, 81-98.

Irish, J.D., and Guatelli-Steinberg, D., 2003. Ancient teeth and modern human origins: an expanded comparison of African Plio-Pleistocene and recent world dental samples. *J. Hum. Evol.* 45, 113-144.

Irish, J.D., Guatelli-Steinberg, D., Legge, S.S., de Ruiter, D.J., and Berger, L.R., 2013. Dental morphology and the phylogenetic "place" of *Australopithecus sediba*. *Science* 340, 1233062

Jernvall, J., 2000. Linking development with generation of novelty in mammalian teeth. *PNAS* 97, 2641-2645.

Jernvall, J., and Thesleff, I., 2000. Reiterative signaling and patterning during mammalian tooth morphogenesis. *Mech. Dev.* 92, 19-29.

Jernvall, J., Kettunen, P., Karavanova, I., Martin, L.B., and Thesleff, I., 1994. Evidence for the role of the enamel knot as a control center in mammalian tooth cusp formation: non-dividing cells express growth stimulating Fgf-4 gene. *Int. J. Dev. Biol.* 38, 463-469.

Johanson, D., and White, T., 1979. A systematic assessment of early African hominids. *Science* 203, 321-330.

Kassai, Y., Munne, P., Hotta, Y., Penttila, E., Kavanagh, K., Ohbayashi, N., Takada, S., Thesleff, I., Jernvall, J., and Itoh, N., 2005. Regulation of mammalian tooth cusp patterning by ectodin. *Science* 309, 2067-2070.

- Kay, R.F., 1977. The evolution of molar occlusion in the Cercopithecidae and early catarrhines. *Am. J. Phys. Anth.* 46, 327-352.
- Keranen, S., Aberg, T., Kettunen, P., Thesleff, I., and Jernvall, J., 1998. Association of developmental regulatory genes with the development of different molar tooth shapes in two species of rodents. *Dev. Genes Evol.* 208, 477-486.
- Kimbel, W.H., and Deleuzene, L.K., 2009. "Lucy" redux: A review of research on *Australopithecus afarensis*. *Am. J. Phys. Anth.* 140, 2-48.
- Kluge, A.G., 1989. A concern for evidence and a phylogenetic hypothesis of relationships among *Epicrates* (Boidae, Serpentes). *Syst. Biol.* 38, 7-25.
- Koenigswald, G.H.R., 1940. Neue Pithecanthropus-Funde 1936-1938: ein Beitrag zur Kenntnis der Praehominiden. Landsdrukkerij.
- Kollar, E.J. and Baird, G.A., 1969. The influence of the dental papilla on the development of tooth shape in embryonic mouse tooth germs. *J. Embryol. Exp. Morphol.* 21, 131-148.
- Kondo, S., and Townsend, G.C., 2006. Associations between Carabelli trait and cusp areas in human permanent maxillary first molars. *Am. J. Phys. Anth.* 129, 196-203.
- Kono, R.T., 2004. Molar enamel thickness and distribution patterns in extant great apes and humans: new insights based on a 3-dimensional whole crown perspective. *Anthr. Sci.* 112, 121-146.
- Kraus, B.S., 1952. Morphologic relationships between enamel and dentin surfaces of lower first molar teeth. *J. Dent. Res.* 31, 248-256.
- Kraus, B.S., and Furr, M.L., 1953. Lower first premolars. I. A definition and classification of discrete morphologic traits. *J. Dent. Res.* 32, 554-564.
- Kubo, D., Kono, R.T., and Kaifu, Y., 2013. Brain size of *Homo floresiensis* and its evolutionary implications. *Proc. R. Soc. B.* 280, 20130338
- Leakey, R.E.F., 1974. Further evidence of Lower Pleistocene hominids from East Rudolf, North Kenya, 1973. *Nature* 248, 653-656.
- Leakey, L.S.B., Tobias, P.V., and Napier, J.R., 1964. A new species of the genus *Homo* from Olduvai Gorge. *Nature* 202, 7-9.
- Lee-Thorp, J.A., van der Merwe, N.J., and Brain, C., 1994. Diet of *Australopithecus robustus* at Swartkrans from stable carbon isotopic analysis. *J. Hum. Evol.* 27, 361-372.
- Lee-Thorp, J.A., Sponheimer, M., and van der Merwe, N.J., 2003. What do stable isotopes tell us about hominid dietary and ecological niches in the Pliocene? *Int. J. Ost.* 13, 104-113.
- Leonard, W.R., and Hegmon, M., 1987. Evolution of P3 Morphology in *Australopithecus afarensis*. *Am. J. Phys. Anth.* 73, 41-63.
- Lieberman, D.E., Wood, B.A., and Pilbeam, D.R., 1996. Homoplasy and early *Homo*: an analysis of the evolutionary relationships of *H. habilis sensu stricto* and *H. rudolfensis*. *J. Hum. Evol.* 30, 97-120.

- Linde, A., 1984. *Dentin and Dentinogenesis*, Vols. I and I, CRC Press
- Linde, A. and Goldberg, M., 1993. *Dentinogenesis*. *Crit. Rev. Or. Biol. Med.* 4, 679-728.
- Lucas, P.W., Corlett, R.T., and Luke, D.A., 1985. Plio-Pleistocene hominid diets: an approach combining masticatory and ecological analysis. *J. Hum. Evol.* 14, 187-202.
- Ludwig, F.J., 1957. The mandibular second premolars: morphologic variation and inheritance. *J. Dent. Res.* 36, 263-273.
- Macho, G.A., and Thackeray, J.F., 1992. Computed tomography and enamel thickness of maxillary molars of Plio-Pleistocene hominids from Sterkfontein, Swartkrans, and Kromdraai (South Africa): An exploratory study. *Am. J. Phys. Anth.* 89, 133-143.
- Manthi, F.K., Plavcan J.M., Ward, C.V., 2012. New hominin fossils from Kanapoi, Kenya, and the mosaic evolution of canine teeth in early hominins. *S. Afr. J. Sci.* 108, 1-9
- Martin, L., 1985. Significance of enamel thickness in hominoid evolution. *Nature* 314, 260-263.
- Martínez de Pinillos, M., Martínón-Torres, M., Skinner, M.M., Arsuaga, J.L., Gracia-Téllez, A., Martínez, I., Martín-Francés, L., and Bermúdez de Castro, J.M., 2014. Trigonid crests expression in Atapuerca-Sima de los Huesos lower molars: Internal and external morphological expression and evolutionary inferences. *Comptes Rendus Palevol* 13, 205-221.
- Martinón-Torres, M., Bastir, M., Bermúdez de Castro, J.M., Gomez, A., Sarmiento, S., Muela, A., and Arsuaga, J.L., 2006. Hominin lower second premolar morphology: evolutionary inferences through geometric morphometric analysis. *J. Hum. Evol.* 50, 523-533.
- Martinón-Torres, M., de Castro, J.M.B., Gómez-Robles, A., Prado-Simón, L., and Arsuaga, J.L., 2012. Morphological description and comparison of the dental remains from Atapuerca-Sima de los Huesos site (Spain). *J. Hum. Evol.* 62, 7-58.
- Martínez de Pinillos, M., Martínón-Torres, M., Skinner, M.M., Arsuaga, J.L., Gracia-Téllez, A., Martínez, I., Martín-Francés, L., and de Castro, J.M.B., 2014. Trigonid crests expression in Atapuerca-Sima de los Huesos lower molars: Internal and external morphological expression and evolutionary inferences. *Comptes Rendus Palevol*, 13, 205-221.
- McCollum, M.A., 1999. The robust australopithecine face: a morphogenetic perspective. *Science*, 284, 301-305.
- Miletich, I. and Sharpe, P.T., 2003. Normal and abnormal dental development. *Human molecular genetics*, 12(suppl\_1), pp.R69-R73.
- Moggi-Cecchi, J., Tobias, P.V., and Beynon, A.D., 1998. The mixed dentition and associated skull fragments of a juvenile fossil hominid from Sterkfontein, South Africa. *Am. J. Phys. Anth.* 106, 425-465.
- Moggi-Cecchi, J., Grine, F.E., and Tobias, P.V., 2006. Early hominid dental remains from Members 4 and 5 of the Sterkfontein Formation (1966-1996 excavations): catalogue, individual associations, morphological descriptions and initial metrical analysis. *J. Hum. Evol.* 50, 239-328.

- Molnar, S., 1971. Human tooth wear, tooth function and cultural variability. *Am. J. Phys. Anth.* 34, 175-189.
- Molnar, S., and Gantt, D.G., 1977. Functional implications of primate enamel thickness. *Am. J. Phys. Anth.* 46, 447-454.
- Moore, N.C., Thackeray, J.F., Hublin, J.J., and Skinner, M.M., 2016. Premolar root and canal variation in South African Plio-Pleistocene specimens attributed to *Australopithecus africanus* and *Paranthropus robustus*. *J. Hum. Evol.* 93, 46-62.
- Morita, W., Yano, W., Nagaoka, T., Abe, M., Ohshima, H., and Nakatsukasa, M., 2014. Patterns of morphological variation in enamel-dentin junction and outer enamel surface of human molars. *J. Anat.* 224, 669-680.
- Morita, W., 2016. Morphological comparison of the enamel–dentine junction and outer enamel surface of molars using a micro-computed tomography technique. *J. Oral Bio.* 58, 95-99.
- Morris, D.H., 1986. Maxillary molar occlusal polygons in five human samples. *Am. J. Phys. Anth.* 70, 333-338.
- Nager, G., 1960. Der vergleich zwischen dem raumlichen verhalten des dentin-kronenreliefs und dem schmelzrelief der zahnkrone. *Acta Anat.* 42, 226–250
- Nanci, A., 2008. *Ten Cate's Oral Histology: Development, Structure, and Function* (Mosby Elsevier)
- Ni, X., Gebo, D.L., Dagosto, M., Meng, J., Tafforeau, P., Flynn, J.J., and Beard, K.C., 2013. The oldest known primate skeleton and early haplorhine evolution. *Nature* 498, 60-64.
- O'Leary, M.A., Bloch, J.I., Flynn, J.J., Gaudin, T.J., Giallombardo, A., Giannini, N.P., Goldberg, S.L., Kraatz, B.P., Luo, Z., Meng, J., Ni, X., Novacek, M.J., Perini, F.A., Randall, Z.S., Rougier, G.W., Sargis, E.J., Silcox, M.T., Simmons, N.B., Spaulding, M., Velazco, P.M., Weksler, M., Wible, J.R., and Cirranello, A.L., 2013. The placental mammal ancestor and the post-K-Pg radiation of placentals. *Science* 339, 662-667.
- Olejniczak, A.J., Martin, L.B., and Ulhaas, L., 2004. Quantification of dentine shape in anthropoid primates. *Annals Anat. – Anat. Anz.* 186, 479-485.
- Olejniczak, A.J., Smith, T.M., Skinner, M.M., Grine, F.E., Feeney, R.N.M., Thackeray, J.F., and Hublin, J.J., 2008. Three-dimensional molar enamel distribution and thickness in *Australopithecus* and *Paranthropus*. *Biol. Letters* 4, 406-410.
- Ortiz, A., Skinner, M.M., Bailey, S.E., and Hublin, J.J., 2012. Carabelli's trait revisited: An examination of mesiolingual features at the enamel–dentine junction and enamel surface of *Pan* and *Homo sapiens* upper molars. *J. Hum. Evol.* 63, 586-596.
- Pan, L., Dumoncel, J., de Beer, F., Hoffman, J., Thackeray, J.F., Duployer, B., Tenailleau, C., and Braga, J., 2016. Further morphological evidence on South African earliest *Homo* lower postcanine dentition: Enamel thickness and enamel dentine junction. *J. Hum. Evol.* 96, 82-96.
- Pan, L., Thackeray, J.F., Dumoncel, J., Zanolli, C., Oettlé, A., de Beer, F., Hoffman, J., Duployer, B., Tenailleau, C., and Braga, J., 2017. Intra-individual metameric variation expressed at the enamel-

- dentine junction of lower post-canine dentition of South African fossil hominins and modern humans. *Am. J. Phys. Anth.* 163, 806-815
- Polly, P.D., 1998. Variability, selection, and constraints: development and evolution in viverravid (Carnivora, Mammalia) molar morphology. *Paleobiol.* 24, 409-429.
- Reif, W.E., 1976. Morphogenesis, pattern formation and function of the dentition of *Heterodontus* (Selachii). *Zoomorphologie*, 83, 1-47.
- Reif, W.E., 1982. Evolution of dermal skeleton and dentition in vertebrates. In: *Evolutionary Biology*, Hecht, M.X. Springer, Boston, MA. pp 287-368
- Richards, M.P., Pettitt, P.B., Stiner, M.C., and Trinkaus, E., 2001. Stable isotope evidence for increasing dietary breadth in the European mid-Upper Paleolithic. *PNAS* 98, 6528-6532.
- Rink, W.J., Mercier, N., Mihailovic, D., Morley, M.W., Thompson, J.W., and Roksandic, M., 2013. New radiometric ages for the BH-1 hominin from Balanica (Serbia): implications for understanding the role of the Balkans in Middle Pleistocene human evolution. *PLoS One* 8, e54608.
- Robinson, J.T., 1956. The dentition of the Australopithecinae. Pretoria: Transvaal Museum.
- Rohlf, F.J., and Slice, D., 1990. Extensions of the Procrustes method for the optimal superimposition of landmarks. *Syst. Biol.* 39, 40-59.
- Roksandic, M., Mihailović, D., Mercier, N., Dimitrijević, V., Morley, M.W., Rakočević, Z., Mihailović, B., Guibert, P., and Babb, J., 2011. A human mandible (BH-1) from the Pleistocene deposits of Mala Balanica cave (Sićevo Gorge, Niš, Serbia). *J. Hum. Evol.* 61, 186-196.
- Rook, D.L., and Hunter, J.P., 2014. Rooting Around the Eutherian Family Tree: the Origin and Relations of the Taeniodonta. *J. Mamm. Evol.* 21, 75-91.
- Ruch, J. V., 1987. Determinisms of odontogenesis. *Cell Biol. Rev.*, 14, 1
- Sakai, T., 1967. Morphologic study of the dentinoenamel junction of the mandibular first premolar. *J. Dent. Res.* 46, 927-932
- Schwartz, G.T., 2000. Taxonomic and functional aspects of the patterning of enamel thickness distribution in extant large-bodied hominoids. *Am. J. Phys. Anth.* 111, 221-244.
- Schour, I. and Massler, M., 1940a Studies in tooth development: the growth pattern of human teeth part II. *J. Am. Dent. Ass.* 27, 1918-1931.
- Schour, I. and Massler, M., 1940b. Studies in tooth development: the growth pattern of human teeth. *J. Am. Dent. Ass.* 27, 1778-1793.
- Scott, G.R., Turner, C.G., 1997. *The anthropology of modern human teeth: Dental morphology and its variation in recent human populations.* Cambridge University Press
- Scott, R.S., Ungar, P.S., Bergstrom, T.S., and Brown, C.A., 2005. Dental microwear texture analysis shows within-species diet variability in fossil hominins. *Nature* 436, 693.

Senut, B., Pickford, M., Gommery, D., Mein, P., Cheboi, K., Coppens, Y., 2001. First hominid from the Miocene (Lukeino Formation, Kenya). *C. R. Acad. Sci.* 332, 137-144.

Singleton, M., Rosenberger, A.L., Robinson, C., and O'Neill, R., 2011. Allometric and metameric shape variation in *Pan* mandibular molars: a digital morphometric analysis. *Anat. Rec.* 294, 322-334.

Skinner, M.M., 2008. Enamel-dentine junction morphology of extant hominoid and fossil hominin mandibular molars. Ph.D. Dissertation, George Washington University

Skinner, M.M., and Gunz, P., 2010. The presence of accessory cusps in chimpanzee lower molars is consistent with a patterning cascade model of development. *J. Anat.* 217, 245-253.

Skinner, M.M., Gunz, P., Wood, B.A., and Hublin, J. 2008a. Enamel-dentine junction (EDJ) morphology distinguishes the lower molars of *Australopithecus africanus* and *Paranthropus robustus*. *J. Hum. Evol.* 55, 979-988.

Skinner, M.M., Wood, B.A., Boesch, C., Olejniczak, A.J., Rosas, A., Smith, T.M., and Hublin, J.J., 2008b. Dental trait expression at the enamel-dentine junction of lower molars in extant and fossil hominoids. *J. Hum. Evol.* 54, 173-186.

Skinner, M.M., Gunz, P., Wood, B.A., Boesch, C., and Hublin, J., 2009a. Discrimination of extant *Pan* species and subspecies using the enamel-dentine junction morphology of lower molars. *Am. J. Phys. Anth.* 140, 234-243.

Skinner, M.M., Wood, B.A. and Hublin, J.J., 2009b. Protostylid expression at the enamel-dentine junction and enamel surface of mandibular molars of *Paranthropus robustus* and *Australopithecus africanus*. *J. Hum. Evol.* 56, 76-85.

Skinner, M.M., Evans, A., Smith, T., Jernvall, J., Tafforeau, P., Kupczik, K., Olejniczak, A.J., Rosas, A., Radovic, J., Thackeray, J.F., Toussaint, M., and Hublin, J.J., 2010. Brief communication: Contributions of enamel-dentine junction shape and enamel deposition to primate molar crown complexity. *Am. J. Phys. Anth.* 142, 157-163.

Skinner, M.M., Alemseged, Z., Gaunitz, C., and Hublin, J., 2015. Enamel thickness trends in Plio-Pleistocene hominin mandibular molars. *J. Hum. Evol.* 85, 35-45.

Skinner, M.M., de Vries, D., Gunz, P., Kupczik, K., Klassen, R.P., Hublin, J., and Roksandic, M., 2016. A dental perspective on the taxonomic affinity of the Balanica mandible (BH-1). *J. Hum. Evol.* 93, 63-81.

Smith, T.M., Olejniczak, A.J., Zermeno, J.P., Tafforeau, P., Skinner, M.M., Hoffmann, A., Radović, J., Toussaint, M., Kruszynski, R., and Menter, C., 2012. Variation in enamel thickness within the genus *Homo*. *J. Hum. Evol.* 62, 395-411.

Sponheimer, M., and Lee-Thorp, J.A., 1999. Isotopic evidence for the diet of an early hominid, *Australopithecus africanus*. *Science* 283, 368-370.

Spoor, F., Gunz, P., Neubauer, S., Stelzer, S., Scott, N., Kwekason, A. and Dean, M.C., 2015. Reconstructed *Homo habilis* type OH 7 suggests deep-rooted species diversity in early *Homo*. *Nature* 519, 83-86.

Stefan, V.H., and Trinkaus, E., 1998. Discrete trait and dental morphometric affinities of the Tabun 2 mandible. *J. Hum. Evol.* 34, 443-468.

Strait, D.S., and Grine, F.E., 2004. Inferring hominoid and early hominid phylogeny using craniodental characters: the role of fossil taxa. *J. Hum. Evol.* 47, 399-452.

Suwa, G., 1990. A comparative analysis of hominid dental remains from the Shungura and Usno Formations, Omo valley, Ethiopia. University of California, Berkeley

Suwa, G., Wood, B.A., and White, T.D., 1994. Further analysis of mandibular molar crown and cusp areas in Pliocene and early Pleistocene hominids. *Am. J. Phys. Anth.* 93, 407-426.

Suwa, G., White, T.D., Howell, F.C., 1996. Mandibular postcanine dentition from the Shungura Formation, Ethiopia: crown morphology, taxonomic allocations, and Plio-Pleistocene hominid evolution. *Am. J. Phys. Anthropol.* 101, 247-282.

Suwa, G., Kono, R.T., Simpson, S.W., Asfaw, B., Lovejoy, C.O., and White, T.D., 2009. Paleobiological implications of the *Ardipithecus ramidus* dentition. *Science* 326, 69-99.

Sponheimer, M., and Lee-Thorp, J.A., 1999. Isotopic evidence for the diet of an early hominid, *Australopithecus africanus*. *Science* 283, 368-370.

Springer, M.S., Burk-Herrick, A., Meredith, R., Eizirik, E., Teeling, E., O'Brien, S.J., and Murphy, W.J. 2007. The adequacy of morphology for reconstructing the early history of placental mammals. *System. Biol.* 56, 673-684.

Strait, D.S., Grine, F.E., and Moniz, M.A., 1997. A reappraisal of early hominid phylogeny. *J. H. Evol.* 32, 17-82.

Swindler, D.R., 2002. *Primate Dentition: An Introduction to the Teeth of Non-human Primates* (Cambridge University Press).

Thackeray, J.F., 2015. Estimating the age and affinities of *Homo naledi*. *S. Afr. J. Sci.* 111, 1-2.

Thesleff, I., 2003. Epithelial-mesenchymal signalling regulating tooth morphogenesis. *J. Cell Sci.* 116, 1647-1648.

Tobias, P.V., 1967. *Olduvai Gorge. Vol 2. The Cranium and Maxillary Dentition of Australopithecus (Zinjanthropus) boisei.* Cambridge University Press

Tobias, P.V., 1971. Human skeletal remains from the Cave of Hearths, Makapansgat, northern Transvaal. *Am. J. Phys. Anth.* 34: 335-367

Townsend, G., Harris, E.F., Lesot, H., Clauss, F. and Brook, A., 2009. Morphogenetic fields within the human dentition: a new, clinically relevant synthesis of an old concept. *Arch. Or. Biol.* 54, S34-S44.

Turner II, C.G., Nichol, C.R., and Scott, G.R., 1991. Scoring Procedures for Key Morphological Traits of the Permanent Dentition: The Arizona State University Dental Anthropology System. In: *Advances in Dental Anthropology*, Kelley, M., and Larsen, C. (Eds.), New York, Wiley Liss, pp. 13-31.

- Ungar, P., 2004. Dental topography and diets of *Australopithecus afarensis* and early *Homo*. *J. Hum. Evol.* 46, 605-622.
- Ungar, P.S., and Grine, F.E., 1991. Incisor size and wear in *Australopithecus africanus* and *Paranthropus robustus*. *J. Hum. Evol.* 20, 313-340.
- von Koenigswald, G., 1952. *Gigantopithecus blacki* von Koenigswald, a giant fossil hominoid from the Pleistocene of southern China. 43, 295–325.
- Walker, A., 1984. Mechanisms of honing in the male baboon canine. *Am. J. Phys. Anth.* 65, 47-60.
- Walker, A., Hoeck, H.N., and Perez, L., 1978. Microwear of mammalian teeth as an indicator of diet. *Science* 201, 908-910.
- Walter, R.C., 1994. Age of Lucy and the First Family: single-crystal  $^{40}\text{Ar}/^{39}\text{Ar}$  dating of the Denen Dora and lower Kada Hadar members of the Hadar Formation, Ethiopia. *Geol.* 22, 6-10.
- Ward, S.C., Johanson, D.C, and Coppens, Y., 1982. Subocclusal Morphology and Alveolar Process Relationships of Hominid Gnathic Elements From the Hadar Formation: 1974-1 977 Collections. *Am. J. Phys. Anth.* 57, 605-630.
- Ward, C., Leakey, M., Walker, A., 1999. The new hominid species *Australopithecus anamensis*. *Evol. Anth.* 7, 197-205.
- Ward, C.V., Leakey, M.G., Walker, A., 2001. Morphology of *Australopithecus anamensis* from Kanapoi and Allia Bay, Kenya. *J. Hum. Evol.* 41, 255-368.
- White, T.D., 1975. Geomorphology to paleoecology: *Gigantopithecus* reappraised. *J. Hum. Evol.* 4, 219-233.
- White, T.D., 1977. New fossil hominids from Laetolil, Tanzania. *Am. J. Phys. Anth.* 46, 197-229.
- White, T.D., Suwa, G., Asfaw, B., 1994. *Australopithecus ramidus*, a new species of early hominid from aramis, ethiopia. *Nature.* 371, 306-312.
- White, T.D., WoldeGabriel, G., Asfaw, B., Ambrose, S., Beyene, Y., Bernor, R.L., Boisserie, J.R., Currie, B., Gilbert, H., Haile-Selassie, Y. and Hart, W.K., 2006. Asa Issie, Aramis and the origin of *Australopithecus*. *Nature* 440, 883-889
- White, T.D., Asfaw, B., Beyene, Y., Haile-Selassie, Y., Lovejoy, C.O., Suwa, G., and WoldeGabriel, G., 2009. *Ardipithecus ramidus* and the paleobiology of early hominids. *Science* 326, 64-86.
- Wollny, G., Kellman, P., Ledesma-Carbayo, M.J., Skinner, M.M., Hublin, J.J., and Hierl, T., 2013. MIA-A free and open source software for gray scale medical image analysis. *Source code Biol. Med.* 8, 20.
- Wood, B.A., 1991. Koobi Fora Research Project: Volume 4. Hominid cranial remains. Oxford: Clarendon Press.
- Wood, B., 1992. Origin and evolution of the genus *Homo*. *Nature* 355, 783-790.
- Wood, B.A., Abbott, S.A., 1983. Analysis of the dental morphology of Plio-Pleistocene hominids. I. Mandibular molars: crown area measurements and morphological traits. *J. Anat.* 136, 197-219.

- Wood, B.A., and Uytterschaut, H., 1987. Analysis of the dental morphology of Plio-Pleistocene hominids. III. Mandibular premolar crowns. *J. Anat.* 154, 121-156.
- Wood, B.A., and Aiello, L.C., 1998. Taxonomic and Functional Implications of Mandibular Scaling in Early Hominins. *Am. J. Phys. Anth.* 105, 523-538
- Wood, B., and Strait, D., 2004. Patterns of resource use in early Homo and Paranthropus. *J. Hum. Evol.* 46, 119-162.
- Wood, B., and Boyle, E.K., 2016. Hominin Taxic Diversity: Fact or Fantasy? *Am. J. Phys. Anth.* 159, 37-78.
- Wood, B.A., Abbott, S.A., and Graham, S.H., 1983. Analysis of the dental morphology of Plio-Pleistocene hominids. II. Mandibular molars--study of cusp areas, fissure pattern and cross sectional shape of the crown. *J. Anat.* 137, 287-314.
- Wood, B.A., Abbott, S.A., and Uytterschaut, H., 1988. Analysis of the dental morphology of Plio-Pleistocene hominids. IV. Mandibular postcanine root morphology. *J. Anat.* 156, 107-139.
- Wu, L., Turner II, C.G., 1993. Variation in the frequency and form of the lower permanent molar middle trigonid crest. *Am. J. Phys. Anth.* 91, 245-248.
- Zack, S.P., 2011. New species of the rare early Eocene creodont Galecyon and the radiation of early Hyaenodontidae. *J. Paleontol.* 85, 315-336.
- Zhang, Y., Jin, C., Kono, R.T., Harrison, T., and Wang, W., 2016. A fourth mandible and associated dental remains of *Gigantopithecus blacki* from the Early Pleistocene Yanliang Cave, Fusui, Guangxi, South China. *Hist. Biol.* 28, 95-104.
- Zingesser, M.R., 1969. Cercopithecoid canine tooth honing mechanisms. *Am. J. Phys. Anth.* 31, 205-213.

# Supplementary information

**Supplementary Table 1.** Detailed study sample, including which analyses each specimen is included in.

Specimen	Side	Site/Origin	Taxonomy	Source	Position basis	Position source	EDJ+ CEJ	CEJ + Med	CEJ only	EDJ only	Ln(CS)	Reconstructed?
ZMB 7814	L	Borneo	<i>Hylobates muelleri</i>	ZMB records	1	ZMB records	Y	Y	Y	Y	3.1940	-
ZMB 7826	L	Borneo	<i>Hylobates muelleri</i>	ZMB records	1	ZMB records	Y	Y	Y	Y	3.2979	-
ZMB 7828	L	Borneo	<i>Hylobates muelleri</i>	ZMB records	1	ZMB records	Y	Y	Y	Y	3.2650	-
ZMB 85368	L	Indonesia/ Malaysia/ Thailand	<i>Hylobates agilis</i>	ZMB records	1	ZMB records	Y	Y	Y	Y	3.2979	Prd
ZMB 6948	R	Borneo	<i>Pongo pygmaeus</i>	ZMB records	1	ZMB records	Y	Y	Y	Y	4.0452	Prd
ZMB 6957	L	Unknown	<i>Pongo pygmaeus</i>	ZMB records	1	ZMB records	Y	Y	Y	Y	3.9166	-
ZMB 12209	R	Sumatra, Indonesia	<i>Pongo pygmaeus</i>	ZMB records	1	ZMB records	Y	Y	Y	Y	4.0985	Prd
ZMB 38607	R	Sumatra, Indonesia	<i>Pongo pygmaeus</i>	ZMB records	1	ZMB records	Y	Y	Y	Y	3.7796	-
ZMB 83509	R	Sumatra, Indonesia	<i>Pongo pygmaeus</i>	ZMB records	1	ZMB records	Y	Y	Y	Y	4.0523	-
ZMB 83511	L	Sumatra, Indonesia	<i>Pongo pygmaeus</i>	ZMB records	1	ZMB records	Y	Y	Y	Y	4.2039	Prd
ZMB 17963	L	Cameroon	<i>Gorilla gorilla</i>	ZMB records	1	ZMB records	Y	Y	Y	Y	4.3722	Prd
ZMB 30940	R	Cameroon	<i>Gorilla gorilla</i>	ZMB records	1	ZMB records	Y	Y	Y	Y	4.3418	-
ZMB 30941	L	Congo	<i>Gorilla gorilla</i>	ZMB records	1	ZMB records	Y	Y	Y	Y	4.2935	Prd
ZMB 31435	R	Cameroon	<i>Gorilla gorilla</i>	ZMB records	1	ZMB records	Y	Y	Y	Y	4.1017	-
ZMB 83561	R	Cameroon	<i>Gorilla gorilla</i>	ZMB records	1	ZMB records	Y	Y	Y	Y	4.3066	Prd
ZMB 11776	L	Taï, Côte d'Ivoire	<i>Pan troglodytes verus</i>	ZMB records	1	ZMB records	Y	Y	Y	Y	3.7974	-
ZMB 11800	R	Taï, Côte d'Ivoire	<i>Pan troglodytes verus</i>	ZMB records	1	ZMB records	Y	Y	Y	Y	3.7896	-
ZMB 11903	R	Taï, Côte d'Ivoire	<i>Pan troglodytes verus</i>	ZMB records	1	ZMB records	Y	Y	Y	Y	3.8208	Prd
ZMB 13430	R	Taï, Côte d'Ivoire	<i>Pan troglodytes verus</i>	ZMB records	1	ZMB records	Y	Y	Y	Y	3.8817	-
ZMB 13437	R	Taï, Côte d'Ivoire	<i>Pan troglodytes verus</i>	ZMB records	1	ZMB records	Y	Y	Y	Y	3.8255	-
KNM-KP 29281	R	Kanapoi, Kenya	<i>Australopithecus anamensis</i>	Ward <i>et al.</i> 2001	1	Ward <i>et al.</i> 2001	Y	Y	Y	Y	3.7852	-
KNM-KP 29286Ai	R	Kanapoi, Kenya	<i>Australopithecus anamensis</i>	Ward <i>et al.</i> 2001	1	Ward <i>et al.</i> 2001	Y	Y	Y	Y	3.8698	-

KNM-KP 53160	L	Kanapoi, Kenya	<i>Australopithecus anamensis</i>	Ward <i>et al.</i> 2017	1	Ward <i>et al.</i> 2017	Y	Y	Y	Y	3.8141	-
AL128-23	R	Hadar, Ethiopia	<i>Australopithecus afarensis</i>	Johanson <i>et al.</i> 1982	1	Johanson <i>et al.</i> 1982	N	Y	Y	N	-	-
AL266-1	R	Hadar, Ethiopia	<i>Australopithecus afarensis</i>	Johanson <i>et al.</i> 1982	1	Johanson <i>et al.</i> 1982	Y	Y	Y	Y	3.7928	Prd
AL277-1	L	Hadar, Ethiopia	<i>Australopithecus afarensis</i>	Johanson <i>et al.</i> 1982	1	Johanson <i>et al.</i> 1982	N	N	Y	N	-	-
AL333-10	L	Hadar, Ethiopia	<i>Australopithecus afarensis</i>	Johanson <i>et al.</i> 1982	3	Johanson <i>et al.</i> 1982	Y	Y	Y	Y	3.8866	Prd
AL333w-1c	R	Hadar, Ethiopia	<i>Australopithecus afarensis</i>	Johanson <i>et al.</i> 1982	2	Johanson <i>et al.</i> 1982	Y	Y	Y	Y	3.8739	-
AL400-1a	R	Hadar, Ethiopia	<i>Australopithecus afarensis</i>	Johanson <i>et al.</i> 1982	1	Johanson <i>et al.</i> 1982	N	N	Y	N	-	-
AL417-1a	L	Hadar, Ethiopia	<i>Australopithecus afarensis</i>	Kimbel <i>et al.</i> 1994	1	Kimbel <i>et al.</i> 1994	N	Y	Y	N	-	-
AL655-1	L	Hadar, Ethiopia	<i>Australopithecus afarensis</i>	Kimbel pers comm	2	Kimbel pers comm	Y	Y	Y	Y	3.8223	-
AL1045	R	Hadar, Ethiopia	<i>Australopithecus afarensis</i>	Kimbel and Delezene, 2009	1	Kimbel and Delezene, 2009	N	N	Y	N	-	-
W8-978	R	Omo, Ethiopia	<i>Australopithecus afarensis</i>	Suwa, 1990	3	Suwa, 1990	Y	Y	Y	Y	3.7729	-
KNM-WT 8556	L	West Turkana, Kenya	<i>Indet</i>	Brown <i>et al.</i> 2001	1	Brown <i>et al.</i> 2001	Y	Y	Y	Y	3.9038	-
STW 7	L	Sterkfontein, South Africa	<i>Australopithecus africanus</i>	Moggi-Cecchi <i>et al.</i> 2006	3	Moggi-Cecchi <i>et al.</i> 2006	Y	Y	Y	Y	3.8498	Prd
STW 104	L	Sterkfontein, South Africa	<i>Australopithecus africanus</i>	Moggi-Cecchi <i>et al.</i> 2006	1	Moggi-Cecchi <i>et al.</i> 2006	N	N	N	Y	-	-
STW 142	R	Sterkfontein, South Africa	<i>Australopithecus africanus</i>	Moggi-Cecchi <i>et al.</i> 2006	1	Moggi-Cecchi <i>et al.</i> 2006	N	Y	Y	N	-	Med
STW 193	R	Sterkfontein, South Africa	<i>Australopithecus africanus</i>	Moggi-Cecchi <i>et al.</i> 2006	2	Moggi-Cecchi <i>et al.</i> 2006	N	N	Y	N	-	-
STW 213	R	Sterkfontein, South Africa	<i>Australopithecus africanus</i>	Moggi-Cecchi <i>et al.</i> 2006	2	Moggi-Cecchi <i>et al.</i> 2006	Y	Y	Y	Y	3.7376	Prd
STW 401	R	Sterkfontein, South Africa	<i>Australopithecus africanus</i>	Moggi-Cecchi <i>et al.</i> 2006	3	Moggi-Cecchi <i>et al.</i> 2006	N	Y	Y	N	-	Med

STW 404	R	Sterkfontein, South Africa	<i>Australopithecus africanus</i>	Moggi-Cecchi <i>et al.</i> 2006	1	Moggi-Cecchi <i>et al.</i> 2006	Y	Y	Y	Y	3.7995	Prd
STW 420B	L	Sterkfontein, South Africa	<i>Australopithecus africanus</i>	Moggi-Cecchi <i>et al.</i> 2006	2	Moggi-Cecchi <i>et al.</i> 2006	N	N	N	Y	-	-
STW 498c	L	Sterkfontein, South Africa	<i>Australopithecus africanus</i>	Moggi-Cecchi <i>et al.</i> 2006	1	Moggi-Cecchi <i>et al.</i> 2006	N	Y	Y	N	-	-
STS 24	L	Sterkfontein, South Africa	<i>Australopithecus africanus</i>	Brain, 1981	1	Brain, 1981	N	N	N	Y	-	-
STS 51	R	Sterkfontein, South Africa	<i>Australopithecus africanus</i>	Brain, 1981	2	Brain, 1981	Y	Y	Y	Y	3.8290	-
STS 52b	R	Sterkfontein, South Africa	<i>Australopithecus africanus</i>	Dart, 1954	1	Dart, 1954	Y	Y	Y	Y	3.8690	Prd
Taung1	R	Taung, South Africa	<i>Australopithecus africanus</i>	Dart, 1925	1	Dart, 1925	N	N	N	Y	-	-
DNH8	L	Drimolen, South Africa	<i>Paranthropus robustus</i>	Moggi-Cecchi <i>et al.</i> 2010	1	Moggi-Cecchi <i>et al.</i> 2010	Y	Y	Y	Y	3.8965	-
DNH46	R	Drimolen, South Africa	<i>Paranthropus robustus</i>	Moggi-Cecchi <i>et al.</i> 2010	1	Moggi-Cecchi <i>et al.</i> 2010	Y	Y	Y	Y	3.8126	-
DNH51	R	Drimolen, South Africa	<i>Paranthropus robustus</i>	Moggi-Cecchi <i>et al.</i> 2010	1	Moggi-Cecchi <i>et al.</i> 2010	N	N	Y	N	-	-
DNH107	L	Drimolen, South Africa	<i>Paranthropus robustus</i>	Moggi-Cecchi <i>et al.</i> 2010	1	Moggi-Cecchi <i>et al.</i> 2010	N	N	N	Y	-	-
SK23	L	Swartkrans, South Africa	<i>Paranthropus robustus</i>	Robinson, 1956	1	Robinson, 1956	N	Y	Y	N	-	-
SK30	L	Swartkrans, South Africa	<i>Paranthropus robustus</i>	Robinson, 1956	3	Robinson, 1956	N	N	Y	N	-	-
SK61	R	Swartkrans, South Africa	<i>Paranthropus robustus</i>	Robinson, 1956	1	Robinson, 1956	N	N	N	Y	-	-
SK62	L	Swartkrans, South Africa	<i>Paranthropus robustus</i>	Robinson, 1956	1	Robinson, 1956	N	N	N	Y	-	-
SK63	L	Swartkrans, South Africa	<i>Paranthropus robustus</i>	Robinson, 1956	1	Robinson, 1956	N	N	N	Y	-	-
SK100	R	Swartkrans, South Africa	<i>Paranthropus robustus</i>	Robinson, 1956	3	Oakley, 1977	Y	Y	Y	Y	3.9081	-
SK857	R	Swartkrans, South Africa	<i>Paranthropus robustus</i>	Robinson, 1956	3	Oakley, 1977	Y	Y	Y	Y	3.9203	-
SKW5	R	Swartkrans, South Africa	<i>Paranthropus robustus</i>	Grine, 2004	1	Grine, 2004	Y	Y	Y	Y	3.8375	Prd
KNM-ER 1820	L	Koobi Fora, Kenya	<i>Paranthropus boisei</i>	Wood, 1991	1	Wood, 1991	N	N	N	Y	-	-
KNM-ER 6082	L	Koobi Fora, Kenya	<i>Paranthropus boisei</i>	Wood, 1991	3	Wood, 1991	N	N	N	Y	-	-
KNM-ER 15951H	L	Koobi Fora, Kenya	<i>Paranthropus boisei</i>	Wood and Leakey, 2011	1	Wood and Leakey, 2011	N	N	Y	N	-	-
KNM-WT 16005	L	West Turkana, Kenya	<i>Paranthropus boisei</i>	Leakey and Walker, 1988	1	Leakey and Walker, 1988	Y	Y	Y	Y	4.0496	Prd

L427-7	R	Omo, Ethiopia	<i>Paranthropus boisei</i>	Suwa <i>et al.</i> 1996	1	Suwa <i>et al.</i> 1996	Y	Y	Y	Y	3.9166	-
HCRP-UR 501	R	Uraha, Malawi	<i>Homo rudolfensis</i>	Schrenk <i>et al.</i> 1993	1	Schrenk <i>et al.</i> 1993	N	N	Y	N	-	-
KNM-BK 8518A	R	Baringo, Kenya	<i>Homo sp.</i>	Wood and van Noten, 1986	1	Wood and van Noten, 1986	N	N	Y	N	-	-
KNM-ER 806E	L	Koobi Fora, Kenya	<i>Homo ergaster</i>	Wood, 1991	2	Wood, 1991	N	Y	Y	N	-	-
KNM-ER 992A	R	Koobi Fora, Kenya	<i>Homo sp.</i>	Wood, 1991	1	Wood, 1991	Y	Y	Y	Y	3.8847	Prd
KNM-ER 1507	L	Koobi Fora, Kenya	<i>Homo sp.</i>	Leakey and Wood, 2005	1	Leakey and Wood, 2005	N	N	Y	N	-	-
KNM-ER 1802	R	Koobi Fora, Kenya	<i>Homo sp.</i>	Wood, 1991	1	Wood, 1991	Y	Y	Y	Y	3.9426	-
KNM-ER 5431E	L	Koobi Fora, Kenya	<i>Indet</i>	Wood, 1991	2	Wood, 1991	Y	Y	Y	Y	3.9228	-
KNM-WT 15000B	R	West Turkana, Kenya	<i>Homo ergaster</i>	Walker and Leakey, 1993	1	Walker and Leakey, 1993	N	N	Y	N	-	-
SK 18a	L	Swartkrans, South Africa	<i>Homo sp.</i>	Brain, 1981	2	Brain, 1981	N	N	Y	N	-	-
SK 96	L	Swartkrans, South Africa	<i>Indet – originally P. robustus</i>	Robinson, 1956	2	Robinson, 1956	Y	Y	Y	Y	3.7833	-
SKX 21204	R	Swartkrans, South Africa	<i>Homo sp.</i>	Grine, 1989	1	Grine, 1989	Y	Y	Y	Y	3.6766	-
STW 151	R	Sterkfontein, South Africa	<i>Indet</i>	Moggi-Cecchi <i>et al.</i> 1998	1	Moggi-Cecchi <i>et al.</i> 1998	Y	Y	Y	Y	3.7794	-
S 6a	R	Sangiran, Indonesia	<i>Homo erectus</i>	Grine and Franzen, 1994	2	Grine and Franzen, 1994	Y	Y	Y	Y	3.9230	-
SMF S7 25	R	Sangiran, Indonesia	<i>Homo erectus</i>	Grine and Franzen, 1994	3	Grine and Franzen, 1994	N	N	Y	N	-	-
U.W. 101-0010	R	Rising Star, South Africa	<i>Homo naledi</i>	Berger <i>et al.</i> 2015	1	Berger <i>et al.</i> 2015	N	Y	Y	N	-	-
U.W. 101-0144	L	Rising Star, South Africa	<i>Homo naledi</i>	Berger <i>et al.</i> 2015	3	Berger <i>et al.</i> 2015	Y	Y	Y	Y	3.7228	-
U.W. 101-298	R	Rising Star, South Africa	<i>Homo naledi</i>	Berger <i>et al.</i> 2015	3	Berger <i>et al.</i> 2015	-	-	-	-	-	-
U.W. 101-377	R	Rising Star, South Africa	<i>Homo naledi</i>	Berger <i>et al.</i> 2015	1	Berger <i>et al.</i> 2015	-	-	-	-	-	-
U.W. 101-506	R	Rising Star, South Africa	<i>Homo naledi</i>	Berger <i>et al.</i> 2015	3	Berger <i>et al.</i> 2015	-	-	-	-	-	-
U.W. 101-0850	R	Rising Star, South Africa	<i>Homo naledi</i>	Berger <i>et al.</i>	3	Berger <i>et al.</i>	N	N	Y	N	-	-

				2015		2015						
U.W. 101-0889	L	Rising Star, South Africa	<i>Homo naledi</i>	Berger <i>et al.</i> 2015	3	Berger <i>et al.</i> 2015	Y	Y	Y	Y	3.7221	-
U.W. 101-1261-1283-1371	R	Rising Star, South Africa	<i>Homo naledi</i>	Berger <i>et al.</i> 2015	1	Berger <i>et al.</i> 2015	Y	Y	Y	Y	3.7298	Prd
U.W. 101-1565	L	Rising Star, South Africa	<i>Homo naledi</i>	Berger <i>et al.</i> 2015	1	Berger <i>et al.</i> 2015	Y	Y	Y	Y	3.7509	-
U.W. 102-0023	R	Rising Star, South Africa	<i>Homo naledi</i>	Hawks <i>et al.</i> 2017	3	Hawks <i>et al.</i> 2017	N	N	Y	N	-	-
U.W. 102-0240	L	Rising Star, South Africa	<i>Homo naledi</i>	Hawks <i>et al.</i> 2017	3	Hawks <i>et al.</i> 2017	N	N	Y	N	-	-
Cave of hearths	R	Cave of hearths, South Africa	<i>Indet</i>	Tobias, 1971	1	Tobias, 1971	Y	Y	Y	Y	3.6712	-
Mauer 1	R	Mauer, Germany	<i>Homo heidelbergensis</i>	Schoetensack, 1908	1	Schoetensack, 1908	N	Y	Y	N	-	-
Combe-Grenal I	R	Combe Grenal, France	<i>Homo neanderthalensis</i>	Garralda and Vandermeersch, 2000	1	Garralda and Vandermeersch, 2000	Y	Y	Y	Y	3.8256	-
Combe-Grenal XV	R	Combe Grenal, France	<i>Homo neanderthalensis</i>	Garralda and Vandermeersch, 2000	3	Garralda and Vandermeersch, 2000	N	Y	Y	N	-	-
KRP 51	R	Krapina, Croatia	<i>Homo neanderthalensis</i>	Radovčić, 1988	1	Radovčić, 1988	Y	Y	Y	Y	3.7241	-
KRP 52	L	Krapina, Croatia	<i>Homo neanderthalensis</i>	Radovčić, 1988	1	Radovčić, 1988	Y	Y	Y	Y	3.7228	-
KRP 54	L	Krapina, Croatia	<i>Homo neanderthalensis</i>	Radovčić, 1988	1	Radovčić, 1988	Y	Y	Y	Y	3.7017	-
KRP 55	L	Krapina, Croatia	<i>Homo neanderthalensis</i>	Radovčić, 1988	1	Radovčić, 1988	Y	Y	Y	Y	3.7657	-
KRP 58	R	Krapina, Croatia	<i>Homo neanderthalensis</i>	Radovčić, 1988	1	Radovčić, 1988	N	Y	Y	N	-	-
KRP D27	L	Krapina, Croatia	<i>Homo neanderthalensis</i>	Radovčić, 1988	2	Radovčić, 1988	N	Y	Y	N	-	-
KRP D28	R	Krapina, Croatia	<i>Homo neanderthalensis</i>	Radovčić, 1988	2	Radovčić, 1988	N	Y	Y	N	-	-
KRP D29	R	Krapina, Croatia	<i>Homo neanderthalensis</i>	Radovčić, 1988	2	Radovčić, 1988	N	Y	Y	N	-	-
KRP D33	L	Krapina, Croatia	<i>Homo neanderthalensis</i>	Radovčić, 1988	2	Radovčić, 1988	Y	Y	Y	Y	3.8083	-
KRP D34	R	Krapina, Croatia	<i>Homo neanderthalensis</i>	Radovčić, 1988	3	Radovčić, 1988	Y	Y	Y	Y	3.7947	Prd
KRP D111	L	Krapina, Croatia	<i>Homo neanderthalensis</i>	Radovčić, 1988	3	Radovčić, 1988	Y	Y	Y	Y	3.8778	-

KRP D114	L	Krapina, Croatia	<i>Homo neanderthalensis</i>	Radovčić, 1988	2	Radovčić, 1988	Y	Y	Y	Y	3.7901	-
SCLA 4A 6	R	Scladina, Belgium	<i>Homo neanderthalensis</i>	Toussaint <i>et al.</i> 1998	2	Toussaint <i>et al.</i> 1998	Y	Y	Y	Y	3.7129	-
Irhoud 11	R	Jebel Irhoud, Morocco	<i>Homo sapiens</i>	Hublin <i>et al.</i> 2017	1	Hublin <i>et al.</i> 2017	N	Y	Y	N	-	-
Qafzeh 10	R	Qafzeh, Israel	<i>Homo sapiens</i>	Vandermeersch, 1981	1	Vandermeersch, 1981	Y	Y	Y	Y	3.6412	-
Qafzeh 11	R	Qafzeh, Israel	<i>Homo sapiens</i>	Vandermeersch, 1981	1	Vandermeersch, 1981	Y	Y	Y	Y	3.6379	-
ULAC 1	R	Anatomical collection	<i>Homo sapiens</i>	ULAC records	1	ULAC records	Y	Y	Y	Y	3.5966	-
ULAC 58	L	Anatomical collection	<i>Homo sapiens</i>	ULAC records	1	ULAC records	Y	Y	Y	Y	3.6127	-
ULAC 58	R	Anatomical collection	<i>Homo sapiens</i>	ULAC records	1	ULAC records	-	-	-	-	-	-
ULAC 66	L	Anatomical collection	<i>Homo sapiens</i>	ULAC records	1	ULAC records	Y	Y	Y	Y	3.5099	Prd
ULAC 74	L	Anatomical collection	<i>Homo sapiens</i>	ULAC records	1	ULAC records	N	Y	Y	N	-	-
ULAC 171	L	Anatomical collection	<i>Homo sapiens</i>	ULAC records	1	ULAC records	N	Y	Y	N	-	-
ULAC 522	L	Anatomical collection	<i>Homo sapiens</i>	ULAC records	1	ULAC records	N	Y	Y	N	-	-
ULAC 536	R	Anatomical collection	<i>Homo sapiens</i>	ULAC records	1	ULAC records	Y	Y	Y	Y	3.4920	Prd
ULAC 607	R	Anatomical collection	<i>Homo sapiens</i>	ULAC records	1	ULAC records	N	Y	Y	N	-	-
ULAC 790	L	Anatomical collection	<i>Homo sapiens</i>	ULAC records	1	ULAC records	Y	Y	Y	Y	3.5646	-
ULAC 797	R	Anatomical collection	<i>Homo sapiens</i>	ULAC records	1	ULAC records	Y	Y	Y	Y	3.6305	-
ULAC 801	L	Anatomical collection	<i>Homo sapiens</i>	ULAC records	1	ULAC records	Y	Y	Y	Y	3.6896	-
ULAC 806	L	Anatomical collection	<i>Homo sapiens</i>	ULAC records	1	ULAC records	Y	Y	Y	Y	3.6265	-

**Position basis:** 1 = In jaw, 2 = Associated dentition, 3 = Based on morphology. **Ln(CS)** = Natural logarithm of centroid size; listed for those specimens included in the EDJ+CEJ analysis. **Reconstructed?** = Specimens with reconstructed dentine horns; Prd = Protoconid reconstructed, Med = Metaconid reconstructed. **TC** = Transverse crest form (see Main article for details). **MR** = Marginal ridge; C = Continuous, M = Mesial marginal ridge discontinuous, D = Distal marginal ridge discontinuous, MD = Mesial and distal marginal ridges both discontinuous. **MBG** = Mesial buccal groove, **DBG** = Distal buccal groove; 0 = absent, 1 = minor, 2 = marked (see text for details)

## References

- Berger, L.R., Hawks, J., de Ruiter, D.J., Churchill, S.E., Schmid, P. *et al.* (2015). *Homo naledi*, a new species of the genus *Homo* from the Dinaledi Chamber, South Africa. *Elife* 4, 09560.
- Brain, C.K. (1981). The hunters or the hunted?: an introduction to African cave taphonomy. University of Chicago Press
- Broom, R., and Robinson, J.T. (1952). Swartkrans ape-man. *Paranthropus crassidens*. Transvaal Museum Memoir No. 6
- Brown B., Brown F.H., Walker A. (2001). New hominids from the Lake Turkana Basin, Kenya. *J. Hum. Evol.* 41, 29-44.

- Dart, R.A. (1925). *Australopithecus africanus*: the man-ape of South Africa. *Nature* 115: 195-199
- Dart, R.A. (1954). The second, or adult, female mandible of *Australopithecus prometheus*. *Am. J. Phys. Anthropol.* 12: 313-344.
- Deleuzene L.K., Kimbel W.H. (2011). Evolution of the mandibular third premolar crown in early *australopithecus*. *J. Hum. Evol.* 60, 711-30.
- Garralda, M.D., and Vandermeersch, B. (2000). Les Néandertaliens de la grotte de Combe-Grenal (Domme, Dordogne, France). *Paléo*, 12, 213-259
- Grine, F.E. (1989). New hominid fossils from the Swartkrans Formation (1979–1986 excavations): craniodental specimens. *Am. J. Phys. Anth.* 79, 409-449
- Grine, F.E. (1993). Description and preliminary analysis of new hominid craniodental fossils from the Swartkrans Formation. *Swartkrans: A Cave's Chronicle of Early Man*. Transvaal Museum, Pretoria, 75-116.
- Hawks, J., Elliott, M., Schmid, P., Churchill, S.E., de Ruiter, D.J., Roberts, E.M., *et al.* (2017). New fossil remains of *Homo naledi* from the Lesedi Chamber, South Africa. *eLife* 6, 24232.
- Hublin, J.J., Ben-Ncer, A., Bailey, S.E., Freidline, S.E., Neubauer, S., Skinner, M.M., Bergmann, I., Le Cabec, A., Benazzi, S., Harvati, K., and Gunz, P. (2017). New fossils from Jebel Irhoud, Morocco and the pan-African origin of *Homo sapiens*. *Nature* 546, 289-292
- Johanson D.C., White T.D., Coppens Y. (1982). Dental remains from the Hadar formation, Ethiopia: 1974–1977 collections. *Am. J. Phys. Anthropol.* 57, 545-603.
- Kimbel W.H., Deleuzene L.K. (2009). “Lucy” redux: A review of research on *australopithecus afarensis*. *Am. J. Phys. Anthropol.* 140, 2-48.
- Leakey, R.E.F., and Walker, A. (1988). New *Australopithecus boisei* specimens from east and west Lake Turkana, Kenya. *Am. J. Phys Anth*, 76, 1-24
- Leakey, R.E.F., and Wood, B.A. (1974). New evidence of the genus *Homo* from East Rudolf, Kenya (IV). *Am. J. Phys. Anth.* 41, 237-243.
- Moggi-Cecchi, J., Tobias, P.V., and Beynon, A.D. (1998). The mixed dentition and associated skull fragments of a juvenile fossil hominid from Sterkfontein, South Africa. *Am. J. Phys. Anth.* 106, 425-465
- Moggi-Cecchi J., Grine F.E., Tobias P.V. (2006). Early hominid dental remains from members 4 and 5 of the sterkfontein formation (1966–1996 excavations): Catalogue, individual associations, morphological descriptions and initial metrical analysis. *J. Hum. Evol.* 50, 239-328.
- Moggi-Cecchi, J., Menter, C., Boccone, S., and Keyser, A. (2010). Early hominin dental remains from the Plio-Pleistocene site of Drimolen, South Africa. *J. Hum. Evol.* 58: 374-405.
- Oakley, K., Campbell, B., and Molleson, T. (1977). *Catalogue of fossil hominids part 1: Africa*. London: British Museum of Natural History
- Prat, S., Brugal, J.P., Roche, H., and Texier, P.J. (2003). Nouvelles découvertes de dents d'hominidés dans le membre Kaitio de la formation de Nachukui (1, 65–1, 9 Ma), Ouest du lac Turkana (Kenya). *Comp. Rend. Pal.* 2, 685-693
- Radovčić, J., 1988. The Krapina hominids: an illustrated catalog of skeletal collection. *Mladost*.
- Robinson, J.T. (1956). *The dentition of the Australopithecinae*. Pretoria: Transvaal Museum.
- Schoetensack O. (1908) *Der Unterkiefer des Homo heidelbergensis aus den Sanden von Mauer bei Heidelberg*. Leipzig: W. Engelmann
- Schrenk, F., Bromage, T.G., Betzler, C.G., Ring, U., and Juwayeyi, Y.M. (1993). Oldest *Homo* and Pliocene biogeography of the Malawi rift. *Nature*, 365, 833-836.
- Suwa G. (1990). A comparative analysis of hominid dental remains from the Shungura and Usno Formations, Omo valley, Ethiopia. Ph.D. Dissertation, University of California, Berkeley.
- Tobias, P.V. (1971). Human skeletal remains from the Cave of Hearths, Makapansgat, northern Transvaal. *Am. J. Phys. Anth.* 34, 335-367.
- Toussaint, M., Otte, M., Bonjean, D., Bocherens, H., Falguères, C., and Yokoyama, Y. (1998). Les restes humains néandertaliens immatures de la couche 4A de la grotte Scladina (Andenne, Belgique). *C. R. Acad. Sci. Paris* 326, 737-742.
- Vandermeersch, B. (1981). Les hommes fossiles de Qafzeh (Israël). *Cahiers de paléontologie*
- Walker, A., and Leakey, R.E. eds. (1993). *The Nariokotome Homo erectus skeleton*. Harvard University Press
- Ward, C.V., Leakey, M.G., and Walker, A. (2001). Morphology of *Australopithecus anamensis* from Kanapoi and Allia Bay, Kenya. *J. Hum. Evol.* 41: 255-368.
- Ward C.V., Plavcan J.M., Manthi F.K. (*In Press*). New fossils of *australopithecus anamensis* from kanapoi, West Turkana, kenya (2012–2015). *J. Hum. Evol.*
- Wood, B.A. (1991). *Koobi Fora Research Project: Volume 4. Hominid cranial remains*. Oxford: Clarendon Press

---

**Supplementary Table 2:** Additional information on the modern human sample, as listed in the records of the Anatomical Collection of the University of Leipzig

---

<b>Specimen number</b>	<b>Region</b>	<b>Age</b>	<b>Sex</b>
ULAC_1	"Germany/Rheinland"	Adult	Male
ULAC_58	"Norway"	Adult	Male
ULAC_66	"Norway/Sweden"	Adult	Female
ULAC_74	"Italy (Etruscan, Tarquinii)"	Adult	Male
ULAC_171	"Italy (Etruscan, Tarquinii)"	Adult	Male
ULAC_522	"Egypt (Thebes)"	Adult	Male
ULAC_536	"Egypt (Thebes)"	Adult	Male
ULAC_607	"Egypt (Thebes)"	Adult	Male
ULAC_790	"Africa (Americans/New Orleans)"	Adult	Male
ULAC_797	"Africa (Americans/New Orleans)"	Adult	Male
ULAC_801	"Africa (Americans/New Orleans)"	Adult	Female
ULAC_806	"Africa (Americans/New Orleans)"	Adult	Male

---

**Supplementary Table 3.** CVA classification results for the EDJ+CEJ analysis in shape space.

	Aafa	Hn	Pr	Aafri	Hs	Hnal	Ptv	Gg	Hy	Pp	Correct class	Proportion Correct
AL333w-1c	13	0	0	0	0	0	0	0	0	0	Aafa	1
AL266-1	13	0	0	0	0	0	0	0	0	0	Aafa	1
AL333-10	5	0	0	8	0	0	0	0	0	0	Aafa	0.3846
AL655-1	13	0	0	0	0	0	0	0	0	0	Aafa	1
Combe Grenal I	0	12	0	0	1	0	0	0	0	0	Hn	0.9231
DNH46	0	0	13	0	0	0	0	0	0	0	Pr	1
DNH8	0	0	13	0	0	0	0	0	0	0	Pr	1
ZMB 17963	0	0	0	0	0	0	0	13	0	0	Gg	1
ZMB 30941	0	0	0	0	0	0	0	13	0	0	Gg	1
ZMB 31435	0	0	0	0	0	0	0	13	0	0	Gg	1
ZMB 83561	0	0	0	0	0	0	0	13	0	0	Gg	1
ZMB 30940	0	0	0	0	0	0	0	10	3	0	Gg	0.7692
ZMB 85368	0	0	0	0	0	0	0	0	13	0	Hy	1
ZMB 7814	0	0	0	0	0	0	0	0	13	0	Hy	1
ZMB 7826	0	0	0	0	0	0	0	0	13	0	Hy	1
ZMB 7828	0	0	0	0	0	0	0	0	13	0	Hy	1
KRP 51	0	11	0	0	2	0	0	0	0	0	Hn	0.8462
KRP 52	0	13	0	0	0	0	0	0	0	0	Hn	1
KRP 54	0	13	0	0	0	0	0	0	0	0	Hn	1
KRP 55	0	13	0	0	0	0	0	0	0	0	Hn	1
KRP D111	0	12	0	0	1	0	0	0	0	0	Hn	0.9231
KRP D114	0	13	0	0	0	0	0	0	0	0	Hn	1
KRP D33	0	13	0	0	0	0	0	0	0	0	Hn	1
KRP D34	0	13	0	0	0	0	0	0	0	0	Hn	1
ZMB 12209	0	0	0	0	0	0	0	0	0	13	Pp	1
ZMB 38607	0	0	0	0	0	0	0	0	0	13	Pp	1
ZMB 6948	0	0	0	0	0	0	0	0	0	13	Pp	1
ZMB 83509	0	0	0	0	0	0	0	0	0	13	Pp	1
ZMB 83511	0	0	0	0	0	0	0	0	0	13	Pp	1
ZMB 11776	0	0	0	0	0	0	13	0	0	0	Ptv	1
ZMB 11800	0	0	0	0	0	0	13	0	0	0	Ptv	1
ZMB 11903	0	0	0	0	0	0	13	0	0	0	Ptv	1
ZMB 13430	0	0	0	0	0	0	13	0	0	0	Ptv	1
ZMB 13437	0	0	0	0	0	0	13	0	0	0	Ptv	1
SCLA 4A 6	0	10	0	0	3	0	0	0	0	0	Hn	0.7692
SK100	0	0	13	0	0	0	0	0	0	0	Pr	1
SK857	0	0	13	0	0	0	0	0	0	0	Pr	1
SKW5	1	0	12	0	0	0	0	0	0	0	Pr	0.9231
STS51	0	0	0	13	0	0	0	0	0	0	Aafri	1
STS52b	0	0	0	13	0	0	0	0	0	0	Aafri	1
STW213	2	0	0	11	0	0	0	0	0	0	Aafri	0.8462
STW404	0	0	0	13	0	0	0	0	0	0	Aafri	1
STW7	0	0	0	13	0	0	0	0	0	0	Aafri	1
ULAC 1	0	0	0	0	13	0	0	0	0	0	Hs	1
ULAC 536	0	0	0	0	13	0	0	0	0	0	Hs	1
ULAC 58	0	8	0	0	5	0	0	0	0	0	Hs	0.3846

ULAC 66	0	4	0	0	9	0	0	0	0	0	Hs	0.6923
ULAC 790	0	2	0	0	11	0	0	0	0	0	Hs	0.8462
ULAC 797	0	0	0	0	13	0	0	0	0	0	Hs	1
ULAC 801	1	0	0	0	12	0	0	0	0	0	Hs	0.9231
ULAC 806	0	4	0	0	9	0	0	0	0	0	Hs	0.6923
UW101 1283	0	0	0	0	0	13	0	0	0	0	Hnal	1
UW101 144	0	0	0	0	0	13	0	0	0	0	Hnal	1
UW101 1565	0	0	0	0	0	13	0	0	0	0	Hnal	1
UW101 889	0	0	0	0	0	13	0	0	0	0	Hnal	1
W8-978-LRP3	13	0	0	0	0	0	0	0	0	0	Aafa	1
ZMB 6957	0	0	0	0	0	0	0	0	0	13	Pp	1

Abbreviations: Aafa = *Australopithecus afarensis*, Hn = *Homo neanderthalensis*, Pr = *Paranthropus robustus*, Aafri = *Australopithecus africanus*, Hs = *Homo sapiens*, Hnal = *Homo naledi*, Ptv = *Pan troglodytes verus*, Gg = *Gorilla gorilla*, Hy = *Hylobates*, Pp = *Pongo pygmaeus*

**Supplementary Table 4.** CVA classification results for the EDJ+CEJ analysis in form space

	Aafa	Hn	Pr	Aafri	Hs	Hnal	Ptv	Gg	Hy	Pp	Correct class	Proportion Correct
AL333w-1c	12	0	0	1	0	0	0	0	0	0	Aafa	0.9231
AL266-1	13	0	0	0	0	0	0	0	0	0	Aafa	1
AL333-10	4	0	1	8	0	0	0	0	0	0	Aafa	0.3077
AL655-1	13	0	0	0	0	0	0	0	0	0	Aafa	1
Combe Grenal I	0	13	0	0	0	0	0	0	0	0	Hn	1
DNH46	0	0	13	0	0	0	0	0	0	0	Pr	1
DNH8	0	0	13	0	0	0	0	0	0	0	Pr	1
ZMB 17963	0	0	0	0	0	0	0	13	0	0	Gg	1
ZMB 30941	0	0	0	0	0	0	0	13	0	0	Gg	1
ZMB 31435	0	0	0	0	0	0	0	13	0	0	Gg	1
ZMB 83561	0	0	0	0	0	0	0	13	0	0	Gg	1
ZMB 30940	0	0	0	0	0	0	0	13	0	0	Gg	1
ZMB 85368	0	0	0	0	0	0	0	0	13	0	Hy	1
ZMB7814	0	0	0	0	0	0	0	0	13	0	Hy	1
ZMB7826	0	0	0	0	0	0	0	0	13	0	Hy	1
ZMB7828	0	0	0	0	0	0	0	0	13	0	Hy	1
KRP51	0	13	0	0	0	0	0	0	0	0	Hn	1
KRP 52	0	13	0	0	0	0	0	0	0	0	Hn	1
KRP54	0	13	0	0	0	0	0	0	0	0	Hn	1
KRP55	0	13	0	0	0	0	0	0	0	0	Hn	1
KRP D111	0	13	0	0	0	0	0	0	0	0	Hn	1
KRP D114	0	13	0	0	0	0	0	0	0	0	Hn	1
KRP D33	0	13	0	0	0	0	0	0	0	0	Hn	1
KRP D34	0	13	0	0	0	0	0	0	0	0	Hn	1
ZMB 12209	0	0	0	0	0	0	0	0	0	13	Pp	1
ZMB 38607	0	0	0	0	0	0	1	0	0	12	Pp	0.9231
ZMB 6948	0	0	0	0	0	0	0	0	0	13	Pp	1
ZMB 83509	0	0	0	0	0	0	0	0	0	13	Pp	1
ZMB 83511	0	0	0	0	0	0	0	0	0	13	Pp	1
ZMB 11776	0	0	0	0	0	0	13	0	0	0	Ptv	1
ZMB 11800	0	0	0	0	0	0	13	0	0	0	Ptv	1
ZMB 11903	0	0	0	0	0	0	13	0	0	0	Ptv	1
ZMB 13430	0	0	0	0	0	0	13	0	0	0	Ptv	1
ZMB 13437	0	0	0	0	0	0	13	0	0	0	Ptv	1
SCLA 4A 6	0	12	0	0	1	0	0	0	0	0	Hn	0.9231
SK100	0	0	13	0	0	0	0	0	0	0	Pr	1
SK857	0	0	13	0	0	0	0	0	0	0	Pr	1
SKW5	2	0	10	1	0	0	0	0	0	0	Pr	0.7692
STS51	0	0	0	13	0	0	0	0	0	0	Aafri	1
STS52b	0	0	1	12	0	0	0	0	0	0	Aafri	0.9231
STW213	4	0	0	8	0	1	0	0	0	0	Aafri	0.6154
STW404	1	0	0	12	0	0	0	0	0	0	Aafri	0.9231
STW7	0	0	0	13	0	0	0	0	0	0	Aafri	1
ULAC 1	0	0	0	0	13	0	0	0	0	0	Hs	1
ULAC 536	0	0	0	0	13	0	0	0	0	0	Hs	1
ULAC 58	0	2	0	0	11	0	0	0	0	0	Hs	0.8462

ULAC 66	0	0	0	0	13	0	0	0	0	0	Hs	1
ULAC 790	0	0	0	0	13	0	0	0	0	0	Hs	1
ULAC 797	0	0	0	0	13	0	0	0	0	0	Hs	1
ULAC 801	0	0	0	0	11	2	0	0	0	0	Hs	0.8462
ULAC 806	0	0	0	0	13	0	0	0	0	0	Hs	1
UW101 1283	0	0	0	0	0	13	0	0	0	0	Hnal	1
UW101 144	0	0	0	0	0	13	0	0	0	0	Hnal	1
UW101 1565	0	0	0	0	0	13	0	0	0	0	Hnal	1
UW101 889	0	0	0	0	0	13	0	0	0	0	Hnal	1
W8-978-LRP3	13	0	0	0	0	0	0	0	0	0	Aafa	1
ZMB 6957	0	0	0	0	0	0	0	0	0	13	Pp	1

Abbreviations: Aafa = *Australopithecus afarensis*, Hn = *Homo neanderthalensis*, Pr = *Paranthropus robustus*, Aafri = *Australopithecus africanus*, Hs = *Homo sapiens*, Hnal = *Homo naledi*, Ptv = *Pan troglodytes verus*, Gg = *Gorilla gorilla*, Hy = *Hylobates*, Pp = *Pongo pygmaeus*



STW420B	0	0	12	0	0	0	0	0	0	1	Aafri	0.9231
STW7	0	0	13	0	0	0	0	0	0	0	Aafri	1
Taung1	1	0	12	0	0	0	0	0	0	0	Aafri	0.9231
ULAC 1	0	0	2	11	0	0	0	0	0	0	Hs	0.8462
ULAC 536	0	0	2	11	0	0	0	0	0	0	Hs	0.8462
ULAC 58	0	0	0	7	0	0	0	0	6	0	Hs	0.5385
ULAC 66	0	0	0	13	0	0	0	0	0	0	Hs	1
ULAC 790	0	0	0	10	0	0	0	0	3	0	Hs	0.7692
ULAC 797	0	0	0	13	0	0	0	0	0	0	Hs	1

Abbreviations: Aafa = *Australopithecus afarensis*, Hn = *Homo neanderthalensis*, Pr = *Paranthropus robustus*, Aafri = *Australopithecus africanus*, Hs = *Homo sapiens*, Hnal = *Homo naledi*, Ptv = *Pan troglodytes verus*, Gg = *Gorilla gorilla*, Hy = *Hylobates*, Pp = *Pongo pygmaeus*

**Supplementary Table 6.** CVA classification results for the EDJ analysis in form space

	<b>Aafa</b>	<b>Pr</b>	<b>Aafri</b>	<b>Hs</b>	<b>Ptv</b>	<b>Gg</b>	<b>Hy</b>	<b>Pp</b>	<b>Hn</b>	<b>Hnal</b>	<b>Correct class</b>	<b>Proportion Correct</b>
AL333w-1c	13	0	0	0	0	0	0	0	0	0	Aafa	1
AL266-1	13	0	0	0	0	0	0	0	0	0	Aafa	1
AL333-10	10	0	3	0	0	0	0	0	0	0	Aafa	0.7692
AL655-1	12	0	0	0	0	0	0	0	0	1	Aafa	0.9231
Combe Grenal I	0	0	0	0	0	0	0	0	13	0	Hn	1
DNH107	0	13	0	0	0	0	0	0	0	0	Pr	1
DNH46	0	13	0	0	0	0	0	0	0	0	Pr	1
DNH8	0	13	0	0	0	0	0	0	0	0	Pr	1
ZMB 17963	0	0	0	0	0	13	0	0	0	0	Gg	1
ZMB 30941	0	0	0	0	0	13	0	0	0	0	Gg	1
ZMB 31435	0	0	0	0	0	13	0	0	0	0	Gg	1
ZMB 83561	0	0	0	0	0	13	0	0	0	0	Gg	1
ZMB 30940	0	0	0	0	0	13	0	0	0	0	Gg	1
ZMB 85368	0	0	0	0	0	0	13	0	0	0	Hy	1
ZMB 7814	0	0	0	0	0	0	13	0	0	0	Hy	1
ZMB 7826	0	0	0	0	0	0	13	0	0	0	Hy	1
ZMB 7828	0	0	0	0	0	0	13	0	0	0	Hy	1
KRP51	0	0	0	0	0	0	0	0	13	0	Hn	1
KRP 52	0	0	0	0	0	0	0	0	13	0	Hn	1
KRP54	0	0	0	0	0	0	0	0	13	0	Hn	1
KRP55	0	0	0	0	0	0	0	0	13	0	Hn	1
KRP D111	0	0	0	0	0	0	0	0	13	0	Hn	1
KRP D114	0	0	0	0	0	0	0	0	13	0	Hn	1
KRP D33	0	0	0	0	0	0	0	0	13	0	Hn	1
KRP D34	0	0	0	0	0	0	0	0	13	0	Hn	1
ZMB 12209	0	0	0	0	0	0	0	13	0	0	Pp	1
ZMB 38607	0	0	0	0	0	0	0	13	0	0	Pp	1
ZMB 6948	0	0	0	0	0	0	0	13	0	0	Pp	1
ZMB 83509	0	0	0	0	0	0	0	13	0	0	Pp	1
ZMB 83511	0	0	0	0	0	0	0	13	0	0	Pp	1
ZMB 11776	0	0	0	0	13	0	0	0	0	0	Ptv	1
ZMB 11800	0	0	0	0	13	0	0	0	0	0	Ptv	1
ZMB 11903	0	0	0	0	13	0	0	0	0	0	Ptv	1
ZMB 13430	0	0	0	0	13	0	0	0	0	0	Ptv	1
ZMB 13437	0	0	0	0	13	0	0	0	0	0	Ptv	1
ZMB 6957	0	0	0	0	0	0	0	13	0	0	Pp	1
SCLA 4A 6	0	0	0	0	0	0	0	0	13	0	Hn	1
SK100	0	13	0	0	0	0	0	0	0	0	Pr	1
SK61	0	13	0	0	0	0	0	0	0	0	Pr	1
SK62	0	13	0	0	0	0	0	0	0	0	Pr	1
SK63	0	13	0	0	0	0	0	0	0	0	Pr	1
SK857	0	13	0	0	0	0	0	0	0	0	Pr	1
SKW5	0	6	0	0	0	0	0	0	0	7	Pr	0.4615
STS24	1	0	12	0	0	0	0	0	0	0	Aafri	0.9231
STS51	0	0	13	0	0	0	0	0	0	0	Aafri	1
STS52b	0	0	13	0	0	0	0	0	0	0	Aafri	1
STW104	0	4	9	0	0	0	0	0	0	0	Aafri	0.6923

STW213	2	0	10	0	0	0	0	0	0	0	1	Aafri	0.7692
STW404	0	0	13	0	0	0	0	0	0	0	0	Aafri	1
STW420B	0	0	13	0	0	0	0	0	0	0	0	Aafri	1
STW7	0	0	13	0	0	0	0	0	0	0	0	Aafri	1
Taung1	2	0	11	0	0	0	0	0	0	0	0	Aafri	0.8462
ULAC 1	0	0	0	13	0	0	0	0	0	0	0	Hs	1
ULAC 536	0	0	0	13	0	0	0	0	0	0	0	Hs	1
ULAC 58	0	0	0	6	0	0	0	0	7	0	0	Hs	0.4615
ULAC 66	0	0	0	13	0	0	0	0	0	0	0	Hs	1
ULAC 790	0	0	0	13	0	0	0	0	0	0	0	Hs	1
ULAC 797	0	0	0	13	0	0	0	0	0	0	0	Hs	1
ULAC 801	3	0	1	8	0	0	0	0	0	0	1	Hs	0.6154
ULAC 806	0	0	0	13	0	0	0	0	0	0	0	Hs	1
UW101 1283	0	0	0	0	0	0	0	0	0	0	13	Hnal	1
UW101 144	0	0	0	0	0	0	0	0	0	0	13	Hnal	1
UW101 1565	0	0	0	0	0	0	0	0	0	0	13	Hnal	1
UW101 889	0	0	0	0	0	0	0	0	0	0	13	Hnal	1
W8-978-LRP3	4	0	9	0	0	0	0	0	0	0	0	Aafa	0.3077

Abbreviations: Aafa = *Australopithecus afarensis*, Hn = *Homo neanderthalensis*, Pr = *Paranthropus robustus*, Aafri = *Australopithecus africanus*, Hs = *Homo sapiens*, Hnal = *Homo naledi*, Ptv = *Pan troglodytes verus*, Gg = *Gorilla gorilla*, Hy = *Hylobates*, Pp = *Pongo pygmaeus*

**Supplementary Table 7.** CVA classification results for the CEJ + Med analysis in shape space

	Aafa	Hn	Pr	Aafri	Hs	Hnal	Ptv	Gg	Hy	Pp	Correct class	Proportion Correct
AL333w-1c	10	0	0	3	0	0	0	0	0	0	Aafa	0.7692
AL128-23	5	0	0	8	0	0	0	0	0	0	Aafa	0.3846
AL266-1	8	0	0	5	0	0	0	0	0	0	Aafa	0.6154
AL333-10	3	0	1	9	0	0	0	0	0	0	Aafa	0.2308
AL417-1a	9	1	1	0	2	0	0	0	0	0	Aafa	0.6923
AL655-1	12	0	0	1	0	0	0	0	0	0	Aafa	0.9231
Combe Grenal I	0	13	0	0	0	0	0	0	0	0	Hn	1
Combe XV	0	0	0	0	13	0	0	0	0	0	Hn	0
DNH46	4	0	8	1	0	0	0	0	0	0	Pr	0.6154
DNH8	0	0	13	0	0	0	0	0	0	0	Pr	1
ZMB 17963	0	0	0	0	0	0	0	13	0	0	Gg	1
ZMB 30941	0	0	0	0	0	0	0	13	0	0	Gg	1
ZMB 31435	0	0	0	0	0	0	0	13	0	0	Gg	1
ZMB 83561	0	0	0	0	0	0	1	12	0	0	Gg	0.9231
ZMB ZMB30940	0	0	0	0	0	0	0	5	8	0	Gg	0.3846
ZMB 85368	0	0	0	0	0	0	0	0	13	0	Hy	1
ZMB ZMB7814	0	0	0	0	0	0	0	0	13	0	Hy	1
ZMB ZMB7826	0	0	0	0	0	0	0	0	13	0	Hy	1
ZMB ZMB7828	0	0	0	0	0	0	0	0	13	0	Hy	1
Krapina58	0	12	0	0	1	0	0	0	0	0	Hn	0.9231
KRP51	0	3	0	0	10	0	0	0	0	0	Hn	0.2308
KRP 52	0	13	0	0	0	0	0	0	0	0	Hn	1
KRP54	0	13	0	0	0	0	0	0	0	0	Hn	1
KRP55	0	13	0	0	0	0	0	0	0	0	Hn	1
KRP D111	0	7	0	0	6	0	0	0	0	0	Hn	0.5385
KRP D114	0	13	0	0	0	0	0	0	0	0	Hn	1
KRP D27	0	13	0	0	0	0	0	0	0	0	Hn	1
KRP D28	0	13	0	0	0	0	0	0	0	0	Hn	1
KRP D29	0	13	0	0	0	0	0	0	0	0	Hn	1
KRP D33	0	13	0	0	0	0	0	0	0	0	Hn	1
KRP D34	0	13	0	0	0	0	0	0	0	0	Hn	1
ZMB 12209	0	0	0	0	0	0	0	0	0	13	Pp	1
ZMB 38607	0	0	0	0	0	0	0	0	0	13	Pp	1
ZMB 6948	0	0	0	0	0	0	0	0	0	13	Pp	1
ZMB 83509	0	0	0	0	0	0	0	0	0	13	Pp	1
ZMB 83511	0	0	0	0	0	0	0	0	0	13	Pp	1
ZMB 11776	0	0	0	0	0	0	11	2	0	0	Ptv	0.8462
ZMB 11800	0	0	0	0	0	0	13	0	0	0	Ptv	1
ZMB 11903	0	0	0	0	0	0	13	0	0	0	Ptv	1
ZMB 13430	0	0	0	0	0	0	12	0	1	0	Ptv	0.9231
ZMB 13437	0	0	0	0	0	0	13	0	0	0	Ptv	1
SCLA 4A 6	0	5	0	0	8	0	0	0	0	0	Hn	0.3846
SK100	0	0	13	0	0	0	0	0	0	0	Pr	1
SK23	6	0	5	0	2	0	0	0	0	0	Pr	0.3846
SK857	0	0	13	0	0	0	0	0	0	0	Pr	1
SKW5	1	0	10	2	0	0	0	0	0	0	Pr	0.7692

STS51	0	0	0	13	0	0	0	0	0	0	Aafri	1
STS52b	5	0	0	8	0	0	0	0	0	0	Aafri	0.6154
STW142	3	0	0	10	0	0	0	0	0	0	Aafri	0.7692
STW213	0	0	0	13	0	0	0	0	0	0	Aafri	1
STW401	11	0	2	0	0	0	0	0	0	0	Aafri	0
STW404	13	0	0	0	0	0	0	0	0	0	Aafri	0
STW498c	0	0	0	13	0	0	0	0	0	0	Aafri	1
STW7	0	0	0	13	0	0	0	0	0	0	Aafri	1
ULAC 171	0	7	0	0	6	0	0	0	0	0	Hs	0.4615
ULAC 1	0	0	2	0	11	0	0	0	0	0	Hs	0.8462
ULAC 522	0	0	0	0	13	0	0	0	0	0	Hs	1
ULAC 536	0	0	0	0	13	0	0	0	0	0	Hs	1
ULAC 58	0	1	0	0	12	0	0	0	0	0	Hs	0.9231
ULAC 607	0	0	0	0	13	0	0	0	0	0	Hs	1
ULAC 66	0	13	0	0	0	0	0	0	0	0	Hs	0
ULAC 74	0	0	0	0	13	0	0	0	0	0	Hs	1
ULAC 790	0	1	0	0	12	0	0	0	0	0	Hs	0.9231
ULAC 797	0	0	0	0	13	0	0	0	0	0	Hs	1
ULAC 801	0	0	3	0	10	0	0	0	0	0	Hs	0.7692
ULAC 806	0	0	0	0	13	0	0	0	0	0	Hs	1
UW101 001	0	0	0	0	0	13	0	0	0	0	Hnal	1
UW101 1283	0	0	0	0	0	13	0	0	0	0	Hnal	1
UW101 144	0	0	0	0	0	13	0	0	0	0	Hnal	1
UW101 1565	0	0	0	0	0	13	0	0	0	0	Hnal	1
UW101 889	0	0	0	0	0	13	0	0	0	0	Hnal	1
W8-978-LRP3	13	0	0	0	0	0	0	0	0	0	Aafa	1
ZMB 6957	0	0	0	0	0	0	0	0	0	13	Pp	1

Abbreviations: Aafa = *Australopithecus afarensis*, Hn = *Homo neanderthalensis*, Pr = *Paranthropus robustus*, Aafri = *Australopithecus africanus*, Hs = *Homo sapiens*, Hnal = *Homo naledi*, Ptv = *Pan troglodytes verus*, Gg = *Gorilla gorilla*, Hy = *Hylobates*, Pp = *Pongo pygmaeus*

**Supplementary Table 8.** CVA classification results for the CEJ + Med analysis in form space

	Aafa	Hn	Pr	Aafri	Hs	Hnal	Ptv	Gg	Hy	Pp	Correct class	Proportion Correct
AL333w-1c	7	0	0	6	0	0	0	0	0	0	Aafa	0.5385
AL128-23	13	0	0	0	0	0	0	0	0	0	Aafa	1
AL266-1	13	0	0	0	0	0	0	0	0	0	Aafa	1
AL333-10	2	0	3	8	0	0	0	0	0	0	Aafa	0.1538
AL417-1a	9	4	0	0	0	0	0	0	0	0	Aafa	0.6923
AL655-1	13	0	0	0	0	0	0	0	0	0	Aafa	1
Combe Grenal I	0	13	0	0	0	0	0	0	0	0	Hn	1
Combe XV	0	0	0	0	13	0	0	0	0	0	Hn	0
DNH46	2	0	9	2	0	0	0	0	0	0	Pr	0.6923
DNH8	0	0	12	1	0	0	0	0	0	0	Pr	0.9231
ZMB 17963	0	0	0	0	0	0	0	13	0	0	Gg	1
ZMB 30941	0	0	0	0	0	0	0	13	0	0	Gg	1
ZMB 31435	0	0	0	0	0	0	0	13	0	0	Gg	1
ZMB 83561	0	0	0	0	0	0	0	13	0	0	Gg	1
ZMB 30940	0	0	0	0	0	0	0	13	0	0	Gg	1
ZMB 85368	0	0	0	0	0	0	0	0	13	0	Hy	1
ZMB ZMB7814	0	0	0	0	0	0	0	0	13	0	Hy	1
ZMB ZMB7826	0	0	0	0	0	0	0	0	13	0	Hy	1
ZMB ZMB7828	0	0	0	0	0	0	0	0	13	0	Hy	1
Krapina58	0	13	0	0	0	0	0	0	0	0	Hn	1
KRP51	0	10	0	0	3	0	0	0	0	0	Hn	0.7692
KRP 52	0	13	0	0	0	0	0	0	0	0	Hn	1
KRP54	0	13	0	0	0	0	0	0	0	0	Hn	1
KRP55	0	13	0	0	0	0	0	0	0	0	Hn	1
KRP D111	0	13	0	0	0	0	0	0	0	0	Hn	1
KRP D114	0	13	0	0	0	0	0	0	0	0	Hn	1
KRP D27	0	13	0	0	0	0	0	0	0	0	Hn	1
KRP D28	0	13	0	0	0	0	0	0	0	0	Hn	1
KRP D29	0	13	0	0	0	0	0	0	0	0	Hn	1
KRP D33	0	13	0	0	0	0	0	0	0	0	Hn	1
KRP D34	0	13	0	0	0	0	0	0	0	0	Hn	1
ZMB 12209	0	0	0	0	0	0	0	0	0	13	Pp	1
ZMB 38607	0	0	0	0	0	0	1	0	0	12	Pp	0.9231
ZMB 6948	0	0	0	0	0	0	0	0	0	13	Pp	1
ZMB 83509	0	0	0	0	0	0	0	0	0	13	Pp	1
ZMB 83511	0	0	0	0	0	0	0	0	0	13	Pp	1
ZMB 11776	0	0	0	0	0	0	13	0	0	0	Ptv	1
ZMB 11800	0	0	0	0	0	0	13	0	0	0	Ptv	1
ZMB 11903	0	0	0	0	0	0	13	0	0	0	Ptv	1
ZMB 13430	0	0	0	0	0	0	13	0	0	0	Ptv	1
ZMB 13437	0	0	0	0	0	0	13	0	0	0	Ptv	1
SCLA 4A 6	0	10	0	0	3	0	0	0	0	0	Hn	0.7692
SK100	0	0	13	0	0	0	0	0	0	0	Pr	1
SK23	7	0	6	0	0	0	0	0	0	0	Pr	0.4615

SK857	0	0	13	0	0	0	0	0	0	0	Pr	1
SKW5	4	0	8	1	0	0	0	0	0	0	Pr	0.6154
STS51	0	0	0	13	0	0	0	0	0	0	Aafri	1
STS52b	1	0	0	12	0	0	0	0	0	0	Aafri	0.9231
STW142	5	0	1	7	0	0	0	0	0	0	Aafri	0.5385
STW213	5	0	0	7	0	1	0	0	0	0	Aafri	0.5385
STW401	0	0	4	9	0	0	0	0	0	0	Aafri	0.6923
STW404	11	0	0	2	0	0	0	0	0	0	Aafri	0.1538
STW498c	0	0	1	12	0	0	0	0	0	0	Aafri	0.9231
STW7	0	0	0	13	0	0	0	0	0	0	Aafri	1
ULAC 171	0	0	0	0	13	0	0	0	0	0	Hs	1
ULAC 1	0	0	0	0	13	0	0	0	0	0	Hs	1
ULAC 522	0	0	0	0	13	0	0	0	0	0	Hs	1
ULAC 536	0	0	0	0	13	0	0	0	0	0	Hs	1
ULAC 58	0	0	0	0	13	0	0	0	0	0	Hs	1
ULAC 607	0	0	0	0	13	0	0	0	0	0	Hs	1
ULAC 66	0	1	0	0	12	0	0	0	0	0	Hs	0.9231
ULAC 74	0	0	0	0	13	0	0	0	0	0	Hs	1
ULAC 790	0	0	0	0	13	0	0	0	0	0	Hs	1
ULAC 797	0	0	0	0	13	0	0	0	0	0	Hs	1
ULAC 801	0	0	0	0	12	1	0	0	0	0	Hs	0.9231
ULAC 806	0	0	0	0	13	0	0	0	0	0	Hs	1
UW101 001	1	0	0	0	0	12	0	0	0	0	Hnal	0.9231
UW101 1283	0	0	0	0	0	13	0	0	0	0	Hnal	1
UW101 144	0	0	0	0	0	13	0	0	0	0	Hnal	1
UW101 1565	0	0	0	0	0	13	0	0	0	0	Hnal	1
UW101 889	0	0	0	0	0	13	0	0	0	0	Hnal	1
W8-978-LRP3	13	0	0	0	0	0	0	0	0	0	Aafa	1
ZMB 6957	0	0	0	0	0	0	0	0	0	13	Pp	1

Abbreviations: Aafa = *Australopithecus afarensis*, Hn = *Homo neanderthalensis*, Pr = *Paranthropus robustus*, Aafri = *Australopithecus africanus*, Hs = *Homo sapiens*, Hnal = *Homo naledi*, Ptv = *Pan troglodytes verus*, Gg = *Gorilla gorilla*, Hy = *Hylobates*, Pp = *Pongo pygmaeus*

**Supplementary Table 9.** CVA classification results for the CEJ analysis in form space

	Aafa	Hn	Pr	Aafri	Hs	Hnal	Ptv	Gg	Hy	Pp	Correct class	Proportion Correct
AL277-1	2	0	7	4	0	0	0	0	0	0	Aafa	0.1538
AL333w-1c	8	0	1	4	0	0	0	0	0	0	Aafa	0.6154
AL1045	12	0	0	0	0	1	0	0	0	0	Aafa	0.9231
AL128-23	11	2	0	0	0	0	0	0	0	0	Aafa	0.8462
AL266-1	9	0	0	4	0	0	0	0	0	0	Aafa	0.6923
AL333-10	3	0	0	10	0	0	0	0	0	0	Aafa	0.2308
AL400-1a	9	0	0	4	0	0	0	0	0	0	Aafa	0.6923
AL417-1a	9	4	0	0	0	0	0	0	0	0	Aafa	0.6923
AL655-1	13	0	0	0	0	0	0	0	0	0	Aafa	1
Combe Grenal I	0	13	0	0	0	0	0	0	0	0	Hn	1
Combe XV	0	0	0	0	13	0	0	0	0	0	Hn	0
DNH46	2	0	11	0	0	0	0	0	0	0	Pr	0.8462
DNH51	0	0	13	0	0	0	0	0	0	0	Pr	1
DNH8	0	0	11	2	0	0	0	0	0	0	Pr	0.8462
ZMB 17963	0	0	0	0	0	0	0	13	0	0	Gg	1
ZMB 30941	0	0	0	0	0	0	0	13	0	0	Gg	1
ZMB 31435	0	0	0	0	0	0	0	10	0	3	Gg	0.7692
ZMB 83561	0	0	0	0	0	0	0	13	0	0	Gg	1
ZMB 30940	0	0	0	0	0	0	0	13	0	0	Gg	1
ZMB 85368	0	0	0	0	0	0	0	0	13	0	Hy	1
ZMB ZMB7814	0	0	0	0	0	0	0	0	13	0	Hy	1
ZMB ZMB7826	0	0	0	0	0	0	0	0	13	0	Hy	1
ZMB ZMB7828	0	0	0	0	0	0	0	0	13	0	Hy	1
Krapina58	0	13	0	0	0	0	0	0	0	0	Hn	1
KRP51	0	13	0	0	0	0	0	0	0	0	Hn	1
KRP 52	0	13	0	0	0	0	0	0	0	0	Hn	1
KRP54	0	13	0	0	0	0	0	0	0	0	Hn	1
KRP55	0	13	0	0	0	0	0	0	0	0	Hn	1
KRP D111	0	13	0	0	0	0	0	0	0	0	Hn	1
KRP D114	0	13	0	0	0	0	0	0	0	0	Hn	1
KRP D27	0	13	0	0	0	0	0	0	0	0	Hn	1
KRP D28	0	13	0	0	0	0	0	0	0	0	Hn	1
KRP D29	0	13	0	0	0	0	0	0	0	0	Hn	1
KRP D33	0	13	0	0	0	0	0	0	0	0	Hn	1
KRP D34	0	13	0	0	0	0	0	0	0	0	Hn	1
ZMB 12209	0	0	0	0	0	0	0	0	0	13	Pp	1
ZMB 38607	0	0	0	0	0	0	1	0	0	12	Pp	0.9231
ZMB 6948	0	0	0	0	0	0	0	0	0	13	Pp	1
ZMB 83509	0	0	0	0	0	0	0	0	0	13	Pp	1
ZMB 83511	0	0	0	0	0	0	0	3	0	10	Pp	0.7692
ZMB 11776	0	0	0	0	0	0	13	0	0	0	Ptv	1
ZMB 11800	0	0	0	0	0	0	13	0	0	0	Ptv	1
ZMB 11903	0	0	0	0	0	0	13	0	0	0	Ptv	1
ZMB 13430	0	0	0	0	0	0	13	0	0	0	Ptv	1
ZMB 13437	0	0	0	0	0	0	13	0	0	0	Ptv	1
SCLA 4A 6	0	11	0	0	2	0	0	0	0	0	Hn	0.8462

SK100	0	0	12	1	0	0	0	0	0	0	Pr	0.9231
SK23	9	1	3	0	0	0	0	0	0	0	Pr	0.2308
SK30	1	0	12	0	0	0	0	0	0	0	Pr	0.9231
SK857	0	0	13	0	0	0	0	0	0	0	Pr	1
SKW5	2	0	9	2	0	0	0	0	0	0	Pr	0.6923
STS51	1	0	0	12	0	0	0	0	0	0	Aafri	0.9231
STS52b	4	0	1	8	0	0	0	0	0	0	Aafri	0.6154
STW142	0	0	4	9	0	0	0	0	0	0	Aafri	0.6923
STW193	0	0	0	13	0	0	0	0	0	0	Aafri	1
STW213	0	0	0	5	0	8	0	0	0	0	Aafri	0.3846
STW401	0	0	1	12	0	0	0	0	0	0	Aafri	0.9231
STW404	13	0	0	0	0	0	0	0	0	0	Aafri	0
STW498c	0	0	2	11	0	0	0	0	0	0	Aafri	0.8462
STW7	3	0	0	10	0	0	0	0	0	0	Aafri	0.7692
ULAC 171	0	0	0	0	13	0	0	0	0	0	Hs	1
ULAC 1	0	0	0	0	13	0	0	0	0	0	Hs	1
ULAC 522	0	0	0	0	13	0	0	0	0	0	Hs	1
ULAC 536	0	0	0	0	13	0	0	0	0	0	Hs	1
ULAC 58	0	0	0	0	13	0	0	0	0	0	Hs	1
ULAC 607	0	0	0	0	13	0	0	0	0	0	Hs	1
ULAC 66	0	0	0	0	13	0	0	0	0	0	Hs	1
ULAC 74	0	0	0	0	13	0	0	0	0	0	Hs	1
ULAC 790	0	0	0	0	13	0	0	0	0	0	Hs	1
ULAC 797	0	0	0	0	13	0	0	0	0	0	Hs	1
ULAC 801	0	3	0	0	10	0	0	0	0	0	Hs	0.7692
ULAC 806	0	0	0	0	13	0	0	0	0	0	Hs	1
UW101 001	0	0	0	0	0	13	0	0	0	0	Hnal	1
UW101 1283	0	0	0	0	0	13	0	0	0	0	Hnal	1
UW101 144	0	0	0	0	0	13	0	0	0	0	Hnal	1
UW101 1565	0	0	0	0	0	13	0	0	0	0	Hnal	1
UW101 850	0	0	0	0	0	13	0	0	0	0	Hnal	1
UW101 889	0	0	0	0	0	13	0	0	0	0	Hnal	1
UW102 23	2	0	0	0	0	11	0	0	0	0	Hnal	0.8462
UW102 240	1	0	0	0	0	12	0	0	0	0	Hnal	0.9231
W8-978-LRP3	12	0	0	0	0	1	0	0	0	0	Aafa	0.9231
ZMB 6957	0	0	0	0	0	0	0	0	0	13	Pp	1

Abbreviations: Aafa = *Australopithecus afarensis*, Hn = *Homo neanderthalensis*, Pr = *Paranthropus robustus*, Aafri = *Australopithecus africanus*, Hs = *Homo sapiens*, Hnal = *Homo naledi*, Ptv = *Pan troglodytes verus*, Gg = *Gorilla gorilla*, Hy = *Hylobates*, Pp = *Pongo pygmaeus*

**Supplementary Table 10.** CVA classification results for the CEJ analysis in shape space

	Aafa	Hn	Pr	Aafri	Hs	Hnal	Ptv	Gg	Hy	Pp	Correct class	Proportion Correct
AL277-1	0	0	0	0	13	0	0	0	0	0	Aafa	0
AL333w-1c	10	0	1	2	0	0	0	0	0	0	Aafa	0.7692
AL1045	13	0	0	0	0	0	0	0	0	0	Aafa	1
AL128-23	2	0	3	8	0	0	0	0	0	0	Aafa	0.1538
AL266-1	6	0	0	7	0	0	0	0	0	0	Aafa	0.4615
AL333-10	9	0	0	4	0	0	0	0	0	0	Aafa	0.6923
AL400-1a	10	0	0	3	0	0	0	0	0	0	Aafa	0.7692
AL417-1a	6	0	0	0	7	0	0	0	0	0	Aafa	0.4615
AL655-1	6	0	1	0	0	6	0	0	0	0	Aafa	0.4615
Combe Grenal I	0	13	0	0	0	0	0	0	0	0	Hn	1
Combe XV	0	0	0	0	13	0	0	0	0	0	Hn	0
DNH46	1	0	10	0	0	2	0	0	0	0	Pr	0.7692
DNH51	0	0	13	0	0	0	0	0	0	0	Pr	1
DNH8	0	0	13	0	0	0	0	0	0	0	Pr	1
ZMB 17963	0	0	0	0	0	0	0	13	0	0	Gg	1
ZMB 30941	0	0	0	0	0	0	0	9	0	4	Gg	0.6923
ZMB 31435	0	0	0	0	0	0	0	12	0	1	Gg	0.9231
ZMB 83561	0	0	0	0	0	0	1	12	0	0	Gg	0.9231
ZMB 30940	0	0	0	0	0	0	0	7	6	0	Gg	0.5385
ZMB 85368	0	0	0	0	0	0	0	0	13	0	Hy	1
ZMB ZMB7814	0	0	0	0	0	0	0	0	13	0	Hy	1
ZMB ZMB7826	0	0	0	0	0	0	0	0	13	0	Hy	1
ZMB ZMB7828	0	0	0	0	0	0	0	0	13	0	Hy	1
Krapina58	0	12	0	0	1	0	0	0	0	0	Hn	0.9231
KRP51	0	6	0	0	7	0	0	0	0	0	Hn	0.4615
KRP 52	0	13	0	0	0	0	0	0	0	0	Hn	1
KRP54	0	13	0	0	0	0	0	0	0	0	Hn	1
KRP55	0	13	0	0	0	0	0	0	0	0	Hn	1
KRP D111	0	9	0	0	4	0	0	0	0	0	Hn	0.6923
KRP D114	0	13	0	0	0	0	0	0	0	0	Hn	1
KRP D27	0	13	0	0	0	0	0	0	0	0	Hn	1
KRP D28	0	12	0	0	1	0	0	0	0	0	Hn	0.9231
KRP D29	0	13	0	0	0	0	0	0	0	0	Hn	1
KRP D33	0	13	0	0	0	0	0	0	0	0	Hn	1
KRP D34	0	13	0	0	0	0	0	0	0	0	Hn	1
ZMB 12209	0	0	0	0	0	0	0	0	0	13	Pp	1
ZMB 38607	0	0	0	0	0	0	0	12	0	1	Pp	0.0769
ZMB 6948	0	0	0	0	0	0	0	1	0	12	Pp	0.9231
ZMB 83509	0	0	0	0	0	0	0	0	6	7	Pp	0.5385
ZMB 83511	0	0	0	0	0	0	0	1	0	12	Pp	0.9231
ZMB 11776	0	0	0	0	0	0	4	9	0	0	Ptv	0.3077
ZMB 11800	0	0	0	0	0	0	13	0	0	0	Ptv	1
ZMB 11903	0	0	0	0	0	0	12	0	0	1	Ptv	0.9231
ZMB 13430	0	0	0	0	0	0	13	0	0	0	Ptv	1
ZMB 13437	0	0	0	0	0	0	13	0	0	0	Ptv	1
SCLA 4A 6	0	8	0	0	5	0	0	0	0	0	Hn	0.6154

SK100	0	0	11	0	2	0	0	0	0	0	Pr	0.8462
SK23	0	0	0	0	13	0	0	0	0	0	Pr	0
SK30	0	0	8	0	0	5	0	0	0	0	Pr	0.6154
SK857	0	0	13	0	0	0	0	0	0	0	Pr	1
SKW5	0	0	11	2	0	0	0	0	0	0	Pr	0.8462
STS51	0	0	0	13	0	0	0	0	0	0	Aafri	1
STS52b	7	0	1	5	0	0	0	0	0	0	Aafri	0.3846
STW142	0	0	3	10	0	0	0	0	0	0	Aafri	0.7692
STW193	9	0	0	4	0	0	0	0	0	0	Aafri	0.3077
STW213	0	0	0	11	0	2	0	0	0	0	Aafri	0.8462
STW401	9	0	1	3	0	0	0	0	0	0	Aafri	0.2308
STW404	13	0	0	0	0	0	0	0	0	0	Aafri	0
STW498c	1	0	0	12	0	0	0	0	0	0	Aafri	0.9231
STW7	0	0	0	13	0	0	0	0	0	0	Aafri	1
ULAC 171	0	1	0	0	12	0	0	0	0	0	Hs	0.9231
ULAC 1	0	9	0	0	4	0	0	0	0	0	Hs	0.3077
ULAC 522	0	0	2	0	11	0	0	0	0	0	Hs	0.8462
ULAC 536	0	7	0	0	6	0	0	0	0	0	Hs	0.4615
ULAC 58	0	0	0	0	13	0	0	0	0	0	Hs	1
ULAC 607	0	13	0	0	0	0	0	0	0	0	Hs	0
ULAC 66	0	3	0	0	10	0	0	0	0	0	Hs	0.7692
ULAC 74	0	0	0	0	13	0	0	0	0	0	Hs	1
ULAC 790	0	1	0	0	12	0	0	0	0	0	Hs	0.9231
ULAC 797	0	0	0	0	13	0	0	0	0	0	Hs	1
ULAC 801	0	0	2	0	11	0	0	0	0	0	Hs	0.8462
ULAC 806	0	0	1	0	12	0	0	0	0	0	Hs	0.9231
UW101 001	0	0	0	0	0	13	0	0	0	0	Hnal	1
UW101 1283	0	0	0	0	0	13	0	0	0	0	Hnal	1
UW101 144	0	0	0	0	0	13	0	0	0	0	Hnal	1
UW101 1565	0	0	0	0	0	13	0	0	0	0	Hnal	1
UW101 850	0	0	0	0	0	13	0	0	0	0	Hnal	1
UW101 889	0	0	0	0	0	13	0	0	0	0	Hnal	1
UW102 23	0	0	0	0	0	13	0	0	0	0	Hnal	1
UW102 240	0	0	0	0	0	13	0	0	0	0	Hnal	1
W8-978-LRP3	13	0	0	0	0	0	0	0	0	0	Aafa	1
ZMB 6957	0	0	0	0	0	0	0	0	0	13	Pp	1

Abbreviations: Aafa = *Australopithecus afarensis*, Hn = *Homo neanderthalensis*, Pr = *Paranthropus robustus*, Aafri = *Australopithecus africanus*, Hs = *Homo sapiens*, Hnal = *Homo naledi*, Ptv = *Pan troglodytes verus*, Gg = *Gorilla gorilla*, Hy = *Hylobates*, Pp = *Pongo pygmaeus*

**Supplementary Table 11.** Discrete trait scores, with inter- and intra-observer error test results. The table displays the scorings for the discrete traits by two observers. The results used in the main text of the paper are those of the primary observer's first scores, unless otherwise stated. Disagreements with the primary observers original scores are marked in red, and percent agreement scores are shown at the bottom of the table. Obs. 1-1 = First scores by primary observer; Obs. 1-2 = Second scores by primary observer (used for intra-observer test); Obs. 2-1 = Trait scores by secondary observer (used for inter-observer test)

Specimen	Transverse Crest			Marginal Ridge			Mesial Buccal Grooves			Distal Buccal Grooves		
	Obs. 1-1	Obs 1-2	Obs 2-1	Obs. 1-1	Obs 1-2	Obs 2-1	Obs. 1-1	Obs 1-2	Obs 2-1	Obs. 1-1	Obs 1-2	Obs 2-1
ZMB 7814	3	3	3	-	-	-	0	0	0	0	0	0
ZMB 7826	2	2	2	-	-	-	1	0	1	0	0	0
ZMB 7828	3	3	3	-	-	-	0	0	0	0	0	0
ZMB 85368	2	2	1	-	-	-	0	0	0	0	0	0
ZMB 6948	1	1	1	-	-	-	0	0	1	0	0	0
ZMB 6957	1	1	1	-	-	-	0	0	0	0	0	1
ZMB 12209	1	1	1	-	-	-	0	0	0	0	0	0
ZMB 38607	1	1	1	-	-	-	0	0	0	0	0	0
ZMB 83509	1	1	1	-	-	-	0	0	0	0	0	0
ZMB 83511	1	1	1	-	-	-	0	0	0	0	0	1
ZMB 17963	2	2	2	-	-	-	1	0	1	1	0	1
ZMB 30940	2	2	2	-	-	-	0	0	1	1	0	0
ZMB 30941	2	2	2	-	-	-	0	0	1	1	1	1
ZMB 31435	2	2	2	-	-	-	1	0	1	1	1	1
ZMB 83561	2	2	1	-	-	-	0	0	1	1	0	1
ZMB 11776	3	3	3	-	-	-	1	0	1	1	1	1
ZMB 11800	3	3	3	-	-	-	1	0	1	1	1	1
ZMB 11903	3	3	3	-	-	-	1	0	1	1	1	1
ZMB 13430	2	2	2	-	-	-	0	0	1	1	0	0
ZMB 13437	3	2	3	-	-	-	0	0	0	1	0	2
KNM-KP 29281	-	-	-	M	M	M	2	2	1	1	2	2
KNM-KP 29286Ai	1	1	1	M	M	M	2	2	2	2	2	2
KNM-KP 53160	1	1	1	M	M	M	2	2	2	1	2	2
AL266-1	1	1	1	M	M	M	1	1	1	1	1	1
AL333-10	1	1	1	C	C	C	2	1	2	2	1	2
AL333w-1c	1	1	1	M	M	M	2	2	2	2	1	2
AL655-1	1	1	1	-	-	-	-	-	-	-	-	-
W8-978	-	-	-	C	C	C	2	1	1	1	1	2
KNM-WT 8556	1	1	1	C	C	C	2	1	1	1	1	1
STW 7	1	1	1	C	C	C	1	2	2	1	1	1
STW 104	1	1	1	C	C	C	2	2	2	1	1	1
STW 142	-	-	-	C	C	C	2	2	2	1	1	2
STW 193	-	-	-	-	-	-	2	2	2	1	1	2
STW 213	1	1	1	M	M	M	2	2	2	2	2	2
STW 401	-	-	-	D	D	D	2	2	2	2	1	2
STW 404	-	-	-	C	C	C	2	2	1	1	1	2
STW 420B	1	1	1	C	C	C	2	2	2	2	2	2
STW 498c	-	-	-	C	C	C	2	2	2	1	1	1
STS 24	1	1	1	C	C	C	1	1	1	1	1	1
STS 51	1	1	1	C	C	C	2	2	1	1	1	2
STS 52b	-	-	-	C	C	C	2	2	2	2	2	2
Taung1	1	1	1	M	M	D	2	1	1	1	1	2
DNH8	1	1	4	C	C	C	0	0	0	1	1	2

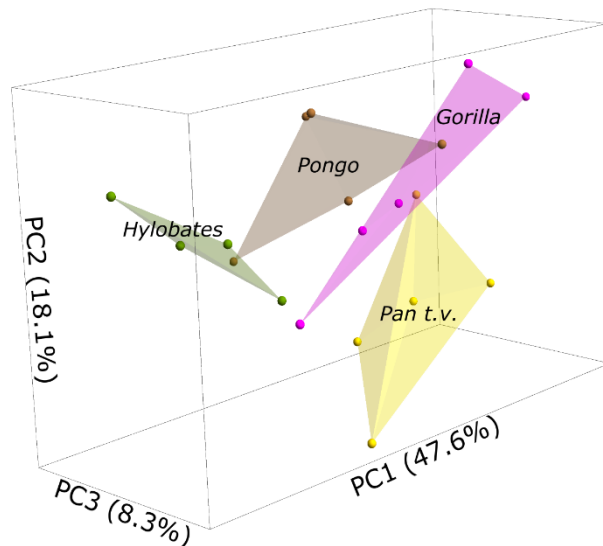
DNH46	1	1	1	-	-	-	-	-	-	-	-	-
DNH51	-	-	-	C	C	C	0	0	0	1	0	0
DNH107	1	1	4	C	C	C	0	1	0	2	2	2
SK23	-	-	-	C	C	C	0	0	0	0	0	0
SK30	-	-	-	-	-	-	0	1	0	1	1	1
SK61	1	1	1	C	C	C	0	1	0	1	1	0
SK62	1	1	1	C	C	C	1	1	0	2	2	2
SK63	-	-	-	-	-	-	0	0	0	1	1	2
SK100	1	1	1	C	C	C	1	0	1	1	1	2
SK857	1	1	4	C	C	C	0	0	0	0	1	0
SKW5	-	-	-	C	C	C	0	0	1	1	1	1
KNM-ER 1820	1	1	1	C	C	C	-	-	-	-	-	-
KNM-ER 6082	0	0	2	C	C	C	-	-	-	-	-	-
KNM-ER 15951H	-	-	-	-	-	-	0	0	0	0	0	0
KNM-WT 16005	1	1	1	C	C	C	0	0	0	1	0	1
L427-7	0	0	0	-	-	-	2	1	2	2	2	2
KNM-ER 806E	-	-	-	-	-	-	2	2	2	0	1	1
KNM-ER 992A	-	-	-	-	-	-	-	-	-	-	-	-
KNM-ER 5431E	2	2	2	C	C	C	-	-	-	-	-	-
SK 96	1	1	1	C	C	C	0	1	0	1	1	1
SKX 21204	1	1	1	C	C	C	2	2	2	1	2	2
STW 151	1	1	1	C	C	C	2	2	1	2	2	1
S 6a	1	1	1	C	C	C	2	1	2	1	1	2
U.W. 101-0010	-	-	-	C	C	C	1	1	1	1	1	1
U.W. 101-0144	1	1	1	C	C	C	1	1	1	0	1	1
U.W. 101-0850	-	-	-	-	-	-	1	1	1	1	1	1
U.W. 101-0889	1	1	1	C	C	C	1	1	1	1	1	1
U.W. 101-1261	1	1	1	C	C	C	1	1	1	1	1	1
U.W. 101-1565	1	1	1	C	C	C	0	1	0	1	1	1
U.W. 102-0023	-	-	-	-	-	-	1	1	1	1	1	1
Cave of hearths	1	1	1	M	M	M	0	0	0	0	0	0
Mauer 1	-	-	-	MD	MD	MD	0	0	0	0	0	0
Combe-Grenal I	1	1	4	C	C	C	1	0	0	0	0	0
Combe-Grenal XV	-	-	-	-	-	-	-	-	-	-	-	-
KRP 51	1	1	1	C	C	C	1	1	0	1	0	1
KRP 52	4	4	4	C	C	C	1	1	0	0	0	0
KRP 54	4	4	4	M	M	M	0	0	0	0	0	0
KRP 55	1	1	1	C	C	C	0	0	0	0	0	0
KRP 58	-	-	-	C	M	M	1	0	0	0	0	0
KRP D27	-	-	-	C	C	C	1	0	0	0	0	0
KRP D28	-	-	-	M	M	M	0	0	0	0	0	0
KRP D29	-	-	-	M	M	M	0	0	0	0	0	0
KRP D33	4	4	4	C	C	C	0	0	0	0	0	0
KRP D34	-	-	-	-	-	-	1	1	1	1	0	1
KRP D111	1	1	1	M	M	M	1	1	1	1	0	1
KRP D114	4	4	4	C	C	C	1	0	0	0	0	0
SCLA 4A 6	1	1	1	C	C	C	0	0	0	0	0	0
Irhoud 11	-	-	-	M	M	M	1	1	1	0	1	1
Qafzeh 10	1	1	1	C	C	C	0	0	0	0	0	0

Qafzeh 11	1	1	1	M	M	M	0	0	0	0	0	0
ULAC 1	-	-	-	C	C	C	0	0	0	0	0	0
ULAC 58	1	1	1	M	M	M	0	0	0	0	0	0
ULAC 66	0	0	0	MD	MD	MD	0	0	0	0	0	0
ULAC 74	-	-	-	C	C	C	0	0	0	1	0	0
ULAC 171	0	0	0	MD	MD	MD	0	0	0	0	0	0
ULAC 522	-	-	-	C	C	C	0	0	0	0	0	0
ULAC 536	1	1	1	C	C	C	0	0	0	0	0	0
ULAC 607	-	-	-	C	C	C	0	1	0	0	0	0
ULAC 790	-	-	-	MD	MD	MD	0	0	0	0	0	0
ULAC 797	0	0	0	C	D	C	0	0	0	0	0	0
ULAC 801	1	1	1	D	D	D	1	1	1	1	1	1
ULAC 806	0	0	0	MD	MD	MD	0	0	0	0	0	0
% Agreement:		98.6%	90.4%		97.2%	97.2%		75.5%	78.6%		78.6%	74.5%

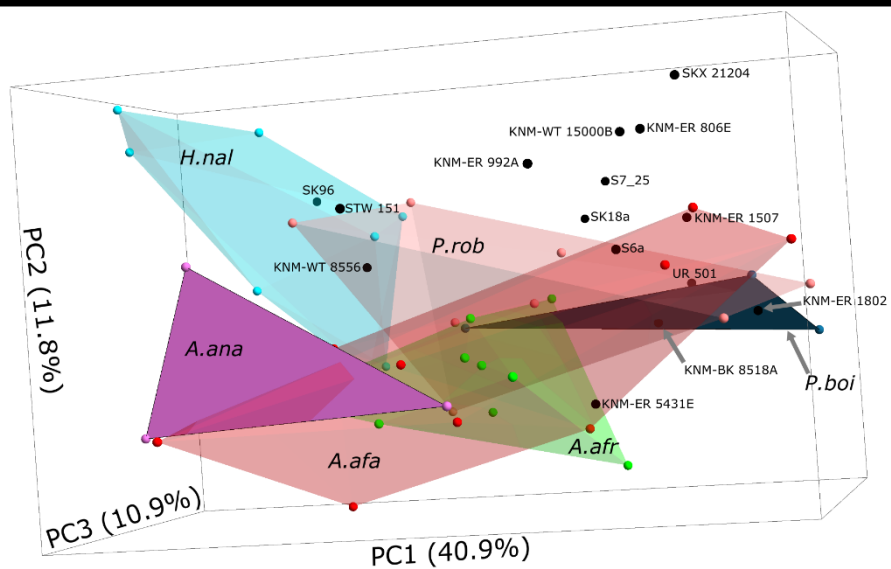
**Supplementary Table 12.** Protoconid form results. Note:  
 The vast majority of specimens display a simple conic  
 dentine horn, and therefore only the exceptions are listed  
 here

<i>Protoconid form</i>	<i>Specimens</i>
Flattened protoconid ridge	ULAC 790
Longitudinally expanded	UW101-144, UW101-889 (and antimeres UW101-506, UW101-377)
Transversely expanded	ULAC 58

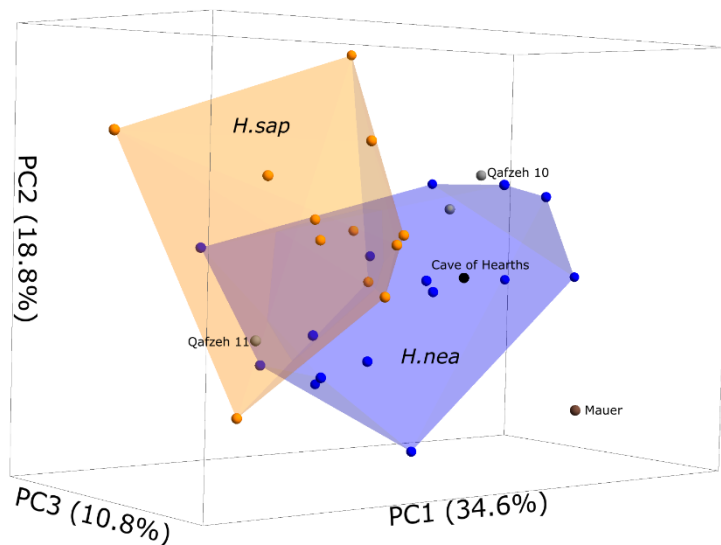
Non-hominin apes



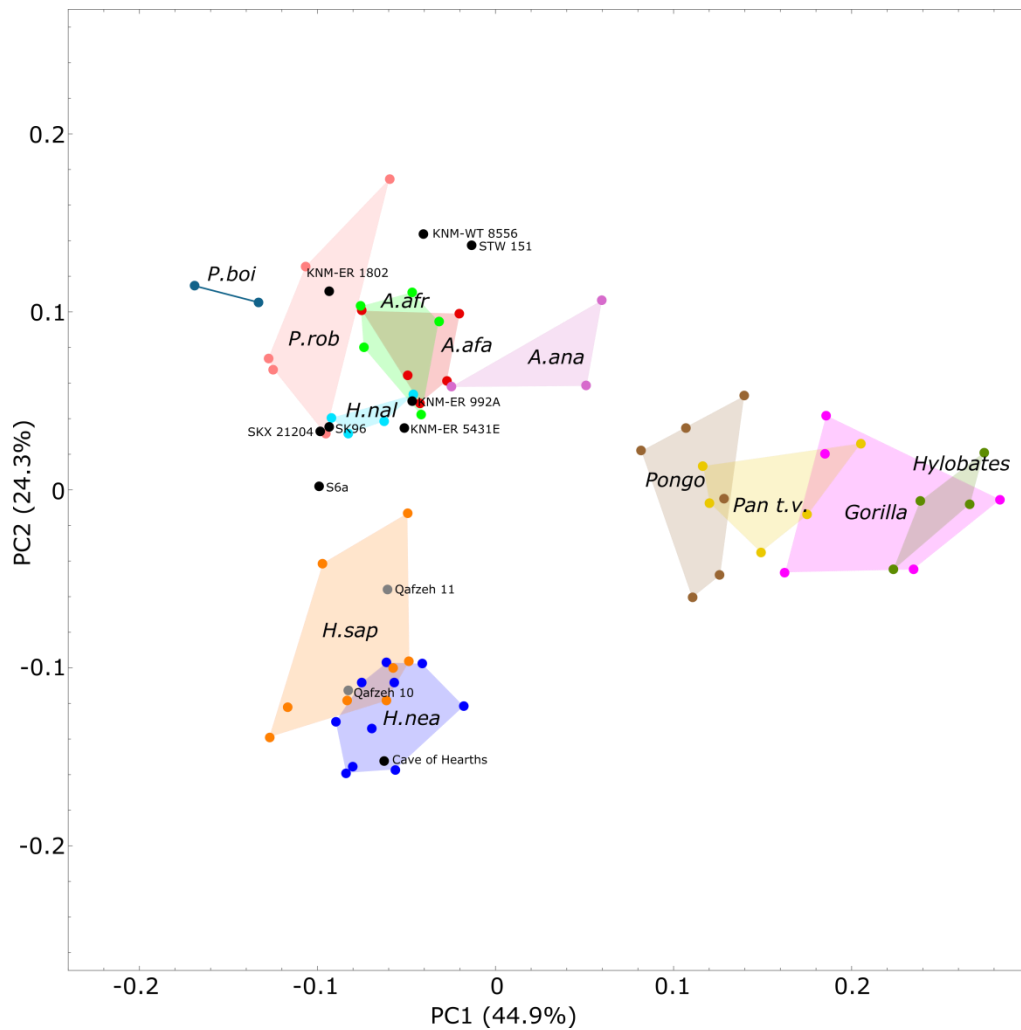
Plio-Pleistocene hominins



Late-Pleistocene hominins



**Supplementary Figure 1.** PCA plots of CEJ shape. Percentages in brackets indicate the proportion of the total variation in the sample which is explained by each principle component. Abbreviations: PC = Principal Component, *Pan t.v* = *Pan troglodytes verus*; *A.ana* = *Australopithecus anamensis*; *A.afa* = *Australopithecus afarensis*; *A.afr* = *Australopithecus africanus*; *H.nal* = *Homo naledi*; *P.rob* = *Paranthropus robustus*; *P.boi* = *Paranthropus boisei*; *H.sap* = Extant *Homo sapiens*; *H.nea* = *Homo neanderthalensis*



**Supplementary Figure 2.** PCA plot of EDJ + CEJ shape for all specimens. Percentages in brackets indicate the proportion of the total variation in the sample which is explained by each principle component. Abbreviations: PC = Principal Component, *Pan t.v* = *Pan troglodytes verus*; *A. ana* = *Australopithecus anamensis*; *A. afa* = *Australopithecus afarensis*; *A. afr* = *Australopithecus africanus*; *H. nal* = *Homo naledi*; *P. rob* = *Paranthropus robustus*; *P. boi* = *Paranthropus boisei*; *H. sap* = Extant *Homo sapiens*; *H. nea* = *Homo neanderthalensis*